

Devonian and Mississippian Sappington Formation in Southwest Montana: Stratigraphic
Framework and Facies Relationships

A Thesis

Presented in Partial Fulfillment of the Requirements for the

Degree of Master of Science

with a

Major in Geology

in the

College of Graduate Studies

University of Idaho

by

Aaron P. Rodriguez

December 2014

Major Professor: Peter E. Isaacson, Ph.D.

Authorization to Submit Thesis

This thesis of Aaron Rodriguez, submitted for the degree of Master of Science with a major in Geology and titled “Devonian and Mississippian Sappington Formation in Southwest Montana: Stratigraphic Framework and Facies Relationships,” has been reviewed in final form. Permission, as indicated by the signatures and dates below, is now granted to submit final copies to the College of Graduate Studies for approval.

Major Professor: _____ Date: _____
Peter E. Isaacson, Ph.D

Committee

Members: _____ Date : _____
George W. Grader, Ph.D

_____ Date: _____
Elizabeth J. Cassel, Ph.D

Department

Administrator: _____ Date: _____
Mickey E. Gunter, Ph.D

Discipline's

College Dean: _____ Date: _____
Paul Joyce, Ph.D

Final Approval and Acceptance

Dean of the College

of Graduate Studies: _____ Date: _____
Jie Chen, Ph.D.

Abstract

Hydrocarbon production success from the Bakken Formation of the Williston Basin has led to interest in time-equivalent Devonian-Mississippian strata. One of these Bakken-equivalent formations is the Sappington Formation of western Montana. This regionally <30 ft. to >120 ft. thick mixed carbonate and fine-grained siliciclastic unit occurs between thick Devonian and Mississippian carbonates and was deposited in the low-accommodation intracratonic Sappington Basin of the Central Montana Trough (CMT). Differential foreland subsidence and uplift of the CMT resulted in changing depocenter geometries. Despite the tectonic and paleogeographic differences between the Sappington Basin and the Williston Basin, the Sappington and Bakken share similar intracratonic depositional elements.

This study focused on outcrop Sappington sections in the Three Forks, Montana area. Regionally, the Sappington pinches out to the south and northeast onto the paleogeographic highs of the Beartooth Shelf and Central Montana Uplift. To the west, correlation of Sappington and Antler Foreland Basin units have been complicated by Sevier and Laramide deformation. Within the Sappington Basin thinning and lateral facies relationships suggest significant early western accommodation of facies with potential for local proximal variations.

Similar to the coeval Bakken Formation, the Sappington's three members (Lower, Middle, Upper) are separated by abrupt facies shifts and unconformities. The Lower and Upper Members both display black organic preservation during periods of quiescent anoxic bottom water conditions. Such conditions were driven by early Gondwanan glaciation producing widespread equatorial Late Devonian eustatic effects. The Middle Member is a well oxygenated mix of wave and tidal dominant energies located within the shoreface regime.

The low-accommodation intracratonic character of the Sappington Basin complicates establishment of a sequence stratigraphic framework. Episodic flooding and draining of the Sappington Basin is represented by four prominent unconformities within a succession of rocks averaging 75 ft. in thickness and with a depositional timeline of ~8 million years. Subsequently, lowstand system tracts deposits are not observed in the study area and are represented by stacked sequence boundaries and transgressive surfaces.

Acknowledgements

Thank you to my advisor Peter Isaacson for taking a chance on me and accepting me to study under him at UI. His guidance, support, and loyalty have been tremendously appreciated. Thank you to my unofficial co-advisor George Grader for proposing my thesis project and spending time with me in the field teaching me the rocks. An additional thank you to George for providing me with much needed doses of non-geology related life perspective (i.e. mountain biking, racquetball, chopping wood). Thank you to Ted Doughty for his research and career guidance. Thank you to Liz Cassel for serving on my committee and adding valuable input to improve the quality of my thesis.

Field work in western Montana was the highlight of my research and there are many that need to be thanked for their support. In addition to George and Ted, thank you to John Hohman and John Guthrie for teaching me about a range of geologic concepts including structural geology, sedimentology, stratigraphy, and geochemistry. Thank you to Audrey Warren my fellow graduate student, and Sappington collaborator for her support and encouragement. An additional thank you to my officemate Daisuke Kobayashi for his graduate school mentorship.

Thank you to the following organizations whom provided the funding that made this research possible: PRISEM Geoscience Consulting, Hess Corporation, Rocky Mountain Section of the Society for Sedimentary Geology (RMS-SEPM), American Association of Petroleum Geologists (AAPG), Tobacco Root Geological Society (TRGS), and the University of Idaho.

Lastly, a thank you above all else, to my family for their never ending support of my various life endeavors.

Table of Contents

Authorization to Submit Thesis	ii
Abstract	iii
Acknowledgements	iv
Table of Contents	v
List of Figures	viii
1. Introduction	1
General Statement	1
Objectives	1
Location of Study	1
Previous Work	1
Paleogeographic Setting	3
Paleoclimatic Setting	3
Structural Setting	5
Tectonic History	5
Stratigraphy Under and Overlying the Sappington Formation	6
Figures	7
2. Methods	16
Outcrop Analysis	16
3. Results and Interpretations	17
Stratigraphic Units & Associated Lithofacies	17
Unit 1	18
Unit 2	18
Unit 3	19
Unit 4	19
Unit 5	20
Unit 6	21
Figures	23
Biostratigraphy	37
Conodont Biostratigraphy	37
Recent Conodont Biostratigraphy	38
Palynomorph Biostratigraphy	38
Figures	39
Drivers for Sappington Deposition	42

Facies Analysis.....	43
Lower Member.....	44
Middle Member	46
Upper Member	50
Figures.....	52
Facies Relationships	69
Lower Member.....	69
Middle Member	69
Upper Member	70
Structural Complications	70
Shelf Break.....	71
Figures.....	72
Sequence Stratigraphic Framework.....	76
Lower Member.....	78
Middle Member	79
Upper Member	79
Figures.....	80
4. Discussion	84
Environment Interpretation Comparison.....	84
Sequence Stratigraphic Comparison to Bakken Formation	84
Paleoclimate	85
Figures	87
5. Conclusions	91
6. References	93
7. Appendix – Stratigraphic sections.....	99
Antelope Creek Section.....	99
Ashbough Canyon Section	101
Brown Back Gulch Section	103
Copper City Section	106
Dry Hollow Section.....	109
Frazier Lake Section.....	112
Logan Gulch Section	115
Lone Mountain Section	117
Milligan Canyon Section (Sappington type section).....	119

Moose Creek Section.....	122
Nixon Gulch Section	124
Red Hill Section	127
Storm Castle Section	131
Trident Section	133

List of Figures

Figure 1.1 Map of Sappington outcrop section locations	7
Figure 1.2 Sappington stratigraphy.....	8
Figure 1.3 Paleogeographic map of North America at 345 Ma.....	9
Figure 1.4 Paleogeographic map of North America at 360 Ma.....	10
Figure 1.5 Regional paleogeographic map of the Late Devonian-Early Mississippian	11
Figure 1.6 Hypothetical series of events and consequences leading to Late Devonian-Early Mississippian formation of black shales	12
Figure 1.7 Block diagram of the Southwest Montana Transverse Zone.....	13
Figure 1.8 Geologic map of the Bozeman Quadrangle.....	14
Figure 1.9 Late Devonian-Early Mississippian Antler Convergent Margin.....	15
Figure 3.1 Unit 1 lithofacies	23
Figure 3.2 Lithofacies 1A thin sections	24
Figure 3.3 Lithofacies 1C fauna.....	24
Figure 3.4 Lithofacies 2	25
Figure 3.5 Unit 3 lithofacies	26
Figure 3.6 Lithofacies 3A ichnogenera assemblage	27
Figure 3.7 Lithofacies 3B ichnogenera assemblage	28
Figure 3.8 Unit 4 lithofacies	29
Figure 3.9 Lithofacies 4A	30
Figure 3.10 Lithofacies 4A ichnogenera assemblage	30
Figure 3.11 Lithofacies 4C	31
Figure 3.12 Unit 5 lithofacies	32
Figure 3.13 Lithofacies 5B	33
Figure 3.14 Unit 6 lithofacies	34
Figure 3.15 Lithofacies 6C	35
Figure 3.16 Lithofacies 6D	36
Figure 3.17 Wheeler Diagram of Sappington, upper Three Forks Fm., and lower Lodgepole Fm	39
Figure 3.18 Past and present conodont zone correlation chart	40
Figure 3.19 Picture of <i>Isosticha</i> conodont	41

Figure 3.20 Slug Model across the study area	52
Figure 3.21 Basal U1 regolith.....	53
Figure 3.22 Transgressive lag at the Three Forks – U2 contact	54
Figure 3.23 Lithofacies 1A chert beds	55
Figure 3.24 Cross section of U1	56
Figure 3.25 Outcrop of U1 lithofacies succession	57
Figure 3.26 Schematic representation of the effects of base level change on the Middle Member of the Sappington.....	58
Figure 3.27 Three Forks-U1 contact and U1-U2 contact	58
Figure 3.28 Lithofacies 2 lag channel fill	59
Figure 3.29 Lithofacies 2 oncolite beds	60
Figure 3.30 Lithofacies 3A outcrop	61
Figure 3.31 Lithofacies 3C outcrop	62
Figure 3.32 U4-U5 contact	63
Figure 3.33 Lithofacies 5A outcrop	64
Figure 3.34 Lithofacies 5B outcrop.	65
Figure 3.35 Lithofacies 5C outcrop	66
Figure 3.36 U6 lithofacies (6A, 6B, 6C, 6D) in outcrop	67
Figure 3.37 Scoured Lodgepole – lithofacies 5C contact at Red Hill	68
Figure 3.38 Cross section of study area	72
Figure 3.39 Conceptual model of U5 differential erosion	73
Figure 3.40 Sappington Lower Member isopach.....	74
Figure 3.41 Sappington Middle Member isopach.....	75
Figure 3.42 Sappington Upper Member isopach	76
Figure 3.43 Sequence stratigraphic interpretations.....	81
Figure 3.44 Paleozoic sea-level curve	82
Figure 3.45 U5-U6 contact	83
Figure 4.1 Comparison of U4 interpretations	87
Figure 4.2 Wheeler Diagram comparison of the Bakken Fm. and Sappington Fm.....	88
Figure 4.3 Correlation of unconformities in the Bakken Fm. and Sappington Fm	89
Figure 4.4 Sequence stratigraphy comparison of the Bakken Fm. and Sappington Fm.....	90

1. Introduction

General Statement

The Late Devonian-Early Mississippian Sappington Formation is a thin package of widely occurring mainly siliciclastic rocks situated unconformably between very thick carbonates of the Mississippian above and the Devonian below. The Sappington was deposited in the Sappington Basin of the greater Central Montana Trough (CMT) in present day southwestern Montana. The formation has not been thoroughly studied since the 1960's/1970's and consequently many questions remain regarding enigmatic vertical and lateral facies relationships. Although individual vertical lithostratigraphic stacking patterns are widespread, internal facies changes within these widely observed, primarily fine grained units, are not well understood.

Objectives

The main objectives of this outcrop based study are to 1) synthesize past work on the temporal relationships of the Sappington stratigraphic units, 2) provide detailed Sappington Formation focused lithofacies classifications and depositional environment interpretations, 3) create and review sequence stratigraphic frameworks for the Sappington, 4) interpret the lateral Sappington lithofacies relationships in up- and down-dip oriented directions, and 5) interpret a depositional model for the Sappington Basin during Sappington deposition.

Location of Study

Montana Sappington Formation outcrop sections in this study are located in a west-east corridor between Whitehall and Livingston (Figure 1.1). The red pins represent studied outcrop locations and the yellow pins represent locations from McMannis (1962) where the Sappington is not present. The McMannis (1962) sections were not visited, but were used to show the pinch out of the Sappington onto southeastern paleo-highs. The study sections were chosen for the accessibility and potential up- and down-dip oriented outcrops.

Previous Work

The term "Sappington Sandstone" (the Middle Member in this paper (Figure 1.2) of the Sappington Formation) was first proposed by Berry (1943) for the Milligan Canyon location (Sappington type section) and was named after the nearby town name of Sappington, Montana. Berry (1943) distinguished the stratigraphic unit by the yellow sandstone in between the Three Forks Formation and the Madison Group Limestone. In the 1950's and

1960's the Sappington was the focus of simultaneous studies by separate groups: Achauer (1959), Gutschick (1957, 1959, 1962, 1967), McMannis (1955, 1962), Rau (1962), and Sandberg (1962, 1965, 1967). In the Bridger Mountains, McMannis (1955) added the two "shaley" units (the Lower and Upper Member in this study (Figure 1.2)) thus creating the three member Sappington Formation. Interpretations of lithofacies, depositional environments, paleontology, and biostratigraphy were focused on more extensively by Achauer (1959), Gutschick et al. (1962), Sandberg (1965), and Sandberg et al. (1972).

Gutschick et al. (1962) created a lettered (A-I) nomenclature for the stratigraphy of the Sappington, and Sandberg (1965) created a numerical (1-5) nomenclature. The A-I nomenclature included four different shale lithofacies (lithofacies 1A-1D in this study, Figure 1.2) within the Lower Member (Unit 1 in this study (Figure 1.2) of the Sappington), as well as four stratigraphic unit subdivisions in the Middle Member (Units 2-5 in this paper (Figure 1.2) of the Sappington), and one in the Upper Member (Unit 6 in this paper (Figure 1.2) of the Sappington). Sandberg's (1965) 1-5 nomenclature subdivided the Middle Member into the same stratigraphic unit subdivisions, but did not subdivide the Lower Member and did not include the Upper Member. Sandberg (1967) later classified the Upper Member as a Mississippian age black shale known as the Cottonwood Canyon Member of the Lodgepole Formation. McMannis (1962) discussed the enigmatic relationship of the Upper Member with both the Sappington Formation and the Lodgepole Formation. It was proposed by Sandberg and Klapper (1967) that the Upper Member of the Sappington is equivalent to the Cottonwood Canyon Member of the Lodgepole Formation. Depositional environment interpretations from this era of Sappington investigations varied from shallow marine environments intermittently above wave base (Rau, 1962) to a mix of poorly circulated lagoonal basins (Gutschick et al., 1962) (Sandberg and Klapper, 1967) for the Upper and Lower Members and mud/tidal flats (Gutschick et al., 1962) for the Middle Member.

Recent master degree theses (Schietinger, 2012; Adiguzel, 2014; Nagase, 2014) on the Sappington Formation have been driven by hydrocarbon production success of correlative Late Devonian-Early Mississippian formations (Bakken Formation, Woodford Shale, Antrim Shale, etc.). These studies have provided insights into first order Sappington to

Bakken correlations including isopach maps, as well as general lithofacies classifications, depositional environment interpretations, and sequence stratigraphy interpretations.

Paleogeographic Setting

North America in Late Devonian-Early Mississippian time was partially encircled by convergent plate interactions (Figure 1.3). These convergent boundaries of the North American Plate resulted in high compressive stress and the loading of the crust at the margins of the North American plate. Loading of the margins (Dorobek et al., 1991) led to the formation of intracratonic basins on the North American Plate (

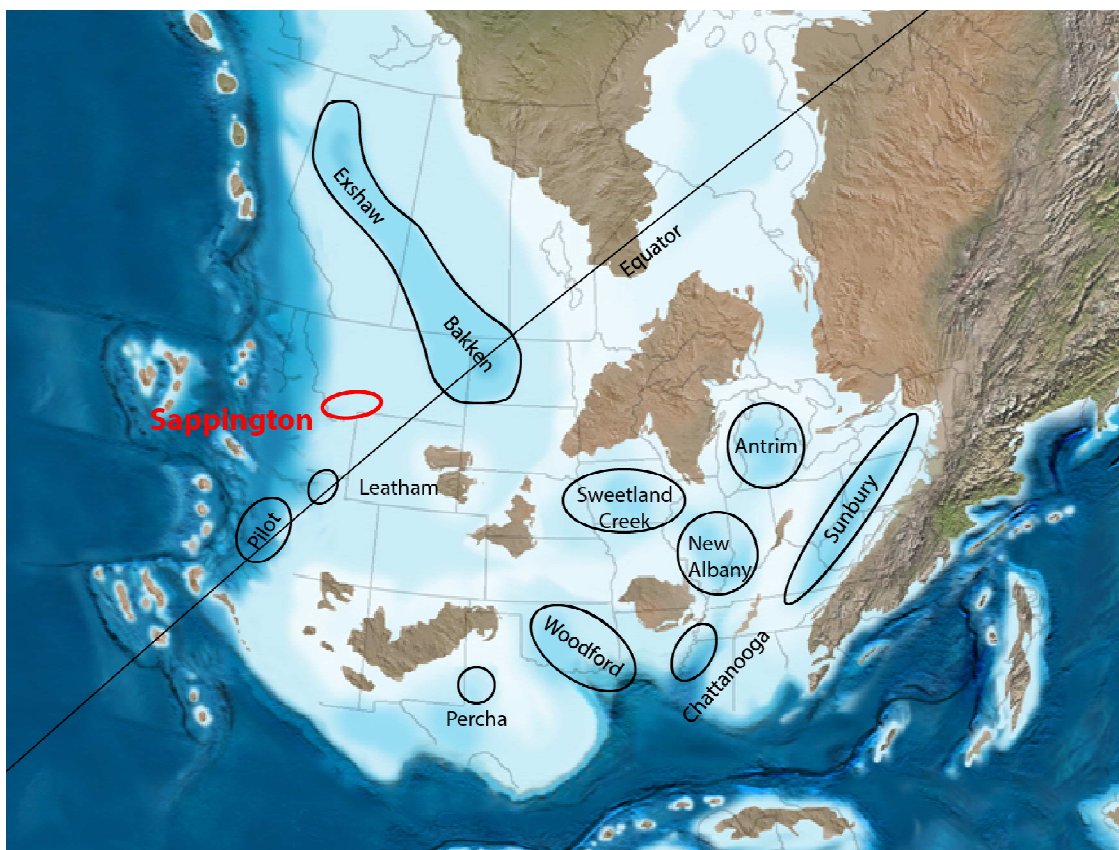


Figure 1.4 Paleogeographic map (Blakey, 2005) of North America at 360 Ma showing Late Devonian basins and the formation that was deposited within the basins.

). Many of these basins are current or proposed targets of hydrocarbon exploration.

The Sappington was deposited in the CMT (**Error! Reference source not found**.Figure 1.5), an intracratonic basin that formed perpendicular to the plate margin and subsided and flooded within a reactivated Precambrian aulacogen. At least two sub-basins (Figure 1.5) existed within the CMT. These basins are the Sappington Basin, which was the

depositional center for the Sappington Formation, and the Cottonwood Canyon Basin, which was the depositional center for the Sappington Upper Member equivalent Cottonwood Canyon Formation. West of the Sappington Basin lie, the Antler Foreland Basin (**Error! Reference source not found.**Figure 1.5), which was created as a flexural response (Dorobek et al., 1991) to the formation and loading of the Antler Highlands inboard of the Antler convergent margin. Flysch deposits of the Lodgepole equivalent McGowan Creek Formation in Idaho are evidence of known Antler Foreland Basin development (Figure 1.9) in the Early Mississippian. However, similar evidence to support Antler Foreland Basin development equivalent to Late Devonian Sappington deposition has not been found. Consequently, the Antler Foreland Basin during the time of Sappington deposition is referred to from this point on as the incipient Antler Foreland Basin. Paleo-highs (Peterson, 1986) existed to the east (Central Montana Uplift) (**Error! Reference source not found.**Figure 1.5), northwest (Montania) (**Error! Reference source not found.**Figure 1.5), and south (Beartooth Shelf) (**Error! Reference source not found.**Figure 1.5). In addition to the Sappington Basin, Cottonwood Canyon Basin, and incipient Antler Foreland Basin, additional regional basins included the Williston Basin (depositional center for the Bakken Formation) and Prophet Trough (Richards et al., 1994) (depositional center for the Exshaw Formation) (Figure 1.5).

Paleoclimatic Setting

During the Late Devonian-Early Mississippian the Sappington Basin was located at similar similar latitudes (

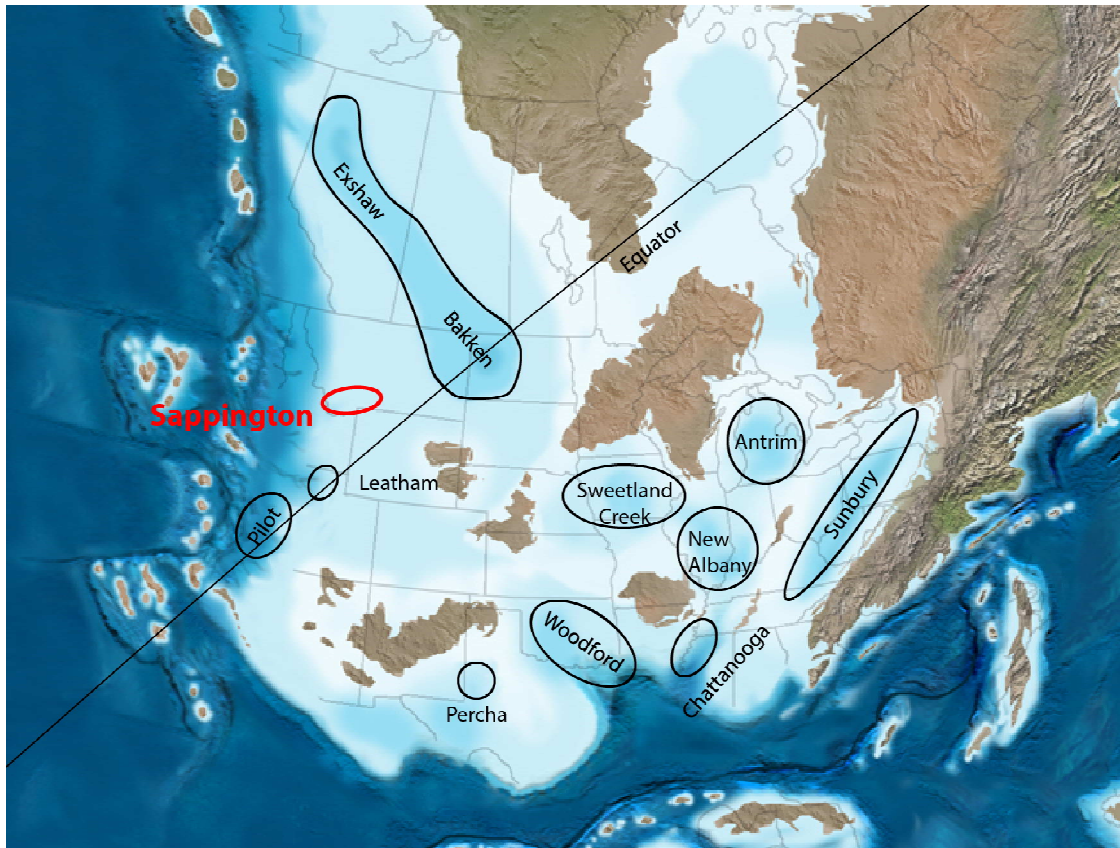


Figure 1.4 Paleogeographic map (Blakey, 2005) of North America at 360 Ma showing Late Devonian basins and the formation that was deposited within the basins.

) to the Williston Basin (Sonnenberg and Pramudito, 2009), just north of the equator in a tropical to subtropical climate. Globally, the Late Devonian-Early Mississippian was at a critical point in the transition from a global greenhouse to icehouse climate (Fischer and Arthur, 1977). Along with local tectonic paleogeography and global eustasy, expanding or contracting climate belts were likely a factor in Three Forks/Sappington sediment supply and depositional changes (Isaacson et al., 2008). Periods of global carbonate demise, such as in the Late Devonian-Early Mississippian, are commonly attributed to one or a combination of the following factors: sea-level changes, temperature, salinity, detrital input, turbidity, and/or eutrophication (Caplan et al., 1996). Studies of the Sappington equivalent Exshaw Formation (western Canada) and underlying Three Forks equivalent Big Valley Formation by Caplan et al. (1996), attribute the mechanism of carbonate demise to a shift from mesotrophic to eutrophic conditions. An influx of nutrients in the Late Devonian created eutrophic

conditions, which resulted in absorption of all the oxygen in the bottom waters and subsequent anoxia and organic preservation (e.g., Caplan et al., 1996; Algeo and Lyons, 2007; Etensohn et al., 2009). This organic preservation is reflected in the character of the Lower Member of the Sappington, Black Shale Member of the Exshaw, and Lower Member of the Bakken. The nutrient influx responsible for the creation of eutrophic marine conditions on the shelf of western paleo North America is proposed to be the upwelling of nutrient-rich deep marine waters (Caplan and Bustin, 1999) associated with an unstable climate. Major changes in land plant evolution also may have played a role in sediment/nutrient supply and eutrophication (Algeo and Scheckler, 2008). Studies of interglacial periods from the Eocene (Frakes et al., 1992) and Quaternary (Anklin et al., 1993) have shown evidence of climatic instability. Caplan and Bustin (1999) suggest similar climatic instability at the Late Devonian-Early Mississippian climate transition. In short, the proposed driving mechanism for this instability is the creation of an unstable ocean through the mixing of water sourced from low and high latitudes driven by the onset of cooling and increased glaciation as Gondwana moved over the South Pole (Caplan and Bustin, 1999). This resulted in oceans becoming susceptible to extensive upwelling and mixing of the water column, which delivered vast amounts of nutrient-rich deep ocean waters to the shelf. The theoretical timeline (Caplan and Bustin, 1999) of the sequence of events responsible for widespread black shale deposition during the Late Devonian-Early Mississippian is provided in Figure 1.6.

Structural Setting

The outcrops in this study are near the Southwest Montana Transverse Zone (SMTZ) within the broader Montana Thrust Belt Province. The SMTZ (Figure 1.8) is a zone of transition between eastward transported, allochthonous thrusting Precambrian through Cretaceous rocks of the Helena Salient to the north and basement-cored Archean uplifts to the south (Schmidt and Neill, 1982). The Helena Salient originated as an eastward promontory of a basin in which Proterozoic Belt Supergroup sediments were deposited (Harlan et al., 2008). As thrusting commenced in western Montana during the Cretaceous (Schmidt and Neill, 1982), thick Precambrian and Paleozoic rocks in the Helena Salient were transported to the east. The Helena Salient can be recognized in structural maps by a large eastward bend in the Cordilleran Fold and Thrust Belt (Harlan et al., 2008). The main thrust

plate of the Helena Salient is the Elk Horn Thrust Plate (Schmidt and Neil, 1982) and the main thrust fault is the Lombard Thrust (Harlan et al., 2008) (Figure 1.8). The Elk Horn Thrust Plate has moved 70 km (Burton et al., 1998) to the east, with several smaller imbricate thrusts with less displacement reaching the Bridger Range to the east.

To the south the Lombard thrust system is suggested to merge with the Cave Fault-Jefferson Canyon Fault system (Schmidt and Neill, 1982). This region marks the boundary of the Helena Salient. There the Willow Creek Fault is acting as a lateral ramp on which the Proterozoic and Paleozoic rocks of the Helena Salient are wrapping up and over the Archean rocks to the south (Figure 1.7).

Tectonic History

Dorobek et al. (1991) documented the tectonic history of the Devonian-Pennsylvanian Antler Convergent Margin, from which the information in the following discussion is derived. Middle to Late Proterozoic rifting in Idaho and Montana created a series of depocenters including the Belt Basin. An eastward extension of the Belt Basin across central Montana, known as the Central Montana Trough, formed within a subsiding aulacogen (Perry, 1995). This rifting in Idaho and Montana initiated a passive margin that lasted until the Early to Middle Devonian, at which time an inferred volcanic arc collided with the western margin of North America, creating a convergent plate margin at the western edge of North America. This period of convergence, known as the Antler Orogeny, resulted in a variety of flexural and compressive responses in-board of the convergent margin. A foredeep, known as the Antler Foreland Basin, began to form in the Early to Middle Devonian in Idaho east of the convergent margin. This foredeep flexural response was induced by the loading of the crust. Devonian to Pennsylvanian eastern migration of the foredeep is supported by the age of synorogenic sediments in Idaho and Montana. East of the Antler Foreland Basin onto the Montana Platform, differential subsidence and uplift from the Late Devonian to Pennsylvanian occurred across a 500 mile wide zone. The axes of the Montana Antler Foreland structures are oriented at high angles to the strike of the Antler Foreland Basin. This indicates that in addition to flexural responses across the Montana Platform, there was reactivation of Proterozoic structures oriented perpendicular to the Antler Convergent Margin. Dorobek et al. (1991) illustrated this by comparing the location and orientation of structural features in the Proterozoic and Devonian-Pennsylvanian.

Isopachs (Figure 3.40, Figure 3.41, Figure 3.42) created of the three members of the Sappington and isopachs of the adjacent Three Forks Formation and Lodgepole Formation from previous work, all support depocenter migration, which is attributed to differential uplift and subsidence on the Montana platform.

Stratigraphy Under and Overlying the Sappington Formation

In the study area, the Sappington is located between the Scallion Member of the Lodgepole Formation above and the Trident Member of the Three Forks Formation below (Figure 1.2). Within this area, the lithologic character of the upper Trident in contact with the Sappington is variable. In relatively higher accommodation portions of the Sappington Basin, to the west the upper Trident is characterized by a brachiopod-rich green shale overlain by a thick wackestone to packstone. In relatively lower accommodation settings, the Trident shale may not be present and the overlying limestone is thinner impacted also under a major unconformity. Throughout the study area, the Sappington is consistently overlain by a crinoidal packstone (base of a Williston Basin-like Scallion Member of the Lodgepole Formation) facies.

Figures

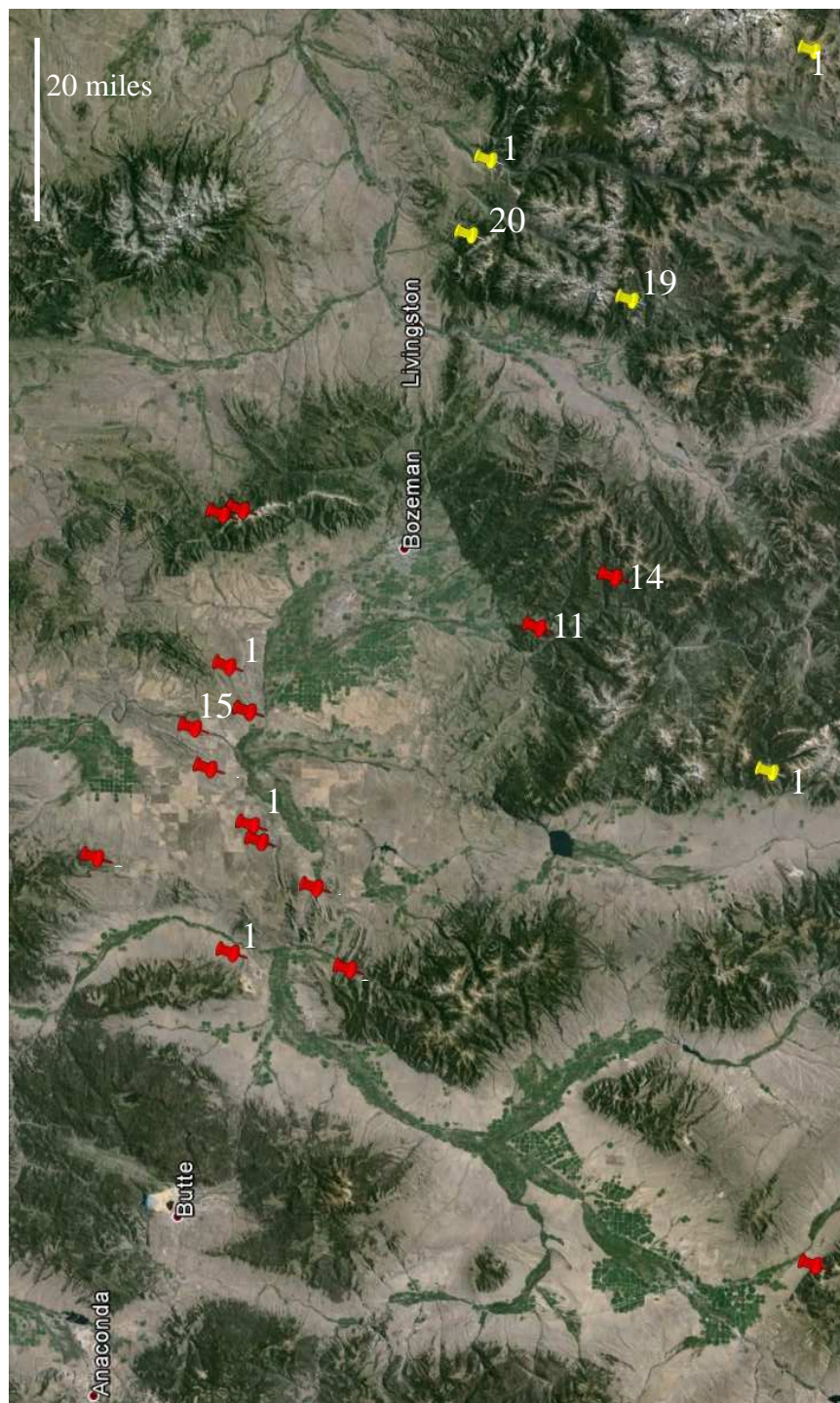


Figure 1.1 Map of Sappington section locations. Red pins represent studied sections (1=Antelope Creek, 2=Ashbough Canyon, 3=Brown Back Gulch, 4=Copper City, 5=Frazier Lake, 6=Hardscrabble, 7=Logan Gulch, 8=Lone Mountain, 9=Dry Hollow, 10= Milligan Canyon, 11=Moose Creek, 12=Nixon Gulch, 13=Red Hill, 14=Moose Creek, 15=Trident). Yellow pins represent McMannis (1962) sections where Sappington is absent (16=Boulder River, 17=Cinnabar Mountain, 18=Cooke City, 19=Mill Creek, 20=Mission Creek).

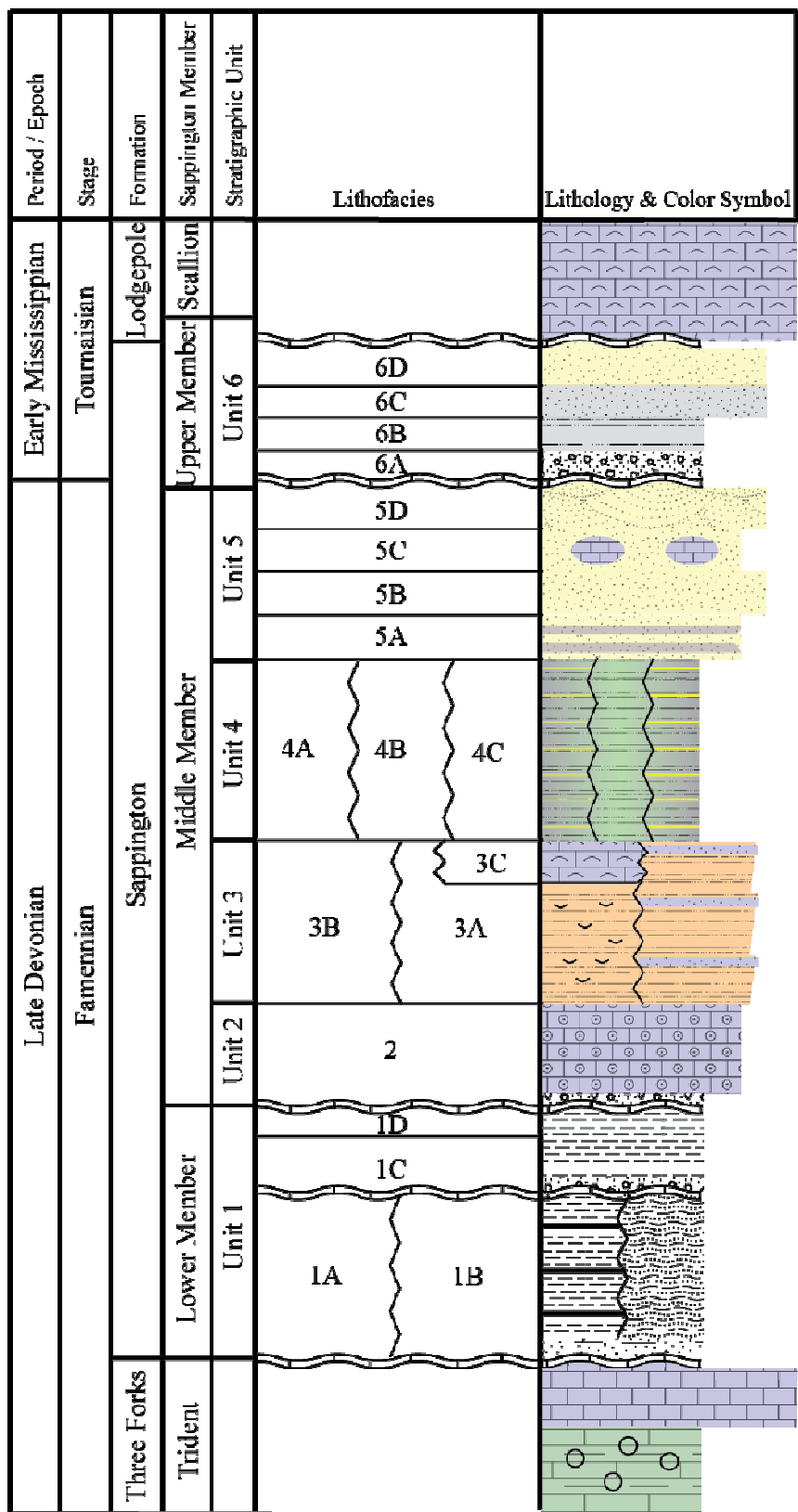


Figure 1.2 Sappington stratigraphy with stratigraphic unit and lithofacies classifications.

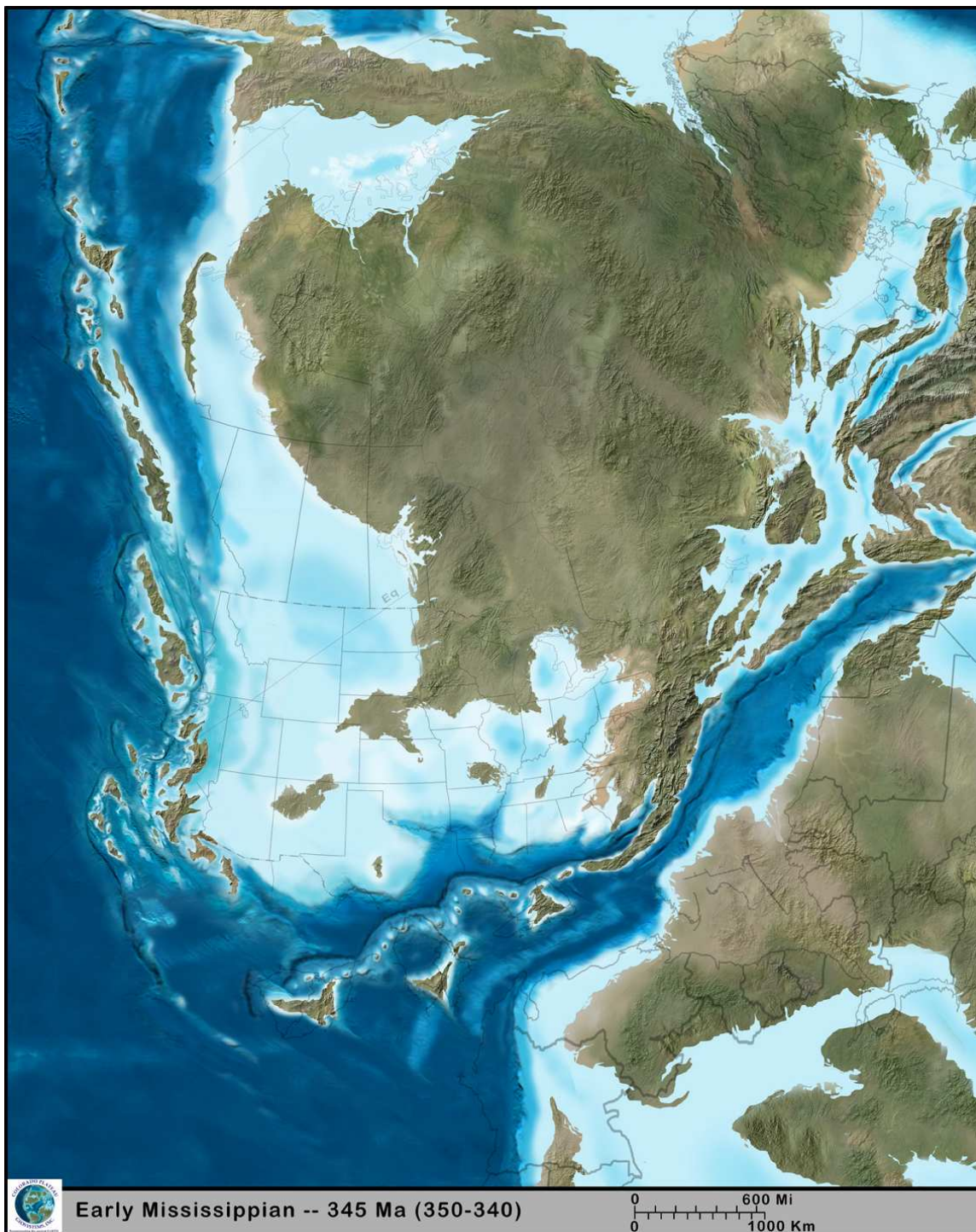


Figure 1.3 Paleogeographic map (Blakey, 2013) of paleo North America at 345 Ma showing western and eastern convergent plate margins.

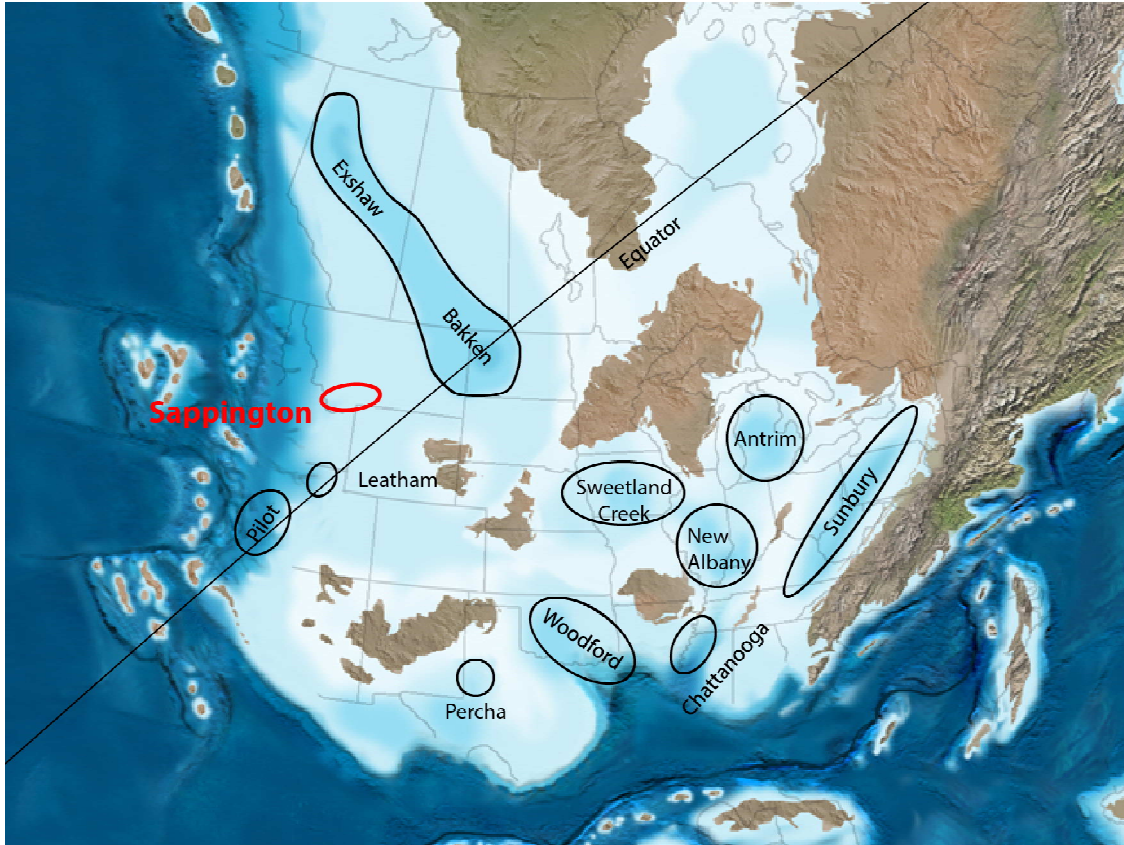


Figure 1.4 Paleogeographic map (Blakey, 2005) of North America at 360 Ma showing Late Devonian basins and the formation that was deposited within the basins.

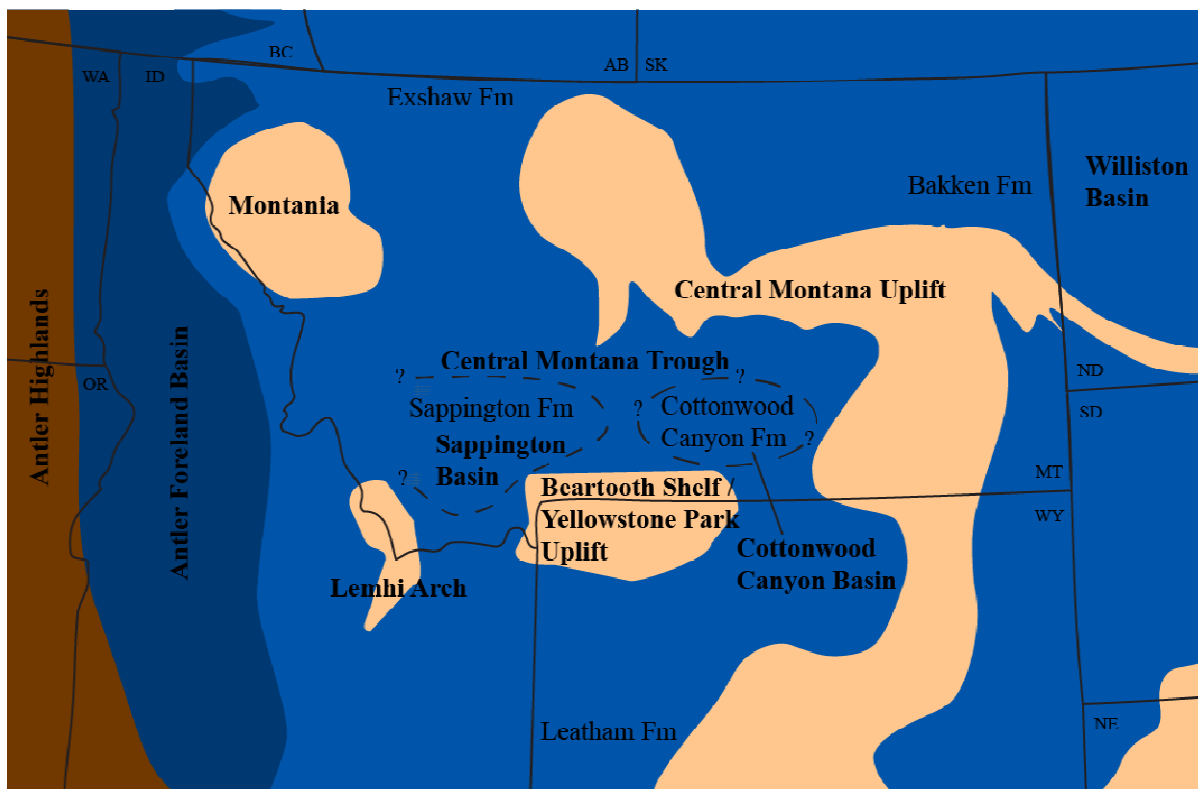


Figure 1.5 Regional paleogeographic map (modified from Grader and Doughty, 2012) of the Late Devonian-Early Mississippian with paleogeographic (Peterson, 1986) features (bold type) and coeval formations. (Color key: light blue = flooded continental shelf, dark blue = foreland basin, dark brown = Antler Orogenic Belt, light brown = intracratonic highlands)

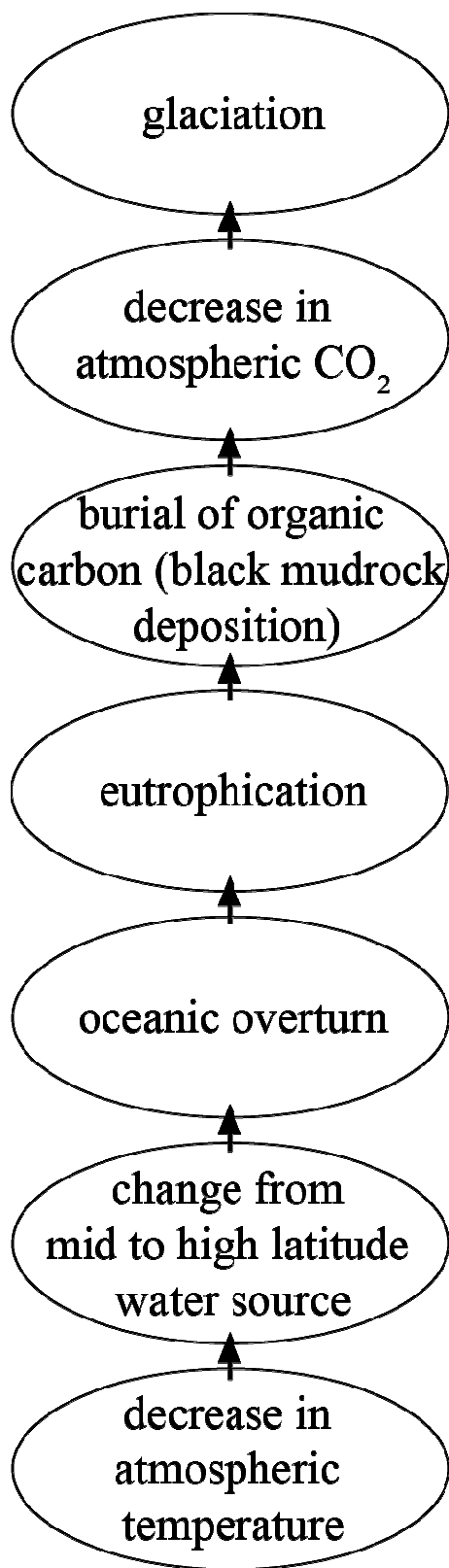


Figure 1.6 Hypothetical series of events and consequences leading to Late Devonian-Early Mississippian formation of black shales (Caplan and Bustin, 1999).

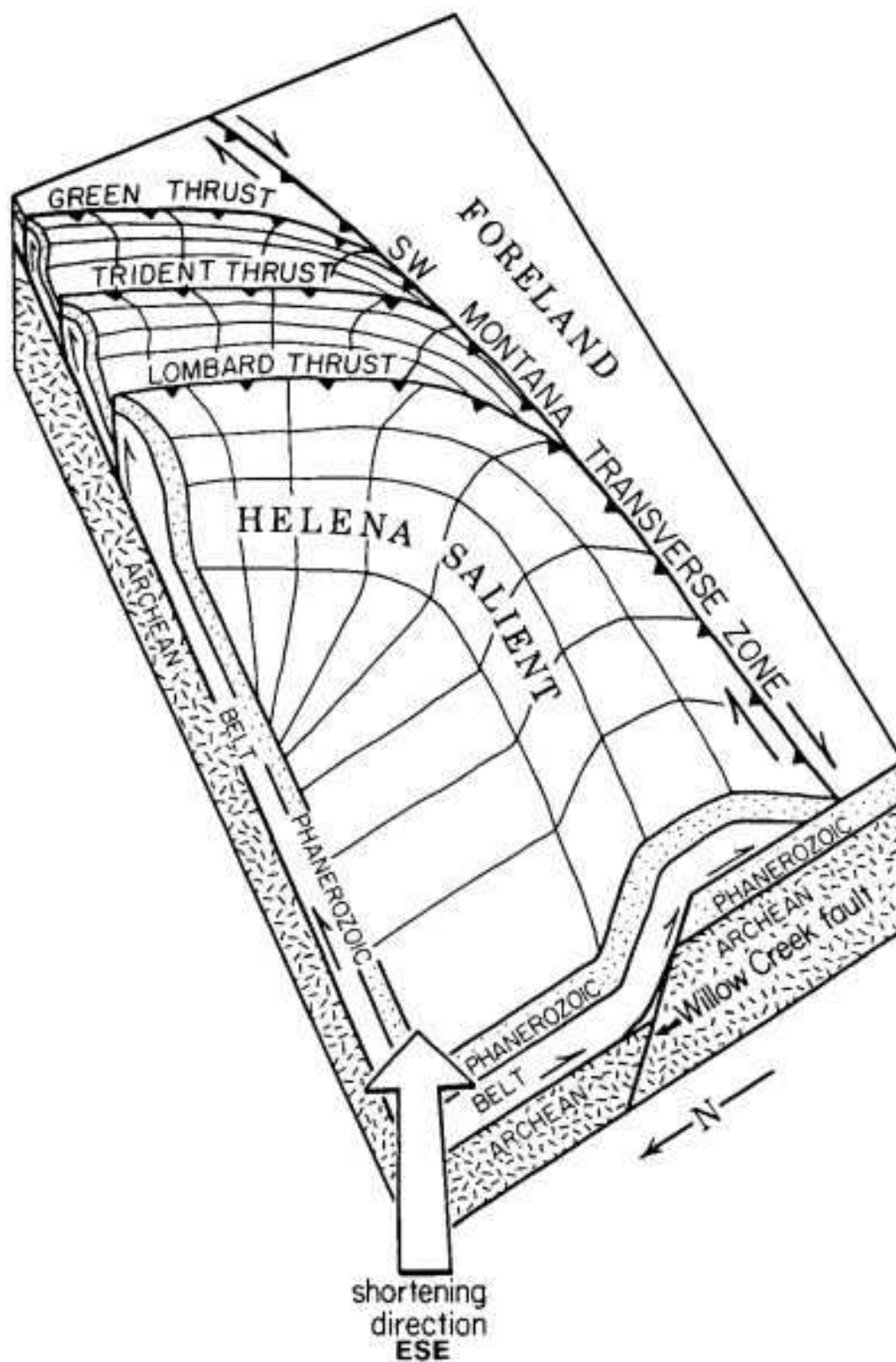


Figure 1.7 Interpretive structural block diagram of Sears (1988) showing the ramping of the Helena Salient over strata to the south.

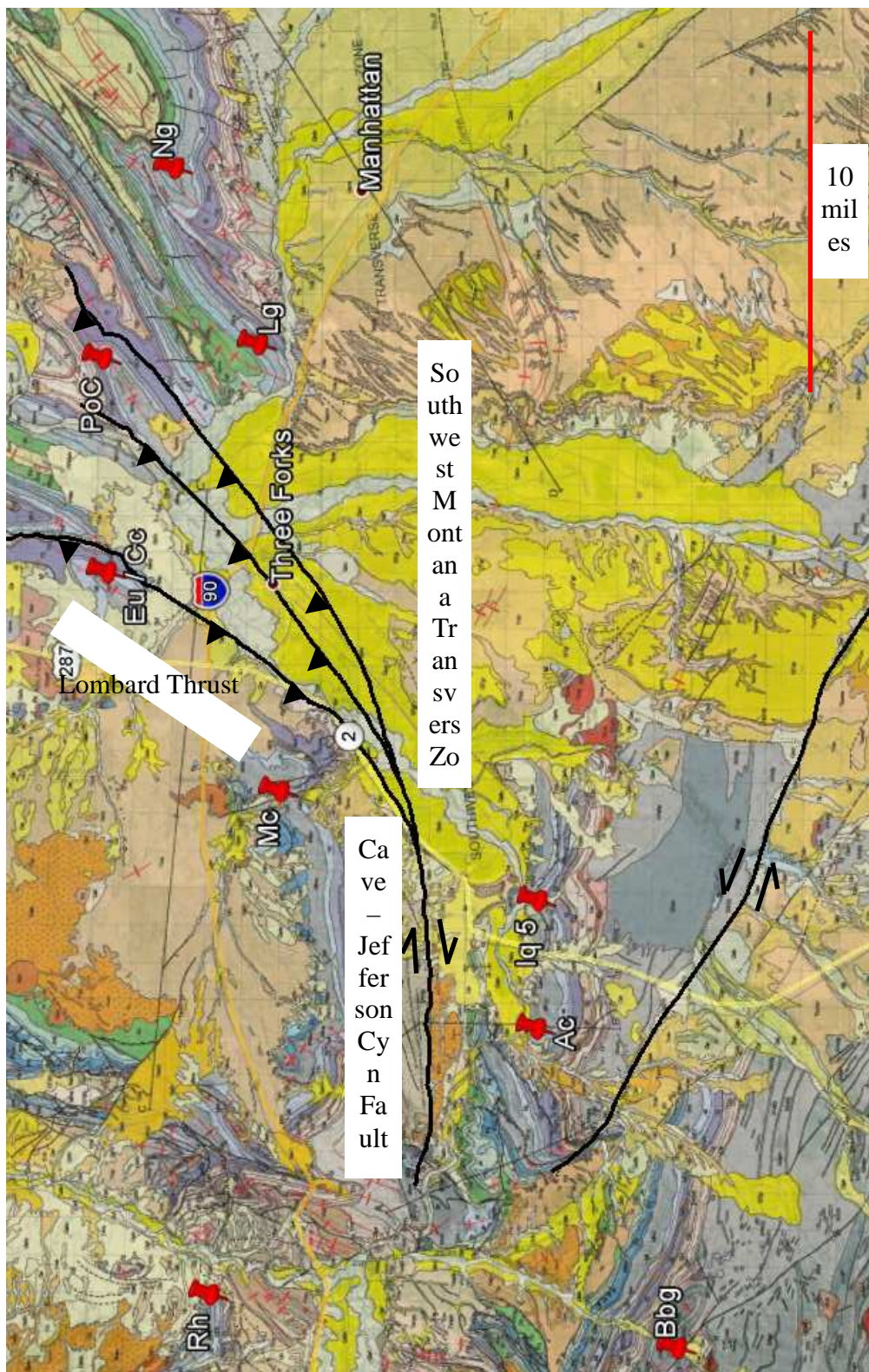


Figure 1.8 Geologic map of the Bozeman Quad (Vuke et al., 2014) with key structural features and studied outcrop sections labeled.

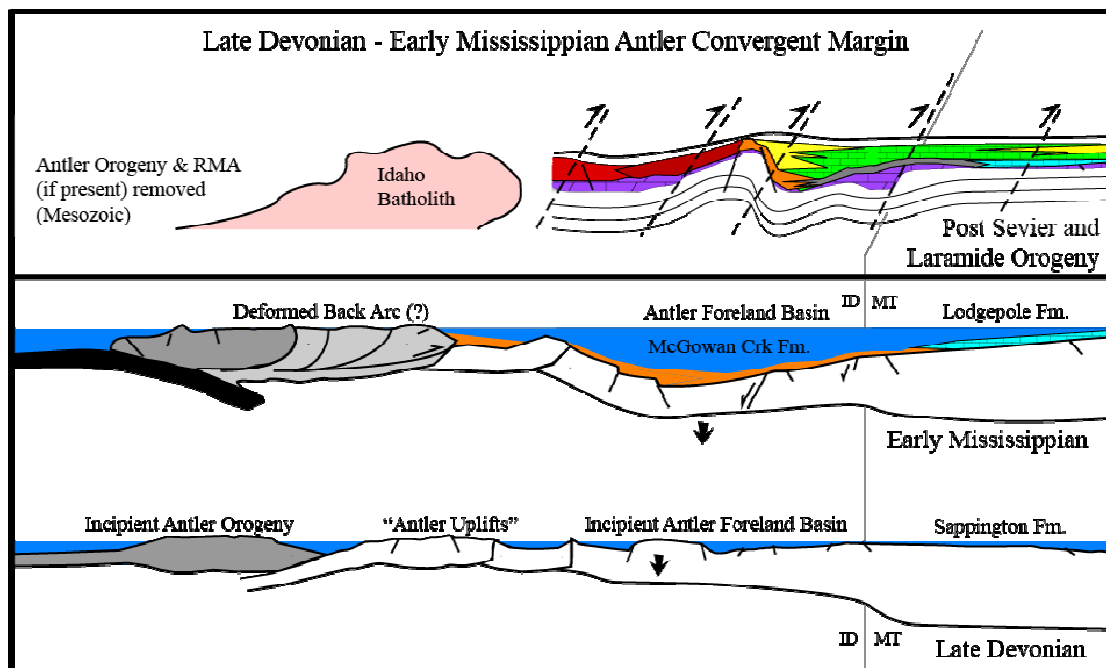


Figure 1.9 Illustration of the Late Devonian-Early Mississippian Antler Convergent Margin (modified from Grader, 2005). Bottom diagram illustrates incipient development of the Antler Foreland Basin during Sappington deposition in the Late Devonian. Middle diagram illustrates full-development of the Antler Foreland Basin during Lodgepole deposition in the Early Mississippian. Upper diagram illustrates post Sevier and Laramide Orogeny deformation of Paleozoic strata. (Color key: blue=water, gray=allochthonous rocks, pink=Idaho Batholith, orange=McGowan Creek Formation (flysch) / distal ramp Lodgepole Formation, light blue=Lodgepole Formation, green/purple/yellow/red=post Lodgepole Formation Paleozoic rocks)

2. Methods

Outcrop Analysis

Nineteen outcrops were visited over multiple weeks in Fall 2013, Spring 2014, and Fall 2014. Of the nineteen outcrops, fourteen stratigraphic sections were created (see Appendix). Outcrop analysis entailed measuring stratigraphic sections, describing lithologic units, identifying sedimentary structures, identifying ichnogenera assemblages, photographic documentation, and sample collection. Sections were measured using a Jacob's Staff, Brunton Compass, and measuring tape. Grain sizes were first described in the field with a hand lens and grain size card. The 2009 GSA 'Geological Rock Color Chart' was used in this study for rock color descriptions.

Laboratory work included sawing hand samples and re-describing using a hand binocular microscope. Thin section work was conducted on Sappington Units 1-6 (Figure 1.2 Sappington stratigraphy with stratigraphic unit and lithofacies classifications) from which exact grain sizes, sorting, and rounding were derived. Sedimentary structures and ichnogenera assemblages were described and photographed. The Pemberton et al. (2011) 'Trace Fossil Atlas' was used towards identification of the ichnogenera, and MacEachern (2014) 'Integrated Ichnology and Sedimentology' aided the identification of sedimentary structures.

3. Results and Interpretations

Stratigraphic Units & Associated Lithofacies

The Sappington Formation is subdivided into 3 latest Devonian-Early Mississippian members (Lower, Middle, and Upper) (Figure 1.2) that represent approximate time and lithostratigraphic units. This three member terminology matches Bakken terminology (Smith et al., 1995), but differs with early Sappington terminology that, 1) included the Sappington as a member of the Three Forks Formation (Sandberg, 1962), and 2) associated the Upper Member with the upper tongue of the Cottonwood Canyon Formation of Wyoming (Sandberg and Klapper, 1967). The Lower and Middle Member Sappington units are approximately equivalent to the Alberta Exshaw Formation and the Upper Member is equivalent to the Banff Formation. These major Sappington units share clear facies analogue and time correlatively with the Bakken (Sandberg and MacQueen, 1970). With the exception that the Bakken Middle Member likely extends into Mississippian time (Smith et al., 1995), and is correlative with a major unconformity in western Montana between the Middle and Upper Members of the Sappington. Overall, these major stratigraphic units seen in the Sappington, Exshaw, and Bakken Formations appear to be mostly time correlative, yet are also time-transgressive (Bustin and Smith, 2000).

The three members of the Sappington can be further divided into six differentiable lithostratigraphic units (U1-U6) (Figure 1.2). These were defined by Gutschick et al. (1962) and Sandberg (1965) and are very useful. However, as one departs the Three Forks area the units become less easily differentiated. Nineteen lithofacies are identified and expanded in this work, with nomenclature that indicates which stratigraphic unit the lithofacies is classified under (1A, 1B, 3A, 3B, etc.) (Figure 1.2). The majority of the grain sizes in the Sappington are coarse-silt to very fine-grained sand.

Like the Exshaw (Richards et al., 1999), Sappington units in the western part of the field area are interpreted as 3rd-order transgressive and regressive depositional cycles. The Upper Member of the Sappington is interpreted as a very thin, laterally discontinuous, shallowing-upward, and unconformity bound sequence, and is included here in the Sappington as U6. Technically U6 is not mappable, often being reduced to a residual unit that thins locally and regionally to a sandstone comprised of phosphatic fish parts. U6 has been associated with the Cottonwood Canyon Formation and the Banff Formation.

Unit 1

Unit 1 is a distinct stratigraphic unit that is situated unconformably between the Three Forks Formation below and Unit 2 of the Sappington Formation above. U1 is composed of four lithofacies (1A, 1B, 1C, 1D) all versions of shale (Figure 3.1). U1 has a thickness range from 0-46.8 ft. and an average thickness of 10.8 ft. In the Three Forks area reaching the Bridger Mountains mean thicknesses are 7 ft. with local anomalies such as the Logan Gulch section where very thin black shale (.3 ft.) appears to fill relief cut into the Trident Limestone. Towards the Sappington Basin margins to the NE and SE basal black shales are very thin to locally missing.

Lithofacies 1A

Lithofacies 1A (Figure 3.1 A) is a black fissile shale with interbeds of bedded chert (avg. .5-4 in. thick). Thin section (Figure 3.2 A) analysis of lithofacies 1A shale show calcite filled fractures (Figure 3.2 A), microfossils, and silt sized grain replaced by chert. Thin section (Figure 3.2 B) analysis of the bedded chert shows unidentifiable tests of siliceous organisms, which are the source of the silica comprising the bedded chert.

Lithofacies 1B

Lithofacies 1B (Figure 3.1 C) is a brownish black carbonaceous mudstone with a contorted glossy texture and slickensides on bedding planes. At some locations 1B appears more blocky and coaly.

Lithofacies 1C

Lithofacies 1C (Figure 3.1 E) is a laminated grayish black fossiliferous mudstone. Observed fossils include conchostracans (Figure 3.1 E & Figure 3.3 B) and echinoderms (Figure 3.3 B). Additional fauna reported from other studies includes brachiopods, conodonts, and plant spores (Gutschick, 1962), as well as Tasmanities (Achauer, 1959). The shale has been silicified and fractures conchoidally between bedding planes.

Lithofacies 1D

Lithofacies 1D (Figure 3.1 F) is a pale green calcareous highly fossiliferous mudstone. Observed fossils include brachiopods and bivalves. Additional fauna reported from other studies includes snails and crinoid stems (Gutschick, 1962).

Unit 2

Unit 2 is an oncolitic silty wackestone that is situated unconformably above U1 of the Sappington and conformably below U3 of the Sappington. The U2-U3 contact is highly gradational complicating accurate thickness measurements for the unit. U2 is comprised of one lithofacies.

Lithofacies 2

Unit 2 (Figure 3.4) is composed of lithofacies 2, which is a light bluish grayish silty wackestone (limestone). Allochems include broken assemblages of oncolites, brachiopods, and crinoid stems. The oncolites are composed of amalgamated algal coatings around a nucleus typically composed of a broken brachiopod (Figure 3.4 A). In addition, lithofacies 2 has a strong siliciclastic presence of silt-sized quartz.

Unit 3

Unit 3 is a calcareous siltstone that is situated conformably between U2 of the Sappington below and U4 of the Sappington above. The highly gradational nature of the U2-U3 contact presented difficulties in measuring accurate thicknesses of U3. The U2-U3 succession has a thickness range of 13.1-34.4 ft. and an average thickness of 26.4 ft. U3 is comprised of 3 lithofacies (3A, 3B, 3C).

Lithofacies 3A

Lithofacies 3A (Figure 3.5 A) is a moderately sorted, subrounded, coarse moderate orange siltstone predominantly composed of quartz clasts. Lithofacies 3A is characterized by a pinching and swelling texture created by a series of stacked wave ripples. Lithofacies 3A has an ichnogenera assemblage of *Teichichnus*, *Planolites*, and *Thalassanoides* (Figure 3.6).

Lithofacies 3B

Lithofacies 3B (Figure 3.5 B) is characterized by a heterolithic sediment assemblage of argillaceous brownish black material and grayish yellow coarse siltstone, lack of distinct sedimentary structures due to prevalent bioturbation (BI 4), and an ichnogenera assemblage of *Nereites*, *Planolites*, *Scolicia* (Figure 3.7).

Lithofacies 3C

Lithofacies 3C (Figure 3.5 C & D) is a moderate yellow calcareous fossiliferous (brachiopods) coarse siltstone. Brachiopods are whole to partially fragmented. Lithofacies 3C has a much higher carbonate content than lithofacies 3B and 3C.

Unit 4

Unit 4 is an argillaceous calcareous siltstone that is situated conformably between U3 of the Sappington below and U5 of the Sappington above. U4 has a thickness range of 2.3-32.8 ft. and an average thickness of 13.6 ft. Unit 4 has significant lateral lithologic, sedimentary structure, and ichnological variability and is subdivided into 3 lithofacies (4A, 4B, and 4C).

Lithofacies 4A

Lithofacies 4A (Figure 3.8 A) has lenticular heterolithically bedded dusky blue mud and starved moderate yellow silt ripples, soft sediment deformation (Figure 3.9 B), and an ichnogenera assemblage (BI 2) of *Chondrites*, *Arenicolites*, *Planolites* (Figure 3.9). The type of *Arenicolites* found in the Sappington is a rare form originally identified as *Bifungites* (Figure 3.10) (Gutschick and Lamborn, 1975).

Lithofacies 4B

Lithofacies 4B (Figure 3.8 B) is characterized by wavy heterolithic bedded grayish blue green mud and moderate yellow silt with combined flow ripples and a low diversity ichnogenera assemblage dominated by *Arenicolites* (*Bifungites*) (Figure 3.10).

Lithofacies 4C

Lithofacies 4C (Figure 3.8 C & D) is characterized by flaser heterolithic bedded dark greenish gray mud and moderate yellow sand with combined flow ripples, tempestites vertically grading from basal large scale wave ripples at the base to parallel laminations to small scale wave ripples at the top (Figure 3.11), ball and pillow soft sediment deformation (Figure 3.11) on the underside of the tempestites, and an ichnogenera (BI 2) assemblage of *Arenicolites* (*Bifungites*), *Chondrites*, *Macaronichnus*, *Planolites* (Figure 3.11).

Unit 5

Unit 5 is a dark yellowish orange well-sorted and subrounded, lower very fine-grained sandstone/coarse siltstone that is situated conformably between U4 of the Sappington below and unconformably between U6 of the Sappington above. U5 has a thickness range of 0-33.5 ft. and an average thickness of 23.8 ft. Unit 5 is comprised of four lithofacies 5A, 5B, 5C, 5D (Figure 3.12).

Lithofacies 5A

Lithofacies 5A (Figure 3.12 A) is a coarse siltstone characterized by interbeds of highly bioturbated sedimentary structure-destroying sand punctuated with parallel laminations and aggrading wave-rippled tempestites.

Lithofacies 5B

Lithofacies 5B (Figure 3.12 B) is characterized by various ripple forms including current ripples, aggrading current ripples, wave ripples, and combined flow ripples. Bedding planes of lithofacies 5B are occasionally found with the trace fossil *Lockeia* (Figure 3.13).

Lithofacies 5C

Lithofacies 5C (Figure 3.12 C) is comprised of heavily bioturbated sedimentary structure-destroying sand with grayish blue wave-rippled sheet and lensoidal geometry tempestites carrying various carbonate debris (i.e., crinoid stems).

Lithofacies 5D

Lithofacies 5D (Figure 3.12 D) is characterized by planar cross-bedding and calcified nodules in some locales.

Unit 6

Unit 6 is a mix of various lithologies situated unconformably between U5 of the Sappington below and the Williston Basin-like Scallion Member of the Lodgepole above. U6 has a thickness range of 0-3.9 ft. and an average thickness of 2.2 ft. Unit 6 is divided into four lithofacies 6A, 6B, 6C, 6D.

Lithofacies 6A

Lithofacies 6A (Figure 3.14 A) is a medium dark gray conglomeratic lag composed of phosphatic fish debris.

Lithofacies 6B

Lithofacies 6B (Figure 3.14 B) is grayish black laminated argillaceous siltstone.

Lithofacies 6C

Lithofacies 6C (Figure 3.14 C) is a dark gray bioturbated laminated siltstone (BI 3) with an ichnogenera assemblage that includes *Chondrites(?)* / *Phycosiphon(?)*, *Planolites*, *Teichichnus* (Figure 3.15).

Lithofacies 6D

Lithofacies 6D (Figure 3.14 D) is a moderate olive brown mixed carbonate clastic with an ichnogenera assemblage that includes *Skolithos* (Figure 3.16).

Figures

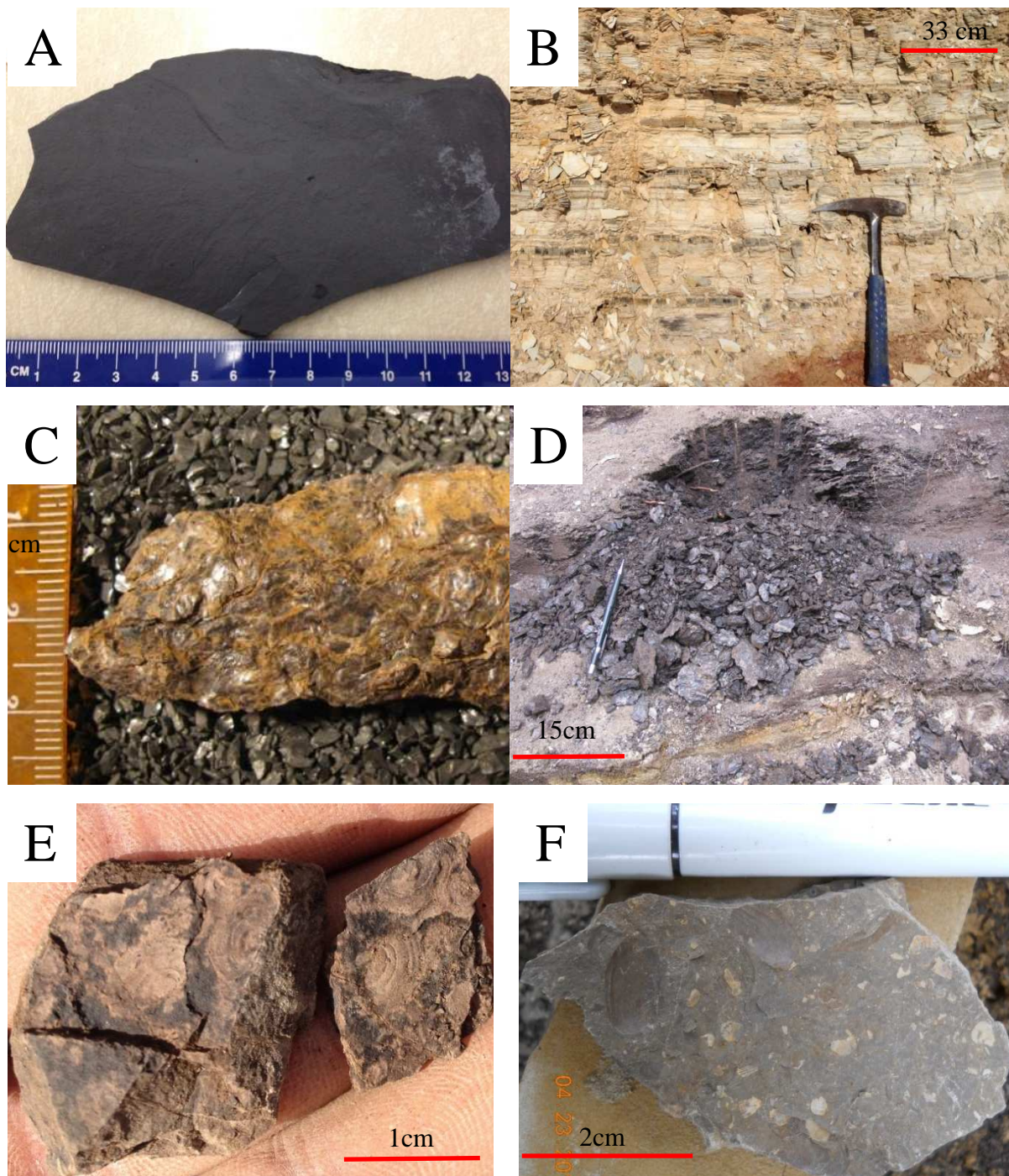


Figure 3.1 Unit 1 lithofacies A) lithofacies 1A hand sample; B) lithofacies 1A outcrop; C) lithofacies 1B hand sample; D) lithofacies 1B outcrop (pen = 14cm); E) lithofacies 1C hand sample; F) lithofacies 1D hand sample

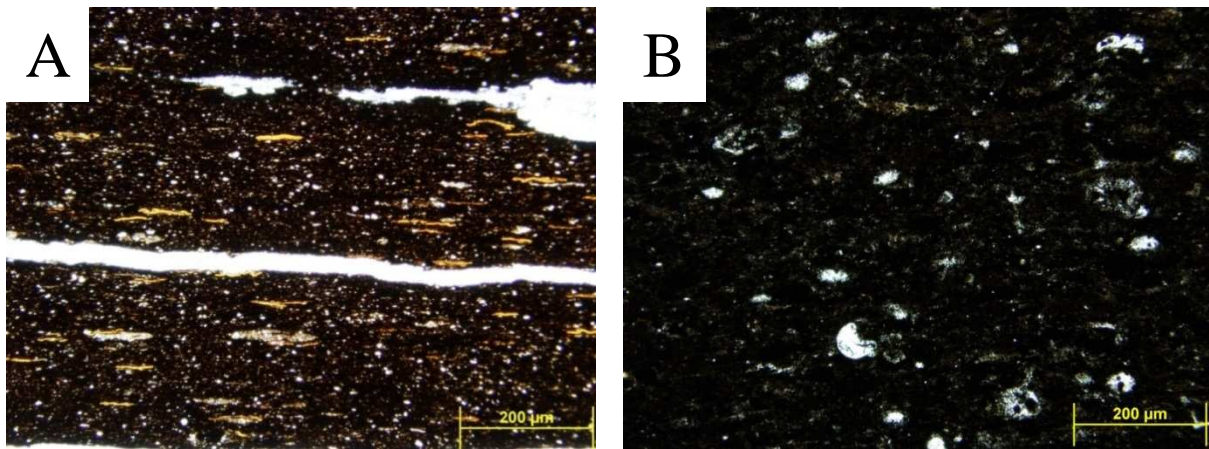


Figure 3.2 Lithofacies 1A thin sections A) shale; B) bedded chert

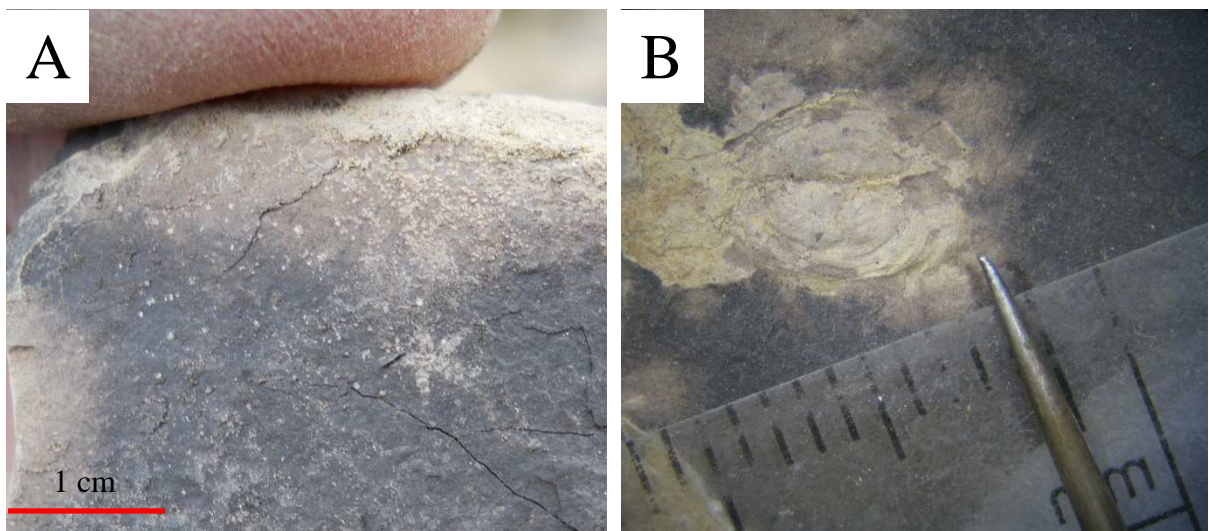


Figure 3.3 Lithofacies 1C fauna A) brittle star; B) conchostracans

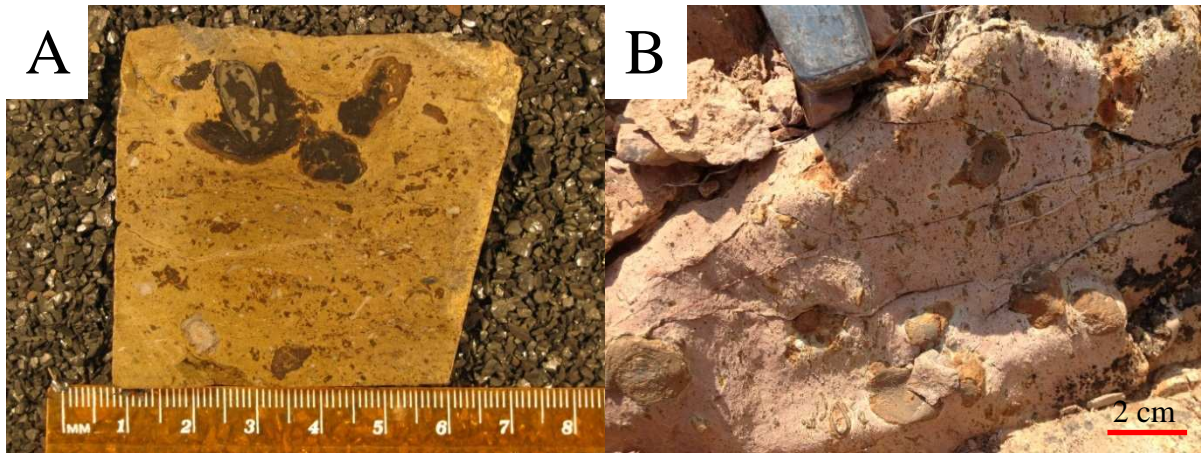


Figure 3.4 Lithofacies 2 A) hand sample cross section view of oncolite with brachiopod nucleus; B) outcrop

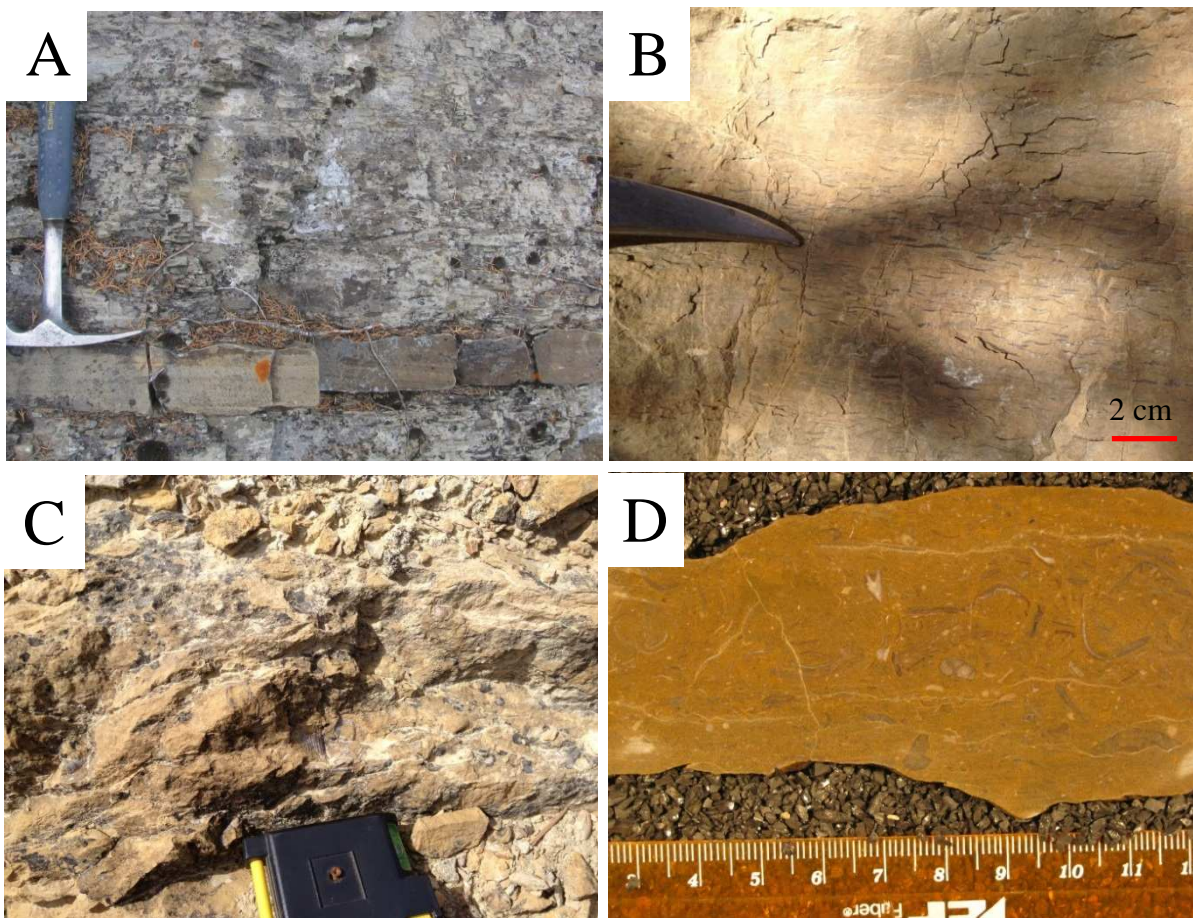


Figure 3.5 Unit 3 lithofacies A) lithofacies 3A outcrop (rock hammer = 33 cm); B) lithofacies 3B outcrop; C) lithofacies 3C outcrop; D) lithofacies 3C hand sample

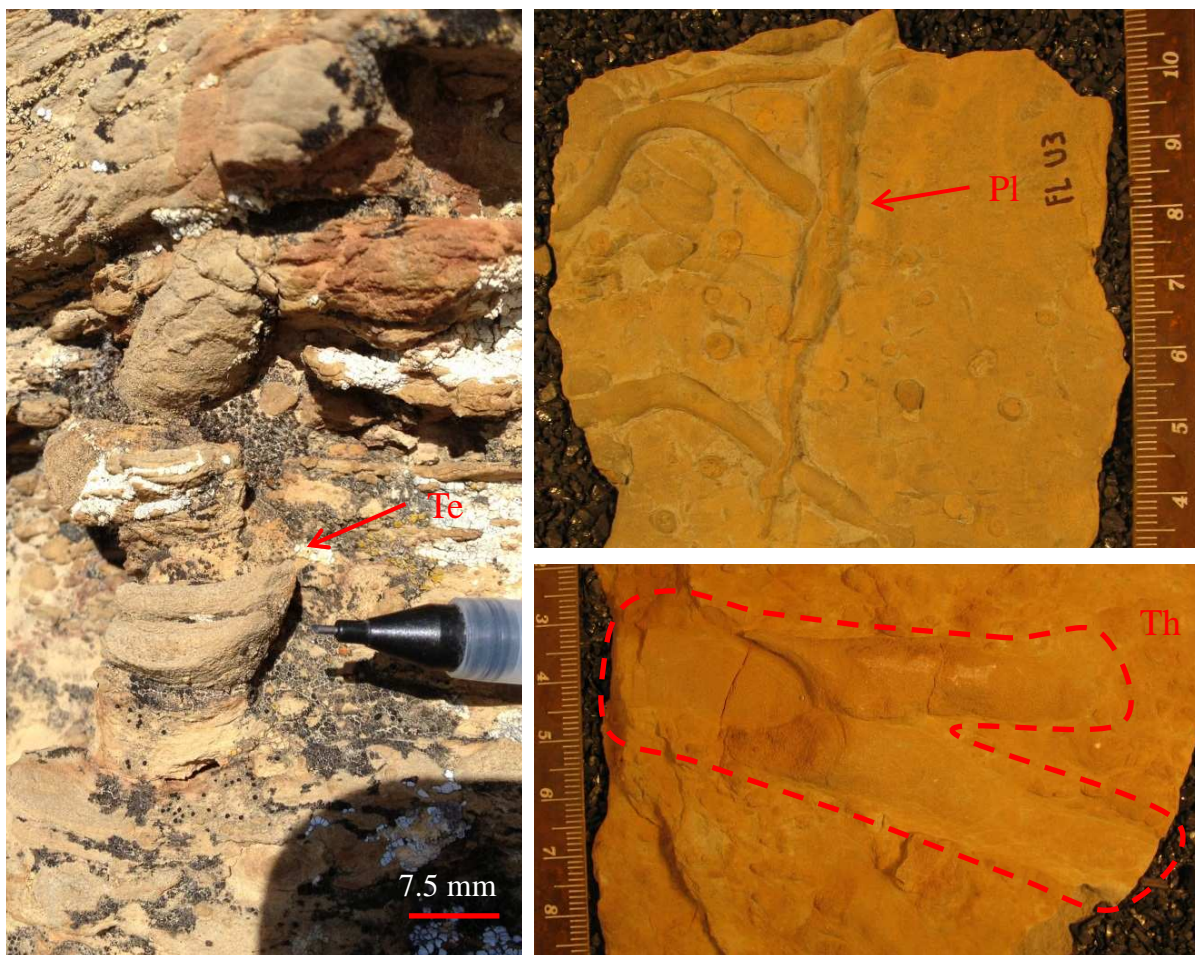


Figure 3.6 Lithofacies 3A ichnogenera assemblage (Pl=*Planolites*, Te=*Teichichnus*, Th=*Thalassanoides*).



Figure 3.7 Lithofacies 3B ichnogenera assemblage (Ne=*Nereites*, Pl=*Planolites*, Sc=*Scolicia*).

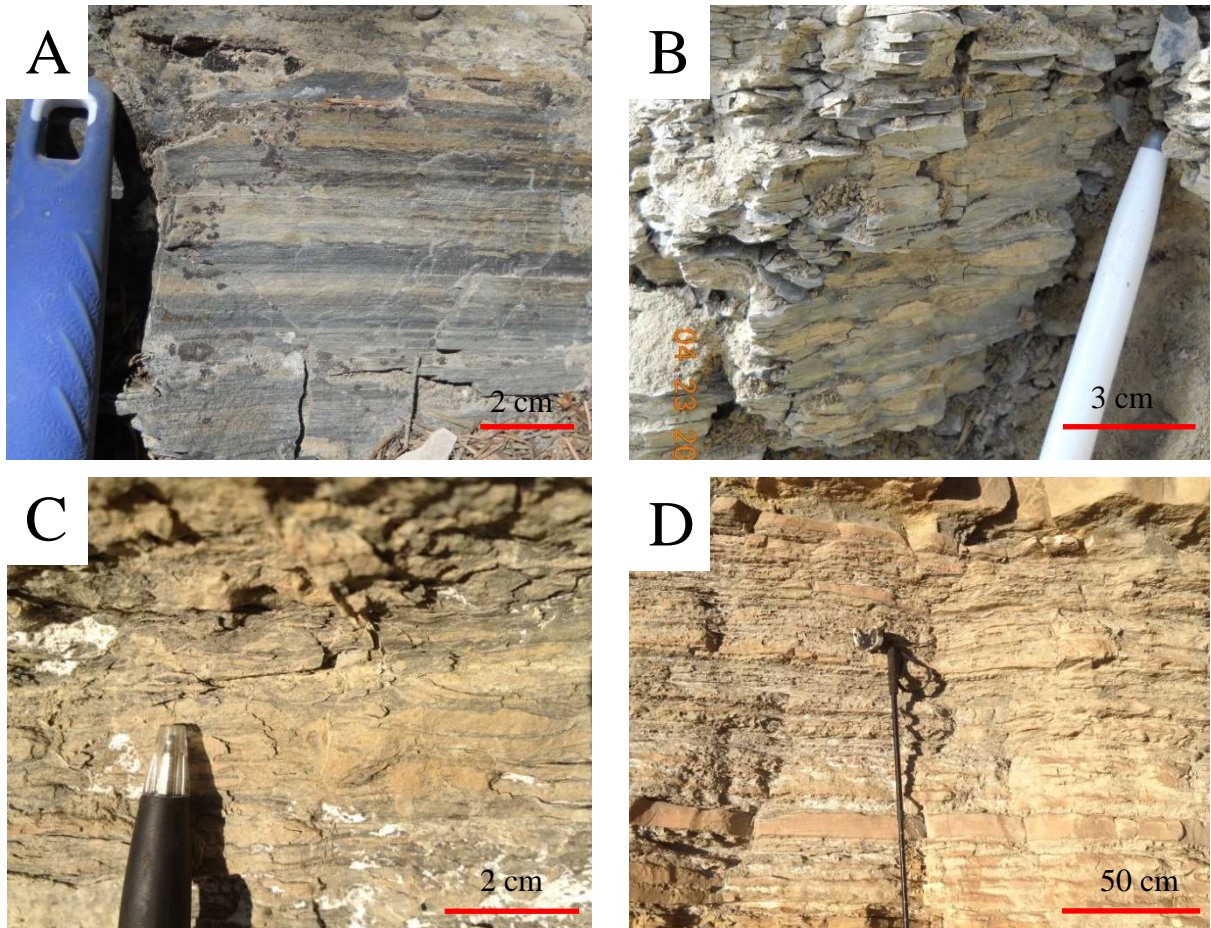


Figure 3.8 Unit 4 lithofacies A) lithofacies 4A outcrop; B) lithofacies 4B outcrop; C) lithofacies 4C outcrop; D) lithofacies 4C outcrop

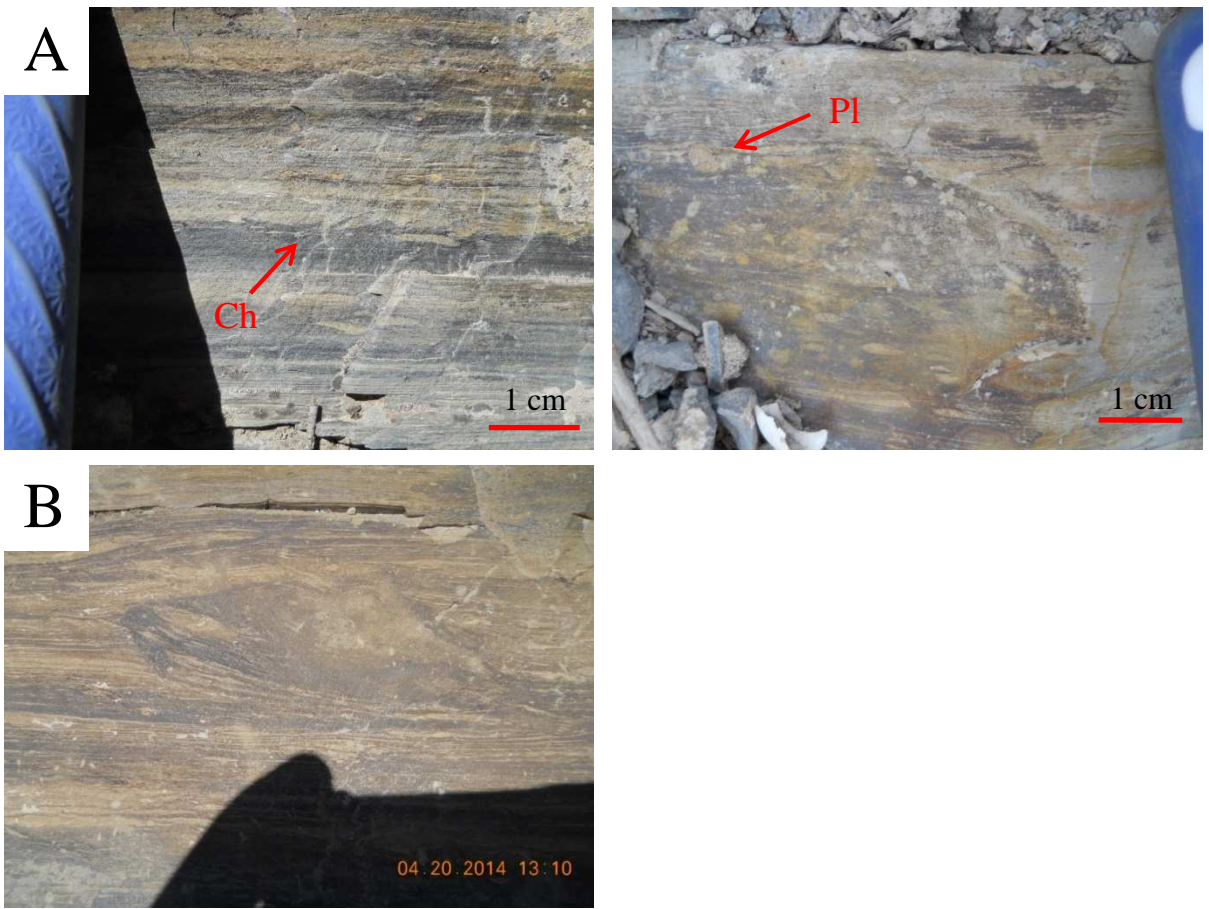


Figure 3.9 Lithofacies 4A (Ch=Chondrites, Pl=Planolites) A) lenticular bedding and starved ripples; B) convolute bedding (soft sediment deformation)

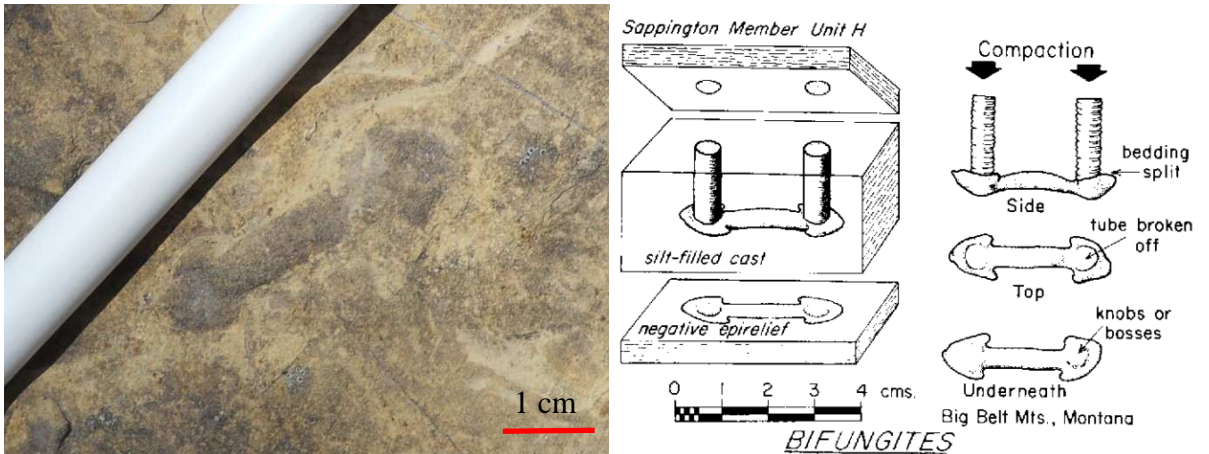
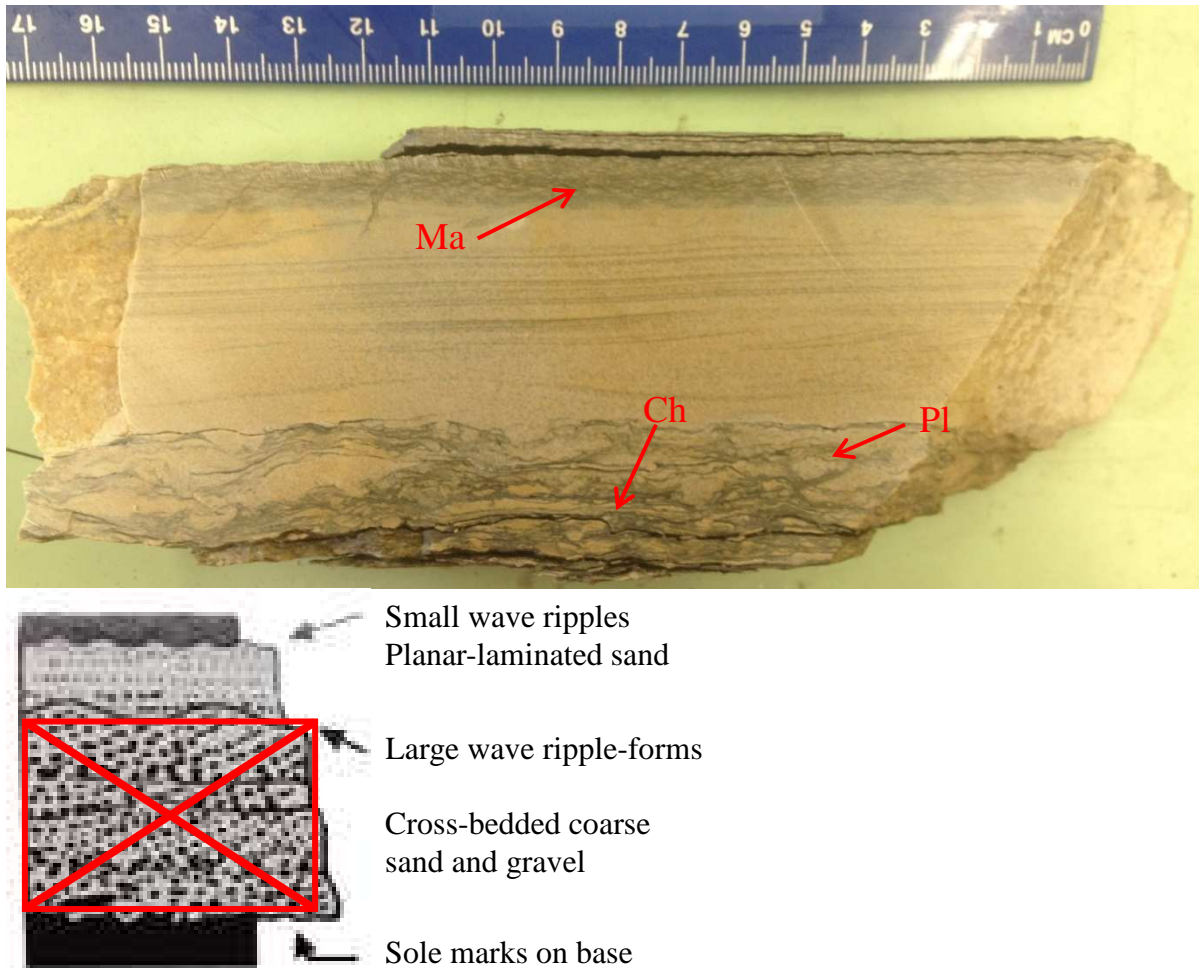


Figure 3.10 Left) picture of *Arenicolites* (*Bifungites*) ichnogenera on bedding plane of lithofacies 4A; Right) illustration of *Bifungites* from Gutschick and Lomborn (1975).



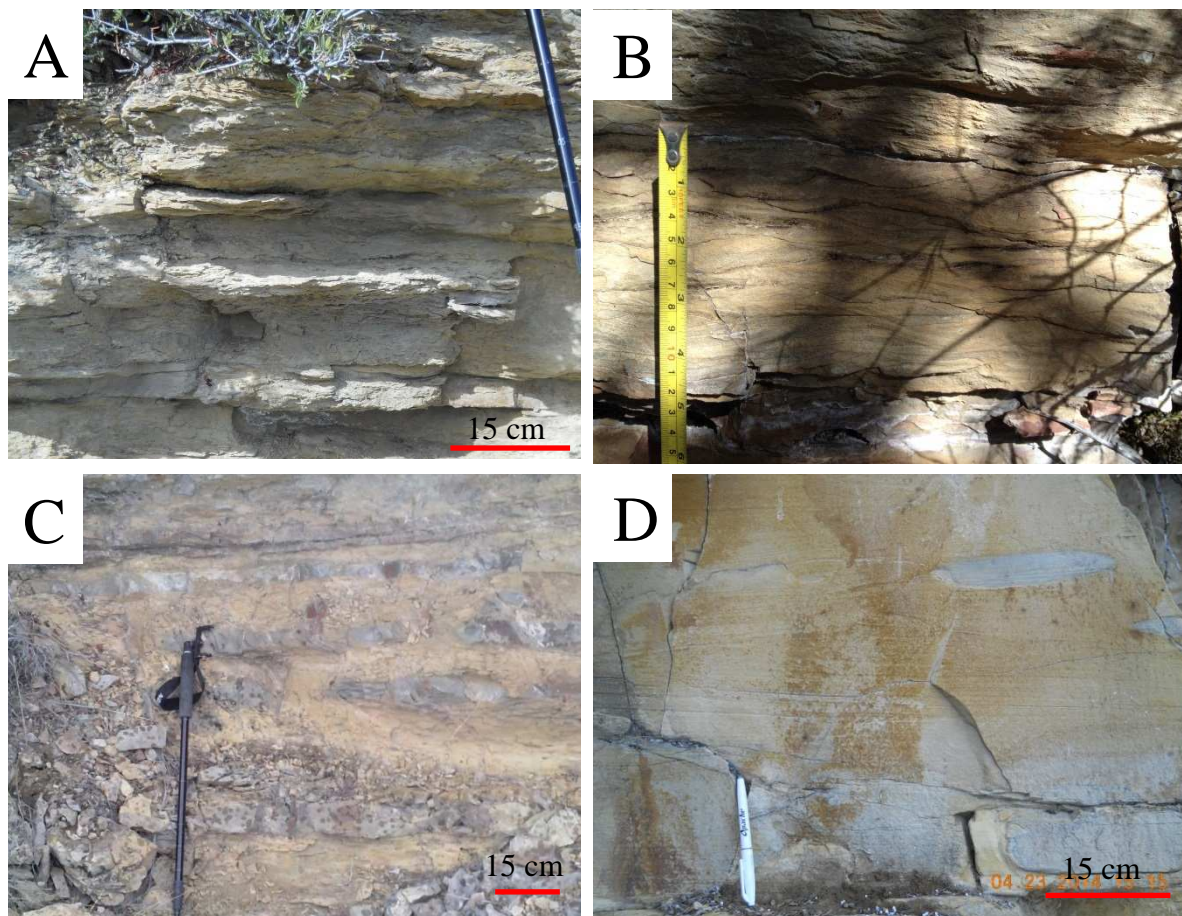


Figure 3.12 Unit 5 lithofacies A) lithofacies 5A outcrop; B) lithofacies 5B outcrop; C) lithofacies 5C outcrop; D) lithofacies 5D outcrop

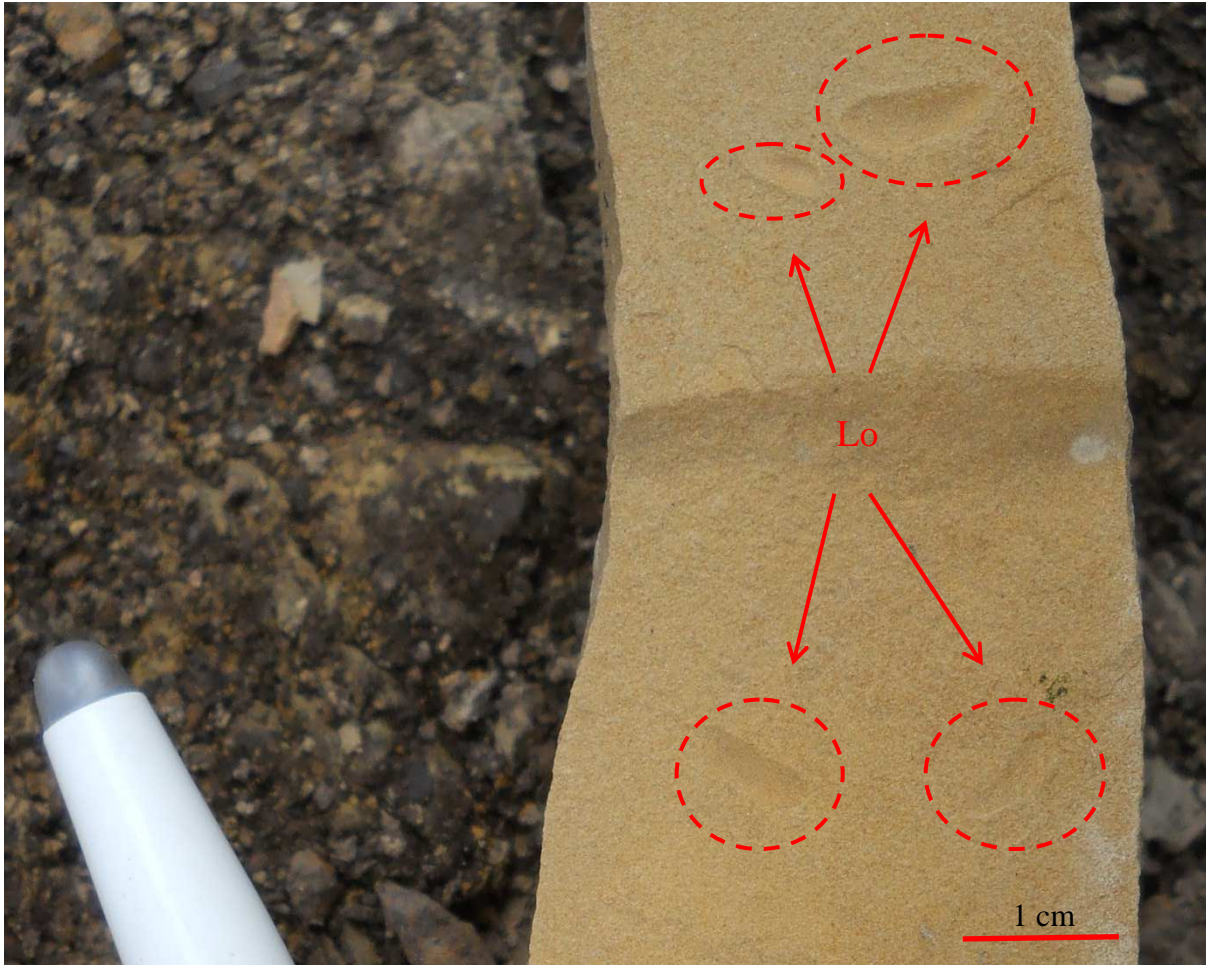


Figure 3.13 Lithofacies 5B bedding plane with *Lockeia* (Lo) trace fossil

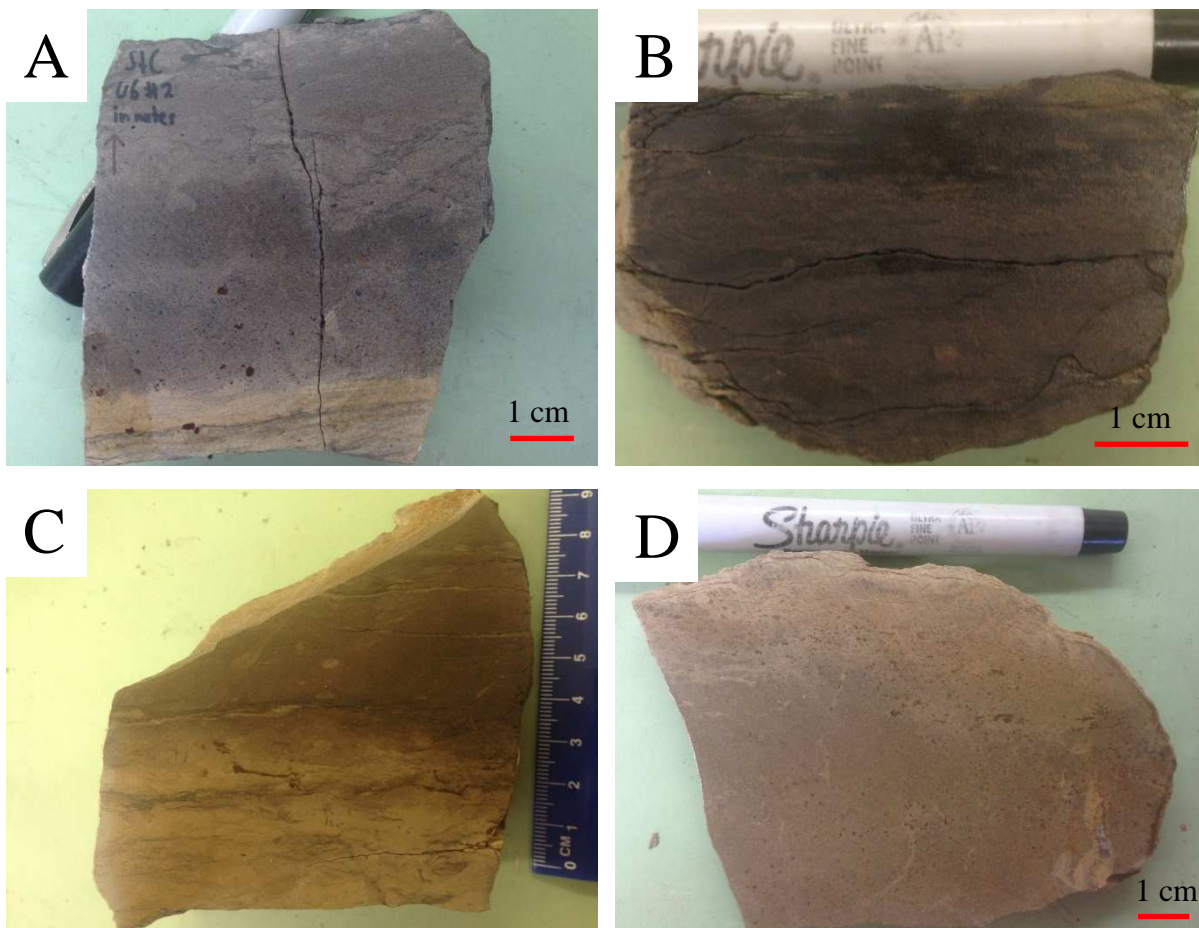


Figure 3.14 Unit 6 lithofacies A) lithofacies 6A hand sample; B) lithofacies 6B hand sample; C) lithofacies 6C hand sample; D) lithofacies 6D hand sample

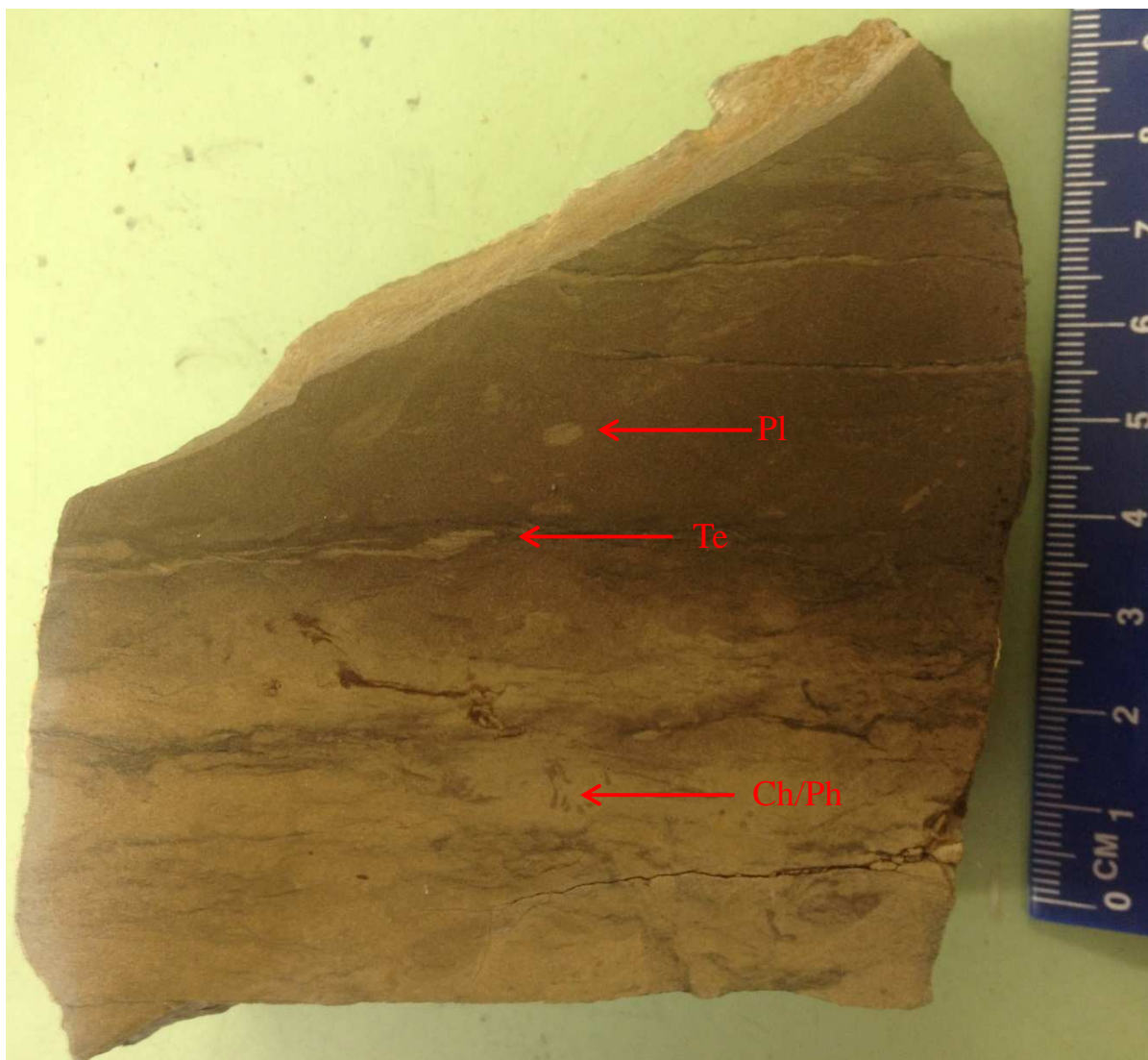


Figure 3.15 Lithofacies 6C (Ch/Ph=Chondrites / Phycosiphon, Pl=Planolites, Te=Teichichnus)



Figure 3.16 Lithofacies 6D (Sk=Skolithos)

Biostratigraphy

Previous conodont biostratigraphic dating of the Sappington Formation was done by multiple studies in the 1950's-70's (Knechtel and Hass, 1953; Sandberg and Klapper, 1967; Sandberg et al., 1972). Currently a conodont study is in progress at the University of Idaho by Dr. Peter E. Isaacson. In addition, there is currently a palynological study being conducted on the Sappington by Audrey Warren at the University of Idaho and Mercedes di Pasquo at Laboratorio de Palinoestratigrafia of Argentina.

A Wheeler Diagram (Figure 3.17) was constructed using conodont results primarily from Sandberg et al. (1972), supplemented with preliminary conodont and palynology results from the University of Idaho. Biostratigraphy was not the main focus nor the objective of this project, but the establishment of a timeline of Sappington deposition complements the Sappington facies analysis and sequence stratigraphic framework of this study. An updated synthesis on the timeline of Sappington deposition was needed since 40 years and numerous additions and revisions to the global conodont zones have occurred since Sandberg et al. (1972).

Conodont Biostratigraphy

The first step in the synthesis was to correlate (Figure 3.18) the conodont zones of 1972 with today's conodont zones. Several papers (Sandberg et al., 1972; Dreesen et al., 1986; Becker et al., 2012; Davydov et al., 2012) were utilized to assemble the correlations shown in Figure 3.18. The correlation was facilitated by the 1-5 Sappington stratigraphic unit nomenclature shown by Sandberg (1965). Sandberg et al. (1972) dated conodonts from the Trident Member of the Three Forks Formation, Sappington Unit 1, Unit 2, Unit 3, Unit 5, and the overlying Lodgepole Formation (equivalent to Unit 6 in this paper). The results from that study are as follows (with their 2012 correlations in parentheses):

Trident member of the Three Forks Formation - *Scaphignathus subserratus* – *Pelekysgnathus inclinatus* (*Palmatolepis rugosa trachytera* and upper *Palmatolepis marginifera*)

- Unit 1 - *Polygnathus styriacus* (*Palmatolepis perlobata postera* and lower *Palmatolepis gracilis expansa*)
- Unit 2 - *Siphonodella praesulcata* (*Siphonodella praesulcata*)
- Unit 3 - *Siphonodella praesulcata* (*Siphonodella praesulcata*)
- Unit 4 - Barren

- Unit 5 - *Siphonodella praesulcata* (*Siphonodella praesulcata*)
- Cottonwood Canyon Member of the Lodgepole Formation (U6) - Lower *Siphonodella crenulata* (Upper *Siphonodella quadruplicata* – *Prognathus andersoni*) (Figure 3.18).

The absence of conodont zone *Spathognathodus costatus* marks an unconformity between Unit 1 and Unit 2 spanning ~1.5 my (Figure 3.17). Between Unit 5 and the Unit 6 there are two conodont zones missing (*Siphonodella sulcata* and *Siphonodella sandbergi* – *Siphonodella duplicata*) marking an unconformity spanning ~4 my (Figure 3.17).

Recent Conodont Biostratigraphy

A preliminary result from an ongoing study at the University of Idaho (P. Isaacson, pers. Commun., 2014) reveals *Siphonodella isosticha* (Figure 3.19) from the Scallion Member of the Lodgepole Formation. There are no conodont zones missing between the between Unit 6 and the Scallion Member of the Lodgepole Formation, yet the sharp lithologic contact between the units and the beveling of uppermost Unit 6 beneath the Scallion still indicates an unconformity. Further, Unit 5 has *Apatognathus varians*, among other taxa. Savoy and Harris (1993) show that *A. varians* occurs at the very latest Famennian, in the uppermost Costigan Member of the Palliser Formation in the Alberta Rockies. This confirms a Devonian age for Unit 5.

Palynomorph Biostratigraphy

Past conodont studies have not yielded results from Unit 4 of the Sappington although Unit 3 and Unit 5 are both *Siphonodella praesulcata* zone. It can be assumed that Unit 4 falls within *Siphonodella praesulcata* as well. Based on this assumption, placement of the Devonian-Mississippian boundary falls within the unconformity between Unit 5 and Unit 6. Encouraging preliminary results from an ongoing study with Sappington collaborators Audrey Warren at the University of Idaho and Mercedes di Pasquo at Laboratorio de Palinoestratigrafía of Diamante, Argentina have new implications for the placement of the Devonian-Mississippian boundary. *Retisopora lepidophyta* a cosmopolitan miospore index taxon for the latest Devonian was recovered from Unit 4.

Figures

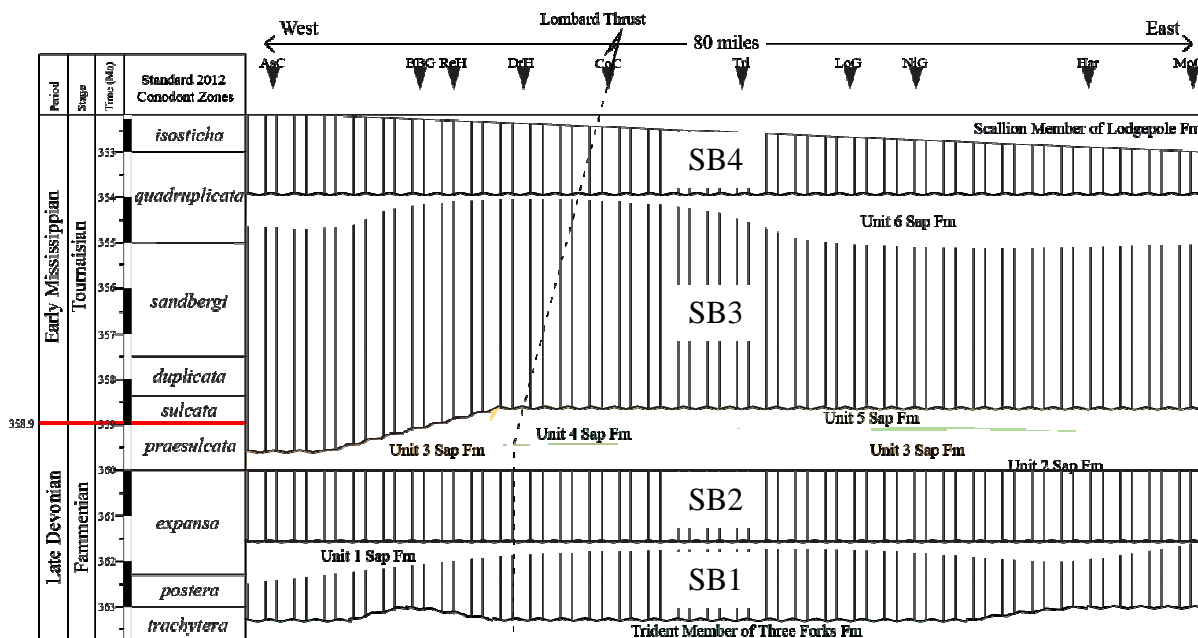


Figure 3.17 Wheeler Diagram of Sappington, upper Three Forks Fm., and lower Lodgepole Fm. showing temporal relationships of stratigraphic units, variation with location in the basin, and location of sequence boundaries (see Sequence Stratigraphic Framework section). (AsC=Ashbough Canyon, BBG=Brown Back Gulch, CoC=Copper City, DrH=Dry Hollow, Har=Hardscrabble, LoG=Logan Gulch, MoC=Moose Creek, NiG=Nixon Gulch, ReH=Red Hill, Tri=Trident).

Period	Stage	Age (Ma)	Standard 2012 Conodont Zones (Becker et al., 2012) & (Davydov et al., 2012)	Rocky Mountain and Great Basin Conodont Zone (Sandberg et al., 1972)
Mississippian	Toumaesian	350	<i>Gnathodus typicus</i> - <i>Siphonodella isosticha</i>	<i>Upper Siphonodella</i> <i>crenulata</i>
		351		
		352		
		353	<i>Upper Siphonodella</i> <i>quadrifidata</i> - <i>Prognathus andersoni</i>	<i>Lower Siphonodella</i> <i>crenulata</i>
		354		
		355	<i>Siphonodella sandbergi</i> - <i>Panognathus andersoni</i>	<i>Siphonodella</i> <i>sandbergi</i> - <i>Siphonodella</i> <i>duplicata</i>
		356		
		357		
		358	<i>Siphonodella</i> <i>duplicata</i>	<i>Siphonodella</i> <i>sulcata</i>
		358	<i>Siphonodella</i> <i>sulcata</i>	
358.9	359	<i>Siphonodella</i> <i>praesulcata</i>	<i>Siphonodella</i> <i>praesulcata</i>	
Devonian	Strunian	360	<i>Palmatolepis</i> <i>gracilis expansa</i>	<i>Spathognathodus</i> <i>castatus</i>
		361		
		362	<i>Palmatolepis</i> <i>perlobata postera</i>	<i>Polygnathus styriacus</i>
		363		
	Famennian	364	<i>Palmatolepis</i> <i>rugosa trachytera</i>	<i>Scaphignathus</i> <i>subserriatus</i> - <i>Pelekysgnathus</i> <i>inclinatus</i>
		364	<i>Palmatolepis</i> <i>marginiifera</i>	
		365	<i>Palmatolepis</i> <i>marginifera</i>	<i>Palmatolepis</i> <i>quadrantodiosa</i>

Figure 3.18 Chart showing correlation between past conodont zones and present conodont zones (Sandberg et al., 1972; Becker et al., 2012; Davydov et al., 2012)



Figure 3.19 Picture of *Isosticha* conodont from Scallion Member of Lodgepole Formation at Lewis and Clark Caverns section

Drivers for Sappington Deposition

Deciphering the accommodation effects in a basin of eustasy-driven base level changes from tectonic-driven base level changes is generally a function of scale (Robin et al., 1998). Eustatic driven base level changes can be correlated globally, while tectonic-driven base level changes are localized within a specific basin.

Eustasy is the proposed driving mechanism responsible for periods of Sappington deposition and non-deposition (unconformities) in the Sappington Basin driven by Gondwana glaciation in the Late Devonian-Early Mississippian. Biostratigraphic dating of the Sappington (Knechtel and Hass, 1953; Sandberg and Klapper, 1967; Sandberg et al., 1972; P. Isaacson, pers. Commun., 2014; A. Warren, pers. Commun., 2014) and Bakken (Thrasher, 1985; Huber, 1986; Richards and Higgins, 1988; Richards, 1989; Karma, 1991) indicate correlation of unconformities within both formations (Figure 4.3). These unconformities correspond to periods of global sea-level fall in the Late Devonian-Early Mississippian as outlined in the Paleozoic sea-level curve (Figure 3.44) of Haq and Schutter (2008).

Lower magnitude base level changes in the Sappington Basin associated with differential uplift and subsidence from Antler tectonism (see Tectonic History for further discussion), in conjunction with low-magnitude sea-level changes are the mechanisms responsible for the vertical and lateral facies heterogeneity of the Sappington. Regionally, stratigraphic units of the Sappington and Bakken appear similar. However, discrepancies in lithofacies character exist between the Sappington and Bakken, as well as within the Sappington in the study area of the Sappington Basin. These differences are proposed to be a function of differential tectonism in the two basins.

The proposed mechanisms for the abundance of organic preservation observed in the Lower and Upper Members of the Sappington are a combination of transgression and eutrophication. Eutrophication (see Paleoclimate Setting for further discussion) resulted from the upwelling of deep nutrient-rich bottom waters (Caplan and Bustin, 1999) and/or the inundation of bottom water environments with plant matter (Algeo and Scheckler, 1998) from Late Devonian land plant diversification.

Facies Analysis

The depositional center for the Sappington Formation was the Sappington Basin of the greater Central Montana Trough (CMT) (**Error! Reference source not found.**Figure 1.5), a paleotopographic low that formed along the margins of a west-east-oriented reactivated Precambrian aulacogen (Maughan, 1989). The Sappington Basin was a low-accommodation intracratonic shelfal basin that did not support substantial water depths. This low-accommodation interpretation of the Sappington Basin is supported by low-accommodation depositional systems, several unconformities in a relatively short time interval, and aggradation / poorly developed progradation. The basin could have resembled a flooded river valley type embayment with Sappington deposition representing valley fill.

The lithofacies of the Sappington, with the exception of lithofacies 1A, do not show a true “deep water” offshore environment. The shallow paleoenvironments had periodic anoxic events created by a combination of eutrophication and transgression. This shallow water, low-accommodation interpretation for the Sappington Basin suggests that average to above average eustatic fluctuations were responsible for the abundance of unconformities in such a short time frame. Interpretation of the Sappington Basin as a deep subsiding basin would require significantly above average, high amplitude, short term sea-level fluctuations (based on the sea-level curve of Haq and Schutter, 2008). A west to east cross-section (Figure 3.38) in the Sappington Basin shows aggradation / poorly developed progradation indicating the lack of a true “shelf break”. A shelf break would be expected in a classic deep subsiding basin, and thus the absence of a shelf break is further evidence of a shallow, low-accommodation basin. A shelf break may be present to the west out of the study area between the Sappington Basin and the incipient Antler Foreland Basin.

The lack of a shelf break and overall low-accommodation of the Sappington Basin complicates fitting a classical sequence stratigraphic model to the Sappington. The southwesternmost Sappington section in this study (Ashbough Canyon) is characterized by an anomalously thick Lower Member and anomalously thin Middle Member when compared with the other studied sections. This is evidence that the Ashbough Sappington section is located in the distal portion of the Sappington Basin in a transitional zone with the incipient Antler Foreland Basin. The interpretation of the Sappington Basin as a low-accommodation depositional basin adequately accounts for the mix of tidal vs. wave dominant energies,

variable levels of oxygenation, and variable salinity levels observed in the Sappington. The depositional environment interpretations for the 19 Sappington lithofacies will be presented here, and a more in-depth lateral equivalency discussion is presented in the Facies Relationships section of this paper.

Lower Member

The Lower Member of the Sappington is composed of lithofacies 1A, 1B, 1C, and 1D and is bound by unconformities (Figure 1.2) with the Three Forks Formation below and with U2 of the Sappington above. U1 was deposited in a low energy, variably stressed salinity, and minimal oxygen (dysoxia/anoxia) environment. Lowermost U1 is characterized by a weathering surface at the top of the Three Forks (Figure 3.25), which is found with an occasionally preserved amalgamation of various weathered clastics and carbonates suggesting a regolith (Figure 3.21). This deposit, along with previous biostratigraphic dating, shows subaerial exposure and non-deposition at the Three Forks-Sappington unconformity.

Above this deposit is a partially pyritized lag composed of fish bones (Figure 3.22) from the re-working of more distal deposition associated with transgression. The U1 lithofacies assemblage present at each section varies with location in the basin. Relative to other U1 lithofacies, lithofacies 1A is the deepest water and most open marine deposit. The majority of outcrop sections containing lithofacies 1A are found to the west (Red Hill, Ashbough Canyon) in the study area. These western sections have abundant bedded chert interbedded with fissile black shale throughout facies 1A. In thin section, the chert beds have pelagic tests of siliceous organisms (Figure 3.2 B). Diagenetic heating of the silica in lithofacies 1A beds concentrated with pelagic tests was remobilized to form chert beds. Lithofacies 1A chert beds are found throughout lithofacies 1A, but are enhanced at sections in close proximity to localized igneous intrusions such as at the Red Hill section (Figure 3.23). In addition, mobilized eolian silt-sized quartz clasts are present through much of the Sappington, being ubiquitous in U2-U6. Further thin section analysis of lithofacies 1A chert beds may reveal silt-sized eolian-derived quartz clasts, which would supply additional silica via the process outlined by Cecil (2004). In addition to the western localities with lithofacies 1A, there are occurrences to the east (Bridger Mountains sections). The eastern occurrences are thinner (16 ft. at Frazier Lake section as opposed to 47 ft. at Ashbough Canyon) and have

fewer chert beds. This eastern lithofacies 1A occurrence was the result of increased accommodation to the east by differential subsidence within the Sappington Basin.

In the central portions of the Sappington Basin, between western and eastern lithofacies 1A deposition, the laterally equivalent lithofacies 1B was deposited. Lithofacies 1B is the proximal lower accommodation equivalent to lithofacies 1A, and represents an up-dip manifestation of the same bottom water eutrophic conditions present during lithofacies 1A deposition. Lithofacies 1B has a thickness range of 6 in.-10 ft. Between lithofacies 1A/1B and lithofacies 1C there is indication of post 1A/1B non-deposition evident by a stained altered surface (Figure 3.25) and previous documentation of a lag by Gutschick and Sandberg (1970). This altered surface was only observed at the Nixon Gulch section where significant time was taken to trench and brush the Lower Member outcrop. This surface is likely present elsewhere, but requires more outcrop preparation to expose it.

A post-unconformity transgression and/or tectonic subsidence flooded an area of the Sappington Basin that was much smaller than lithofacies 1A/1B deposition. This smaller area meant the connectivity between the basin and the open marine environment to the west was less than during lithofacies 1A/1B deposition, which contributed to less mixing of the water column and resultant dysoxia/anoxia. The presence of conchostracans (clam shrimp) and echinoderms (brittle starfish) are evidence of a variable salinity environment. In the modern world, conchostracans (Figure 3.3 B) are restricted to brackish and fresh water environments (Gutschick and Rodriguez, 1978). The most favorable environment for conchostracans are muddy sediment, shallow water depth, and low energy (Gutschick and Sandberg, 1970). Brittle starfish (Figure 3.3 A) are an exclusively marine fauna. The lithofacies 1C faunal assemblage of fresh to brackish water conchostracans paired with normal marine water brittle starfish indicates fluctuating salinity levels in the basin. The small size of the brittle starfish found in lithofacies 1C could be the result of living in a stressful variable salinity environment. The faunal and sedimentologic evidence in lithofacies 1C suggests an environment with fluctuating salinities, low energy, and dysoxic/anoxic conditions. This indicates the presence of shallow, stagnant, and restricted environments in the Sappington Basin.

Lithofacies 1D represents a shift to normal salinity environments through the de-stratifying and mixing of the water column. The black to green rock color transition and the

fauna differences between lithofacies 1C and lithofacies 1D support a transition to a paleoenvironment with normal or close to normal salinity levels. Gutschick and Rodriguez (1967), described the brachiopod assemblages of the Sappington as increasing in diversity between lithofacies 1C and 1D. Increased species diversity shows more favorable environments in which fauna are forced to diversify feeding strategies to compete for resources and thus branch off into various species (G. Pemberton & J. MacEachern pers. Commun., 2014). The difference in brachiopod species diversity from lithofacies 1C to 1D suggests that lithofacies 1C was a more stressful (fluctuating salinities, non-normal marine salinity) living environment than in lithofacies 1D. The creation of a stressed salinity living environment would have been induced by changes in the layout of the basin making it more restricted. A more restricted basin would have variable consequences for levels of salinity through the minimizing of the degree of exchange between basinal water and normal marine waters, increasing of the effects of evaporation, and enhancing of the effects of differential rates of water run-off. Mechanisms for the altering of the basin layout were base level changes induced by eustasy and/or tectonics.

Middle Member

The Middle Member of the Sappington includes U2-U5 and represents a general shallowing-up regressive sequence bounded by unconformities. The Middle Member conformably transitions from a transgressive clastic starved shoreface environment in stratigraphic Unit 2 (U2) to a regressive wave-dominated lower to middle shoreface environment in U3. Sea-level reached a point of maximum flooding extent during U2 deposition (Figure 3.26) at which point the Middle Member transitioned into a regressive phase for U3 through into the U5-U6 unconformity. Alternatively, sea-level stand still and progradational filling of the basin could have occurred in the Middle Member post-U2 deposition. U3 transitions abruptly, although conformably, into a tidal-dominated estuarine environment in U4. The U4 to U5 transition is abrupt but conformable as well, transitioning into a wave-dominated lower shoreface to foreshore environment in U5. A schematic representation of the regression that dominates the Middle Member is present in Figure 3.26.

The surface between U1 and U2 is an unconformity characterized by scouring (Figure 3.277) and lag channel fill (Figure 3.288) associated with a post unconformity transgression.

The predominantly carbonate deposition of U2 contrasts across the unconformity (SB2) with the predominantly siliciclastic deposition of U1.

The fauna in lithofacies 2 consists of brachiopods, crinoid stems, and oncolites. The distribution of fauna in outcrop is evenly distributed or concentrated in event beds (Figure 3.299). Oncolites are mobile (unattached) stromatolites with alternating concentric layers of sediment and algal growth (Gutschick and Perry, 1959). Storm and wave energy rolled the oncolites and trapped cyanobacteria around the nucleus (Shi and Chen, 2006). Distribution and size of the oncolites in lithofacies 2 are controlled by the proximity of the seafloor to storm and fair-weather wave base. Energy levels typical of the middle shoreface would be ideal for oncolite growth. Higher energy levels in the upper shoreface may limit cyanobacteria growth, and lower energy levels typical of the lower shoreface, where the seafloor is below fair weather wave base, would limit the rolling of the oncolites to only during storms. Throughout the study area, lithofacies 2 was deposited in a clastic-starved carbonate-prone shoreface environment. The rate of accommodation creation during U2 deposition was greater than the rate of sedimentation, starving the basin of significant siliciclastic deposition and allowing for carbonate deposition. There was still eolian mobilized silt sedimentation in the basin that hampered carbonate growth, but was not significant enough to completely mask the carbonates.

The predominantly carbonate deposition of U2 gradually transitions into the predominantly siliciclastic deposition of U3 as a result of the slowing of the rate of accommodation space creation, which allowed for the rate of sedimentation to prevail and clastic deposition to return to the basin. Sedimentary structures, grain sizes, and ichnogenera assemblages of lithofacies 3A indicate deposition in a wave-dominated lower to middle shoreface environment. Lithofacies 3A occasionally expresses itself in outcrop as a set of cleaning-up tempestite capping beds (Figure 3.3030). In comparison to lithofacies 3A, lithofacies 3B has greater mud content, lack of distinct sedimentary structures, and a greater Bioturbation Index (BI) indicating a more distal, than lithofacies 3A, environment such as wave-dominated upper offshore. Lithofacies 3C is located in uppermost U3 and is a brachiopod-rich silty carbonate deposited in areas of the basin more sheltered from siliciclastic deposition (Figure 3.31) where brachiopods were able to establish populations.

The transition from U3 to U4 is abrupt but gradational and represents a rapid change in energy from a wave-dominated shoreline to a tidal-dominated estuary. In this study the term “estuary” is defined as a semi-enclosed coastal body of water with a pseudo-barrier system acting as a baffle to open marine wave energy. The tidal-dominated estuarine interpretation of U4 is supported by the heterolithic sedimentary structures (i.e. flaser bedding, lenticular bedding), an impoverished ichnogenera assemblage, and a lack of fauna. The impoverished ichnogenera diversity of U4 dominated by abundant *Arenicolites* (*Bifungites*) is evidence of a stressed living environment. Additionally, the lack of fauna in U4 is another indicator of a stressed living environment. This type of stressed living environment was likely a result of non-normal marine salinities and is suggestive of a brackish water setting, commonly associated with estuaries. The lenticular heterolithic bedding (Figure 3.8A) and ichnogenera assemblage of lithofacies 4A is indicative of a tidal-dominated outer estuary. Lithofacies 4B was deposited in a medial estuary setting and is characterized by wavy heterolithic bedding (Figure 3.8B) and a low-diversity ichnogenera assemblage dominated by abundant *Arenicolites*, which when found in high abundance has been shown to be associated with mixed tidal flats (Pemberton et al., 2011). Lithofacies 4C is distinguished from the other U4 lithofacies by flaser bedding (Figure 3.8C) and interbedded tempestites. As wave energy from storms moved onshore, the disturbance of the seafloor intensified with shallowing water depth leaving behind a distinctive internally stratified tempestite (Figure 3.11) (Plint, 2010). Lithofacies 4C has a much stronger storm wave energy influence (Figure 3.8D) than the other two U4 lithofacies, which is attributed to shallower water depths and a greater fetch. Sand content increases landward due to closer proximity to sediment sources as well as the onshore movement of clastics due to the flood current being the dominant tidal current. This, along with the ichnogenera assemblage, indicates deposition in the mixed tidal- and wave-dominated inner estuary.

Unit 4 is the most peculiar of the Middle Member stratigraphic units because it displays an abrupt (Figure 3.32) yet conformable transition to tide-dominated energy from wave-dominated energies of U3 and U5. The shift from wave- to tidal-dominant energy indicates a change in the layout of the basin that allowed for increased protection from wave energy and increased influence of tidal energy. The formation of a barrier at the mouth of the basin and subsequent creation of an estuary-like environment occurred rapidly in terms of

geologic time, which is expressed by the sharp contacts of U3-U4 and U4-U5. The driving mechanism behind barrier formation could have been one or a combination of an abrupt sea-level fall, tectonically induced uplift, and/or barrier bar formation from changing coastal currents. An abrupt sea-level fall could have exposed a previously submerged subaqueous high(s), which would have acted as a barrier focusing tidal energy across a smaller cross sectional area at the mouth of the estuary and reducing the wave influence in the basin. Additionally, tectonically induced uplift could have had the same effects on the basin. Alternative to a base level change, the strength and/or orientation of coastal currents could have resulted in the formation of a barrier system at the mouth of the estuary, which would have limited wave energy and increased tidal energy. In the absence of additional evidence, the identification of the mechanism driving barrier formation remains enigmatic.

The contact between U4 and U5 is another abrupt but gradational contact and represents a proximal shift in the depositional environment from a tide-dominated estuary in U4 to a wave-dominated shoreline in U5. The proximal shift in environment from U4 to U5 was associated with the introduction of coarser clastics to the system. The coarse-siltstone to very fine-grained sandstone of U5 has the coarsest (other than the lags) clast sizes that are present in the Sappington. The four lithofacies of U5 are characterized by various sedimentary structures representing different forms of sandy shoreface to foreshore environments. Lithofacies 5A, with its interbedded highly bioturbated sand and tempestites (Figure 3.33), is interpreted as being deposited in the lower shoreface. The assemblage of ripple forms (current ripples, aggrading current ripples (Figure 3.34), wave ripples, and combined flow ripples) in lithofacies 5B are indicators of a middle to upper shoreface environment. Lithofacies 5C is a mix of heavily bioturbated sand and tempestites. The tempestites in lithofacies 5C were variably diagenetically calcified and show distinct tempestite internal stratification (Figure 3.35). Various carbonate debris (i.e. crinoid stems) contained in the tempestites are the source of the calcium carbonate that was later remobilized throughout the tempestite bed. Lithofacies 5C was deposited in a lower shoreface environment in close proximity to laterally equivalent carbonate units. The diagnostic sedimentary structure of lithofacies 5D is planar cross beds (Figure 3.12) an indicator of a foreshore environment. At Dry Hollow lithofacies 5D was seen in conjunction with calcified nodules (Figure 3.12).

U5 was deposited in a wide swath stretching at least 40 miles (measured from present outcrop locations not palinspastic reconstructions) perpendicular to the paleoshoreline and measuring at least 30 feet in thickness. This scale of sand deposition is unlikely in a steady state sea-level with the depositional timeline of U5, and thus increased erosion rates are necessary. Increased erosion rates could have been induced by uplift or sea-level fall, both of which would be accompanied by a regressing shoreline. Primary sand deposition takes place in the shoreface and as base level falls distal shoreface environments transition into proximal shoreface environments. This distal to proximal shoreface transition is evident in the generally coarsening-up character of U5. As an area of the basin is subaerially exposed some of the upper poorly consolidated sand bodies are scoured-off and recycled, which means the preserved thickness of U5 is less than what was at one time deposited. Low-magnitude base level changes along with differential erosion rates (Figure 3.39) in different parts of the Sappington Basin is the reason lithofacies associations do not consistently become more proximal up section. U5 deposition ended as sea-level fell out of the Sappington Basin exposing the basin to a period of non-deposition and leading to the U5-U6 unconformity.

Upper Member

U5 and U6 are in unconformable contact across an unconformity (SB3) of ~4 my (Figure 3.17). During that time the Sappington Basin depocenter migrated eastward (Figure 3.20 & Figure 3.38). U6 is comprised of 4 lithofacies (Figure 3.36) partially deposited in a limited oxygen environment. Dysoxic to anoxic conditions were present in subequatorial coeval basins (**Error! Reference source not found.**Figure 1.5) around the world during the earliest Mississippian, such as in the Bakken and Exshaw formations. Similar anoxic deposition took place in U6 of the Sappington during this time, but overall the grain sizes in the Sappington are coarser-grained than the Bakken and Exshaw, an indicator of lower accommodation in the Sappington Basin compared to the Williston Basin and Prophet Trough (Figure 1.5). Lithofacies 6A is a conglomeratic lag, which indicates a post-unconformity transgression. Lithofacies 6B is an argillaceous siltstone deposited in the upper offshore environment. The lithofacies 6C ichnogenera assemblage of *Chondrites(?)* / *Phycosiphon(?)*, *Planolites*, *Teichichnus* (Figure 3.15), along with the mix of dark and light colored silt, is an indicator of episodic oxygenated conditions in lower shoreface water depths. Lithofacies 6D was not deposited under limited oxygen conditions and is a mixed

carbonate clastic with an ichnogenera assemblage that included *Skolithos* (Figure 3.16). The carbonates within lithofacies 6D may indicate the shift in global conditions that lead to widespread carbonate deposition during the Mississippian (e.g., Lodgepole Formation). Lithofacies 6D was likely deposited in a low-energy, carbonate-prone shoreface environment.

U6 is unconformably overlain by a Williston Basin Scallion-like Member of the Lodgepole Formation. The Scallion represents the initial deposits of prolonged carbonate deposition associated with the transition to a global icehouse climate. In outcrop, the Scallion differentially scours the uppermost Sappington Formation (Figure 3.36 and Figure 3.37).

Figures

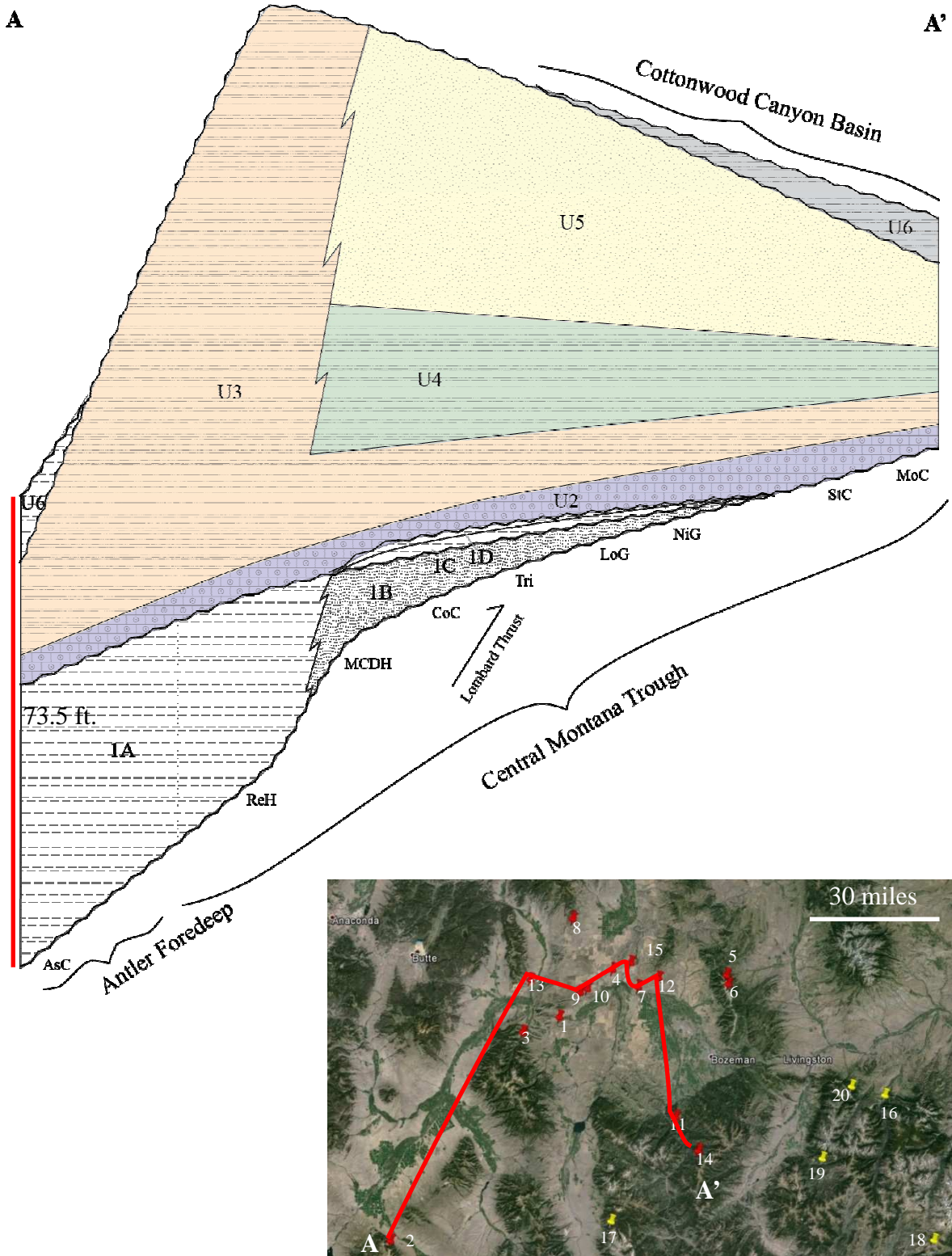


Figure 3.20 Cross section (A-A') showing general facies distribution and relationships in the Sappington Basin.

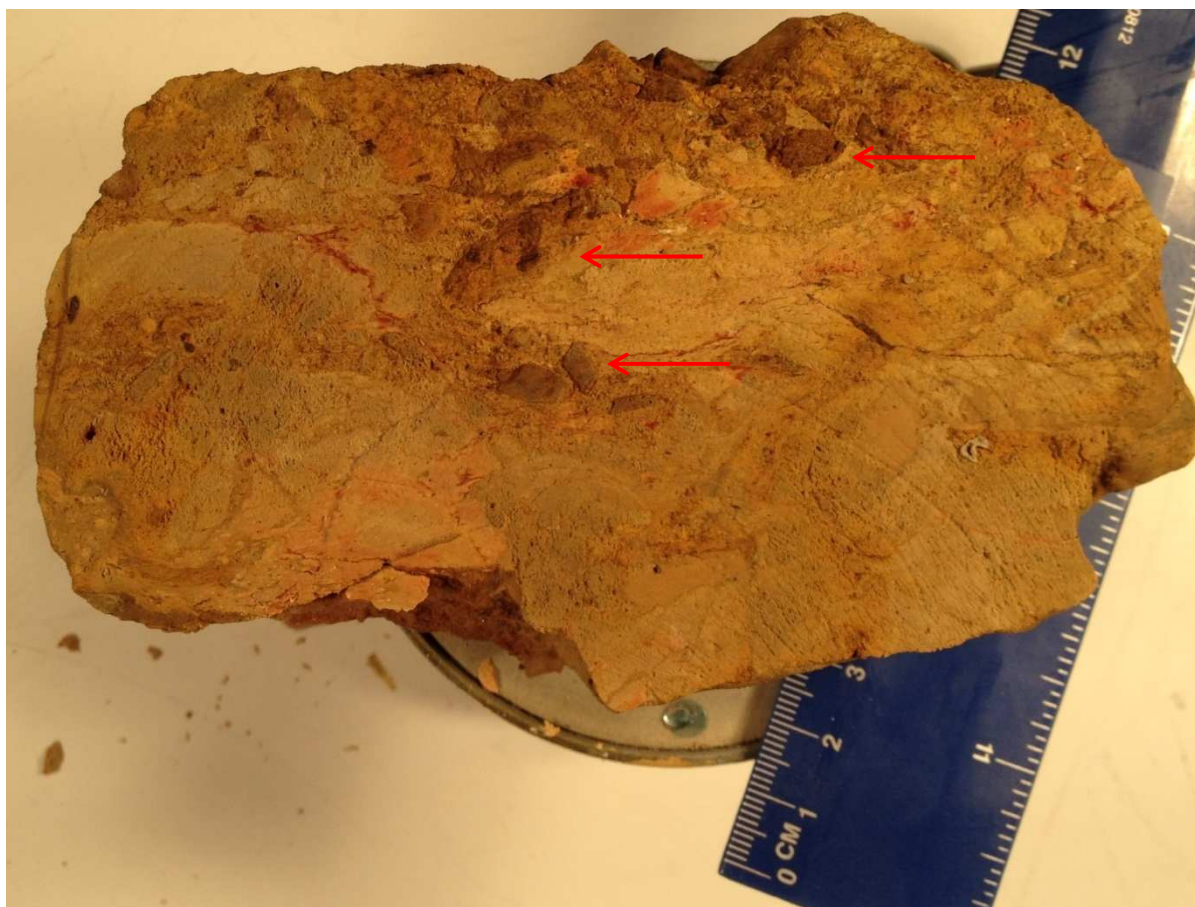


Figure 3.21 Basal U1 regolith (red arrows point to clasts of weathered and re-worked mixed carbonate and clastic debris sitting in clay-rich matrix).



Figure 3.22 Transgressive lag at the Three Forks – U2 contact.



Figure 3.23 Abundant chert beds (red arrows) in lithofacies 1A.

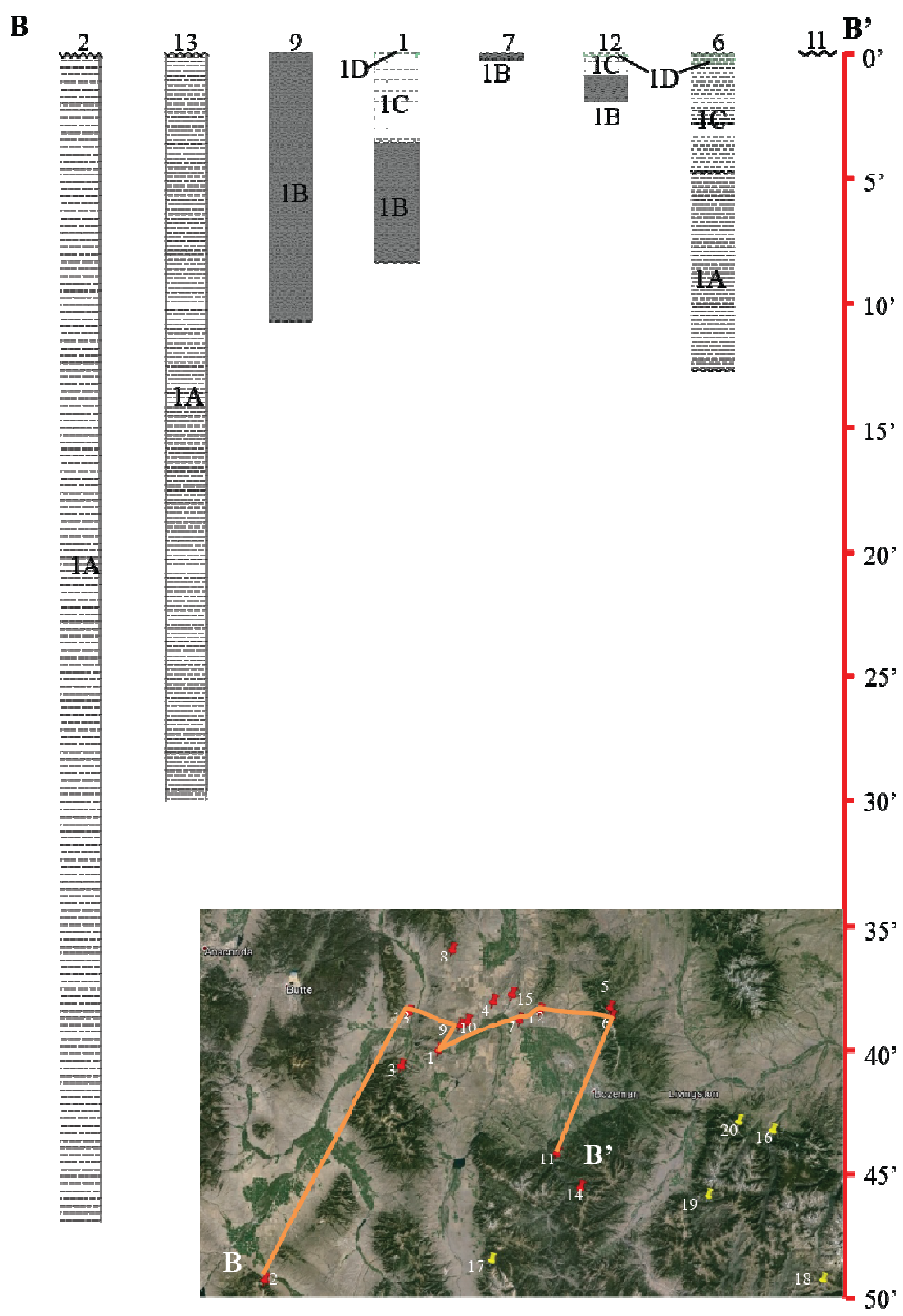


Figure 3.24 Cross section (B-B') of U1 (2-Ashbough Canyon, 13-Red Hill, 9=Dry Hollow, 1=Antelope Creek, 7=Logan Gulch, 12=Nixon Gulch, 6=Hardscrabble).

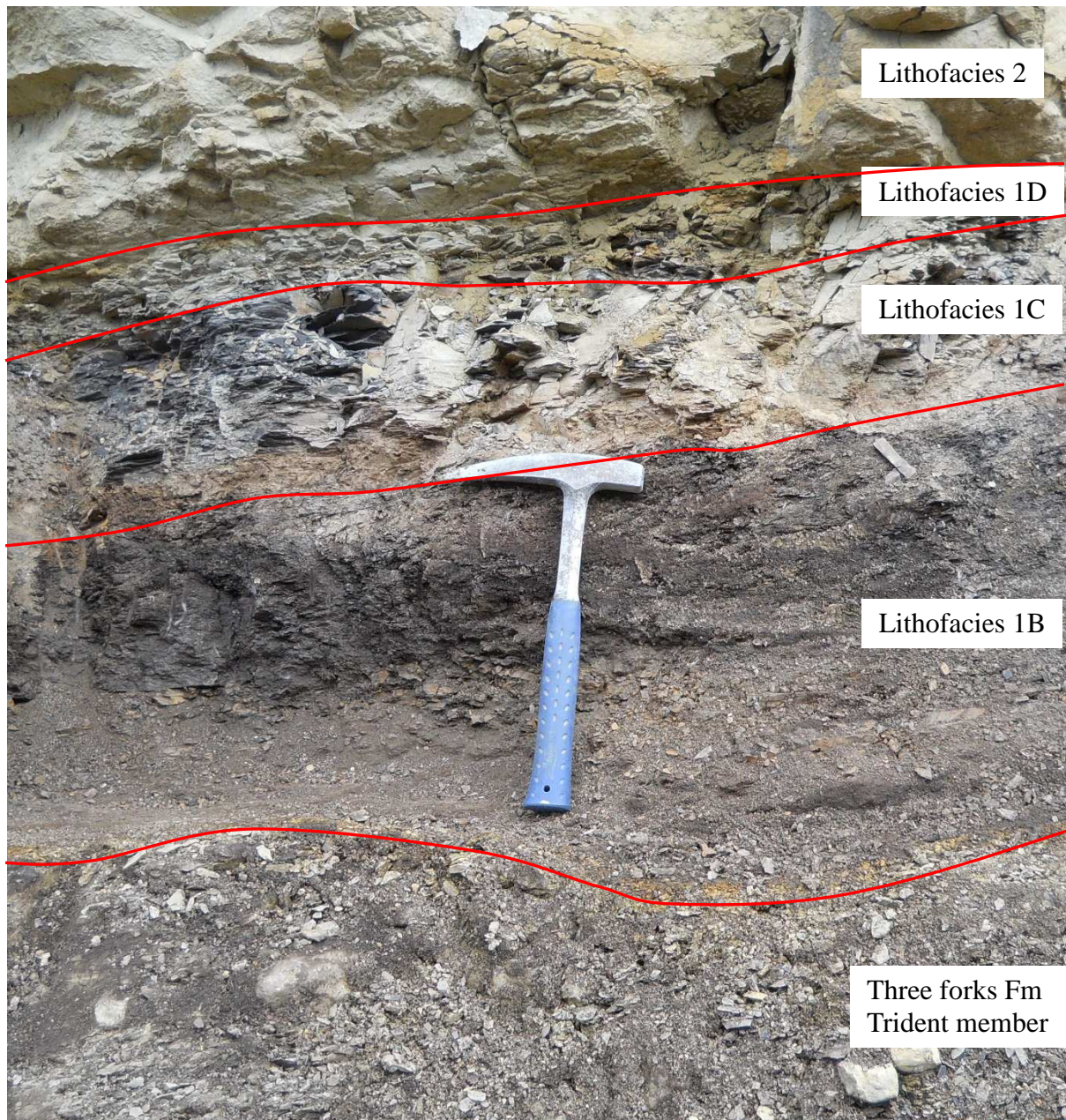


Figure 3.25 Outcrop picture of U1 lithofacies succession (lithofacies 1B, 1C, 1D, 2). Definite unconformities exist at the Three Forks – lithofacies 1B contact, as well as the lithofacies 1D – lithofacies 2 contact. An additional unconformity may exist at the contact lithofacies 1B – lithofacies 1C contact.

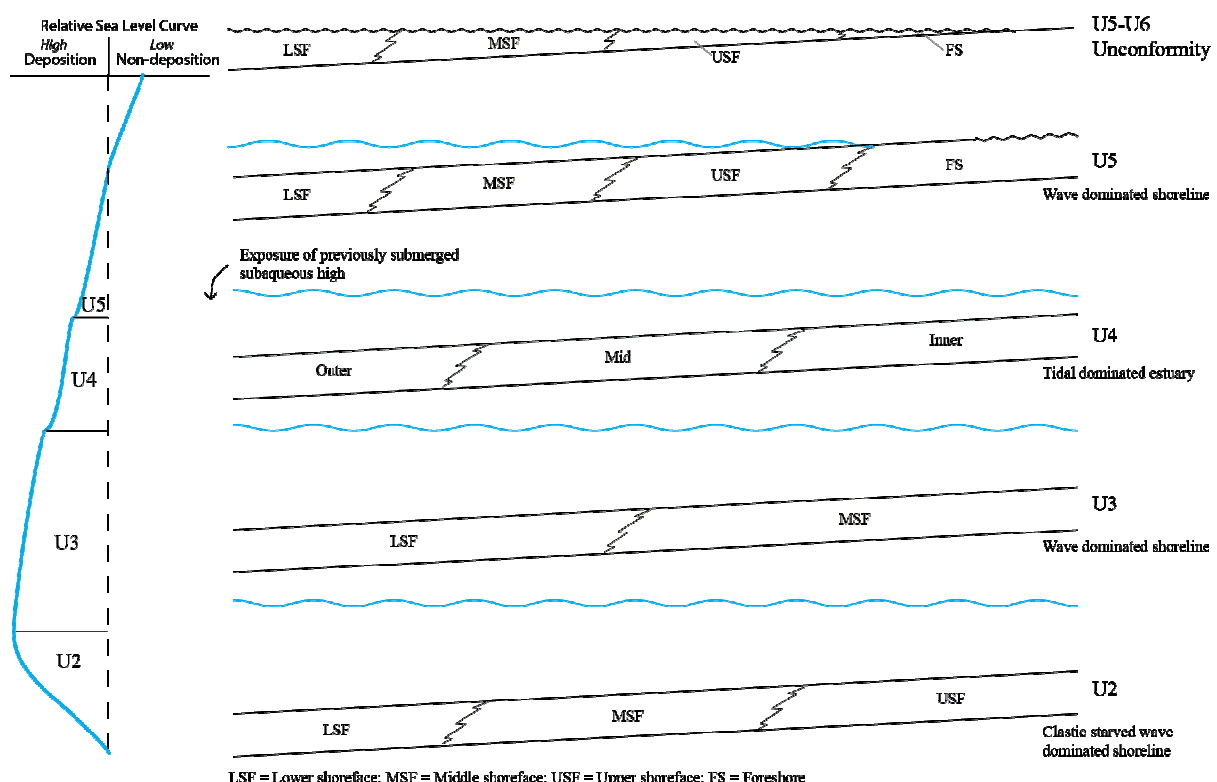


Figure 3.26 A schematic representation of base level changes in the Middle Member of the Sappington. Left) relative sea-level curve showing transgression during U2 followed by regression for U3 through U5-U6 unconformity; Right) diagram showing proximal depositional environment transitions of the Middle Member.



Figure 3.27 Outcrop photo of scoured Three Forks-U1 contact and U1-U2 contact (brush = 30 cm).



Figure 3.28 Outcrop photo of lithofacies 2 lag (brachiopod and crinoid stem fragments) channel fill (red arrows point to some of the larger lags).

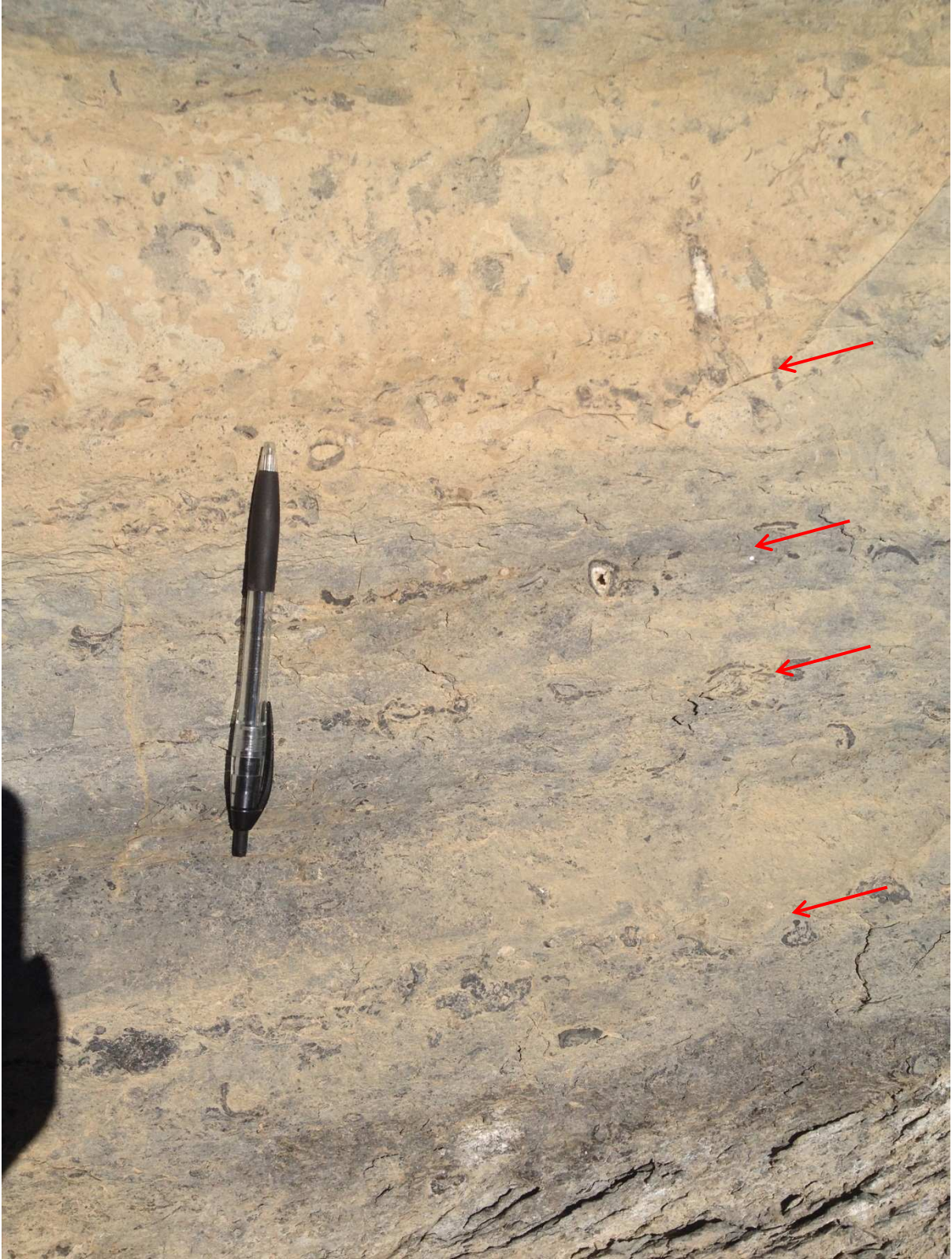


Figure 3.29 Lithofacies 2 fossiliferous (fragmented brachiopods and poorly developed oncolites) tempestites (red arrows) (pen = 14 cm).



Figure 3.30 Outcrop of lithofacies 3A near (red arrows point to tempestite capping beds).

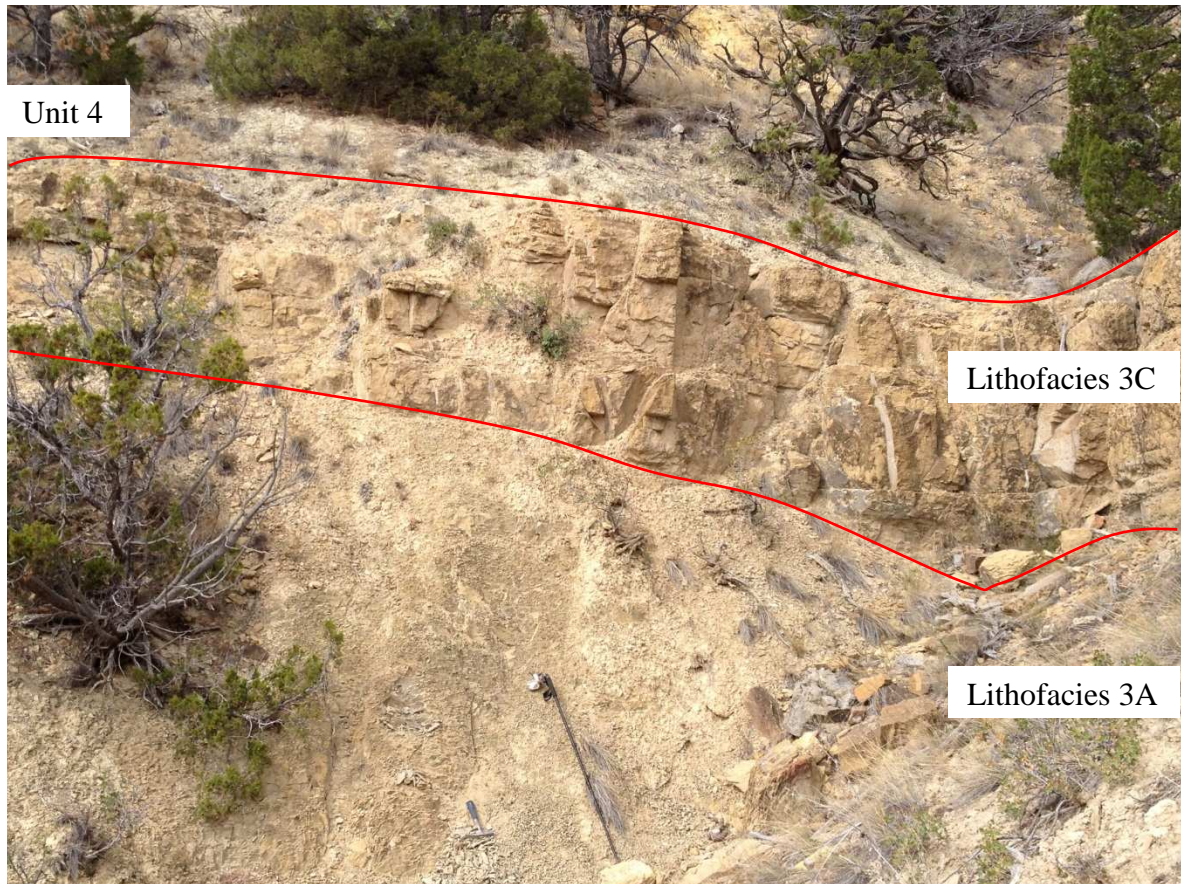


Figure 3.31 Uppermost Unit 3 showing more resistant to weathering carbonate nature of lithofacies 3C (Jacob's Staff in lower portion of picture = 1.5 m).

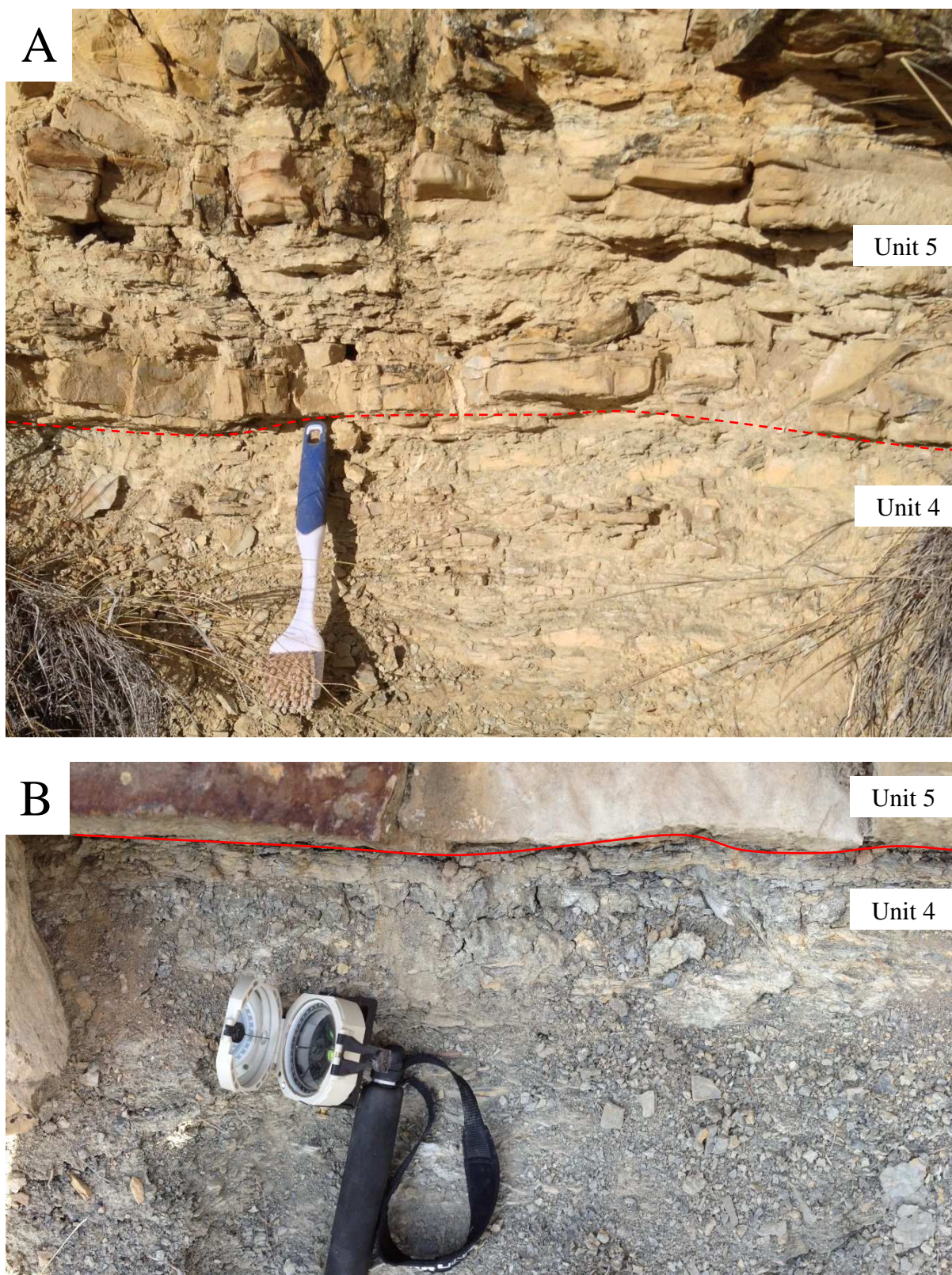


Figure 3.32 U4-U5 contact A) gradational expression (lithofacies 5A) (brush = 30 cm); B) non-gradational expression from (compass width = 8 cm).



Figure 3.33 Lithofacies 5A (red arrows point to tempestites) (compass width = 8 cm).



Figure 3.34 Lithofacies 5B (red arrow points to aggrading current ripples) (pen = 15 cm).



Figure 3.35 Lithofacies 5C Left) tempestite from; Right) outcrop

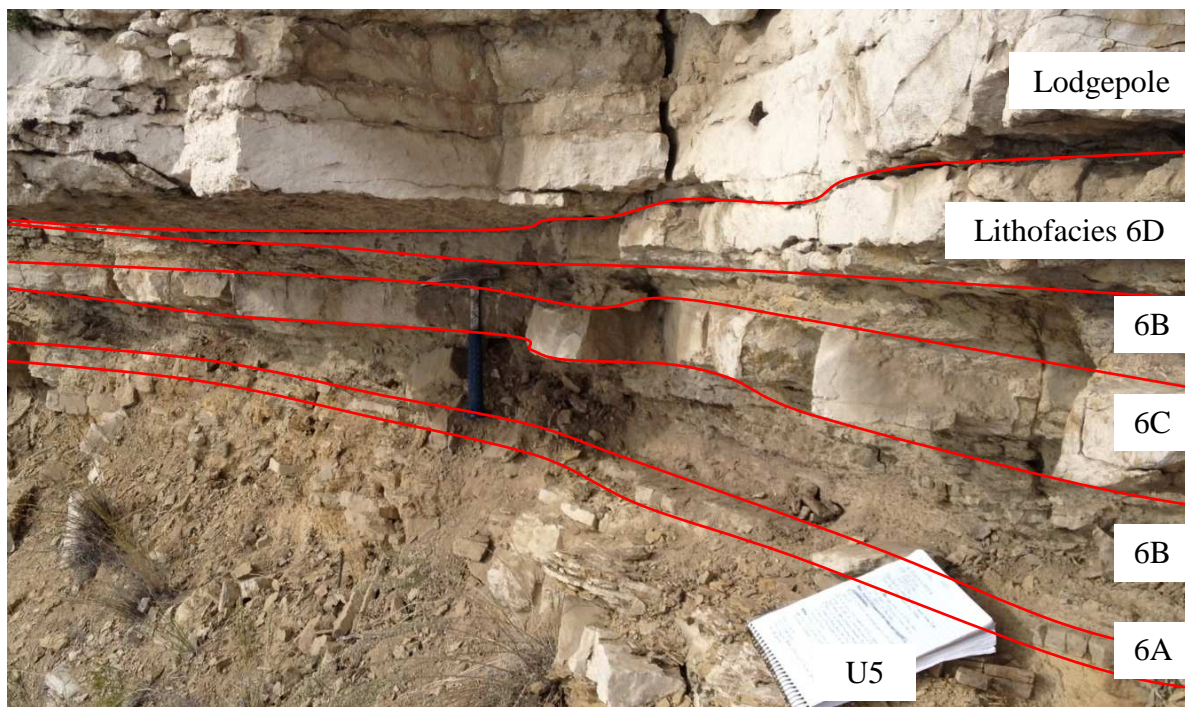


Figure 3.36 U6 lithofacies (6A, 6B, 6C, 6D) in outcrop; lithofacies 6D is being beveled to the left by the overlying Scallion Member of the Lodgepole Formation (notebook length = 23 cm).

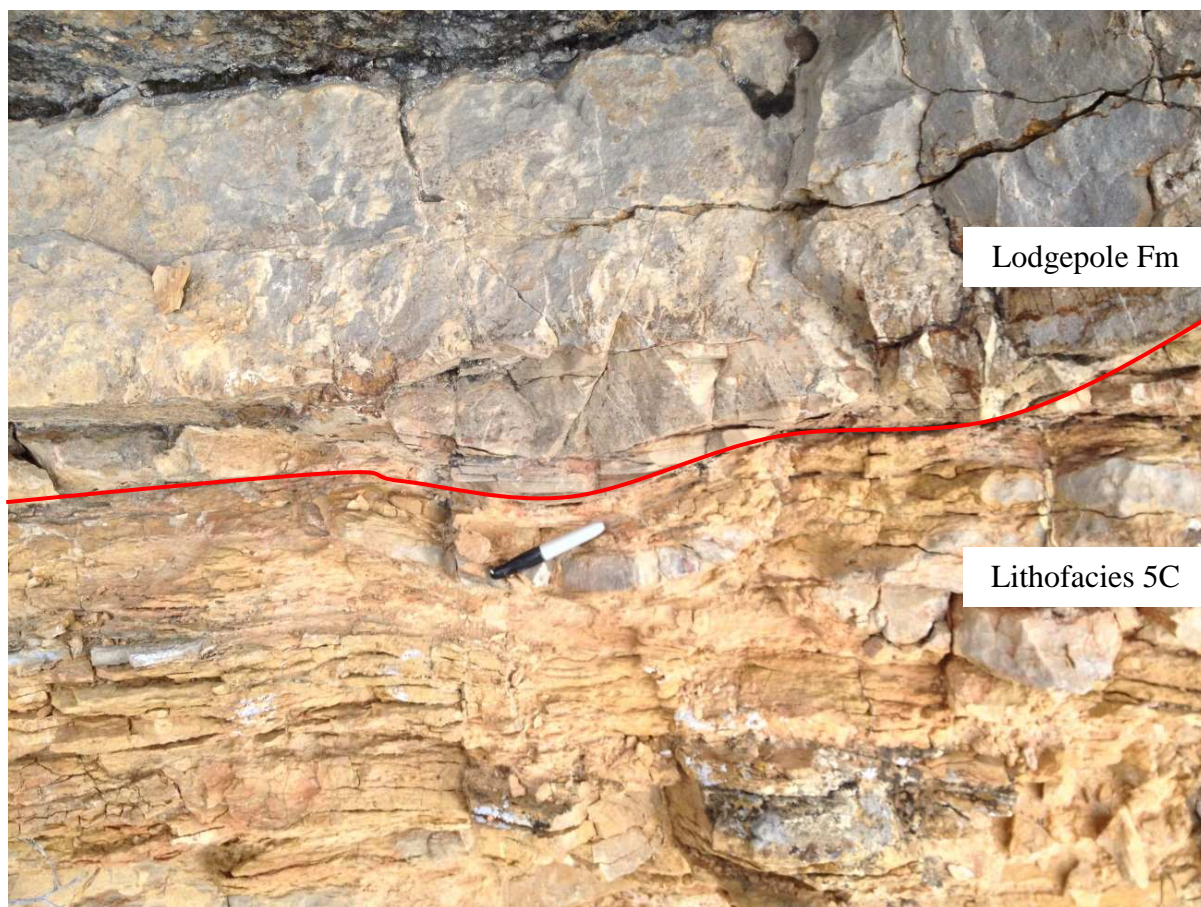


Figure 3.37 Scoured Lodgepole – lithofacies 5C contact (pen = 9 cm).

Facies Relationships

Lower Member

During Lower Member deposition, the majority of the internal Sappington Basin was a broad shallow basin with western distal deepening (Figure 3.38 & Figure 3.24) towards the incipient Antler Foreland Basin and thinning and pinching out to the southeast onto the Beartooth Shelf (Figure 3.40). The area of greatest accommodation lied to the southwest at the Ashbough Canyon section (Figure 3.38), which has at least 47 ft. of Lower Member black shale. Dysoxic/anoxic deposition prevailed as a result of a combination of Late Devonian sea-level rise and eutrophication (see Paleoclimate section). Lithofacies 1A and 1B are time correlative and represent the relatively greater and lesser accommodation equivalents to one another. Lithofacies 1A was deposited under more open marine like conditions to the west and lithofacies 1B was deposited under more terrestrial like conditions to the east. Lithofacies 1C deposition was less widespread than 1A or 1B and was deposited in a variable salinity environment associated with a change in the balance of circulation of normal marine water in the basin and fresh water run-off. Lithofacies 1D was fully marine and more widespread than lithofacies 1C, as a result of greater mixing of open marine and basinal waters.

Middle Member

The Middle Member thins and pinches out (Figure 3.41) to the southeast onto the Beartooth Shelf (Figure 3.38). U2 is found in a similar oncolitic lithologic character throughout the entire study area. In the Lithofacies section of this paper oncolites were proposed to have formed under shoreface energies. If this theory is correct than to the southwest (Ashbough Canyon section), in the portion of the basin with greatest accommodation for Lower Member deposition, shallowing of seafloor relief via tectonic induced uplift would have been required. However, if oncolites can form under a wider range of energy regimes beyond the shoreface, than shallowing of seafloor relief is not required.

Unit 3 is similar in lithologic character (lithofacies 3C) throughout the majority of the study area with the exception of the most proximal outcrop location (Moose Creek) where lithofacies 3B was deposited. The lower energy depositional nature of lithofacies 3B at the most proximal outcrop section is contradictory and may indicate short lived localized subsidence. Unit 4 thickens westward until it disappears between the Red Hill and Dry

Hollow sections. This disappearance at Red Hill is attributed to U4 equivalent deposition out of the estuary on a wave-dominated shoreline in the form lithofacies 3A deposition. The sedimentary structures of U4 transition from flaser to wavy to lenticular bedding from southeast to northwest indicating a proximal to distal transition in the estuary. U5 generally thickens from southeast to northwest until it abruptly thins between the Dry Hollow and Red Hill sections in the same location where U4 disappeared. This abrupt disappearance and paralleling thickness pattern of U4 and U5 is interpreted as the filling of the U4 estuary with coarser clastics during U5 deposition brought on by increased up-dip erosion rates from abrupt sea-level fall or tectonic uplift. Alternatively, the U5 estuary fill depositional pattern could be a result of progradation, but the abrupt nature of the U4-U5 contact supports the preceding interpretation. Within the bounds of the U4 estuary U5 grain sizes and sedimentary structures fine and decrease in energy to the west indicating east to west proximal to distal transition.

Upper Member

During the unconformity between U5 and U6 the area of greatest accommodation in the basin shifted to the east (Figure 3.42). This eastward migration is attributed to increasing eastern subsidence coupled with western uplift during the 4 my of non-deposition between U5 and U6. Previous work (Benson, 1966; Sandberg et al., 1972; Nagase, 2014) has indicated the presence of another basin to the east out of the study area known as the Cottonwood Canyon Basin in which Upper Member Sappington equivalent Cottonwood Canyon Formation was deposited. The relationship between the Cottonwood Canyon Basin and the Sappington Basin has seen little investigation and is largely unknown, but it is possible that by the time of Upper Member Sappington deposition that the Cottonwood Canyon Basin and Sappington Basin had merged.

Structural Complications

Post depositional Laramide and Sevier deformation (Figure 1.9) in the basin needs to be considered when discussing lateral facies relationships and subtleties in basin architecture. Unfortunately, not all of the studied outcrop sections can be treated as being deposited *in situ*. The region's main structural feature is the Lombard Thrust Fault which has transported the Elkhorn Thrust Plate at least 70 km (Burton et al., 1998) to the east. A simple palinspastic restoration was conducted in the isopachs (Figure 3.40, Figure 3.41, Figure 3.42) of the

Sappington's three members to account for Lombard Thrust transport to provide a more accurate visualization of the *in situ* depositional layout in the basin. Five of the western studied sections (Copper City, Dry Hollow, Lone Mountain, Milligan Canyon, Red Hill) are located on the Elkhorn Thrust Plate. Based on its present day location, the Copper City and Trident sections appear to be only 7 km apart, but when considering Elkhorn Thrust Plate translation these two sections were originally deposited approximately 77 km apart. However, a west-east cross section (Figure 3.38) across the fault does not reveal much variation with the exception of the absence of U6 west of the fault. The Lombard Thrust is the most significant, but not the only structural feature in the study area. Thus, to create a true depositional model for the Sappington Basin a more in-depth palinspastic restoration needs to be developed.

Shelf Break

The location/existence of a shelf break in the study area is enigmatic (see Sequence Stratigraphic Framework section for discussion of importance of the shelf break in sequence stratigraphy). Was there enough accommodation in the Sappington Basin to support the existence of a shelf break? Was the Antler Foreland Basin (Figure 1.9) developed enough during the time of Sappington deposition to support a shelf break with the Sappington Basin? The lack of lowstand systems tract lithologies in outcrops within the study area indicates the lack of a shelf break. It is possible that out of the study area to the west that evidence of a shelf break may exist. Flysch deposits of the Lodgepole equivalent McGowan Creek Formation in eastern Idaho are evidence of lowstand deposits by the time of Lodgepole deposition, but to this point similar evidence for the Sappington has not been located.

Figures

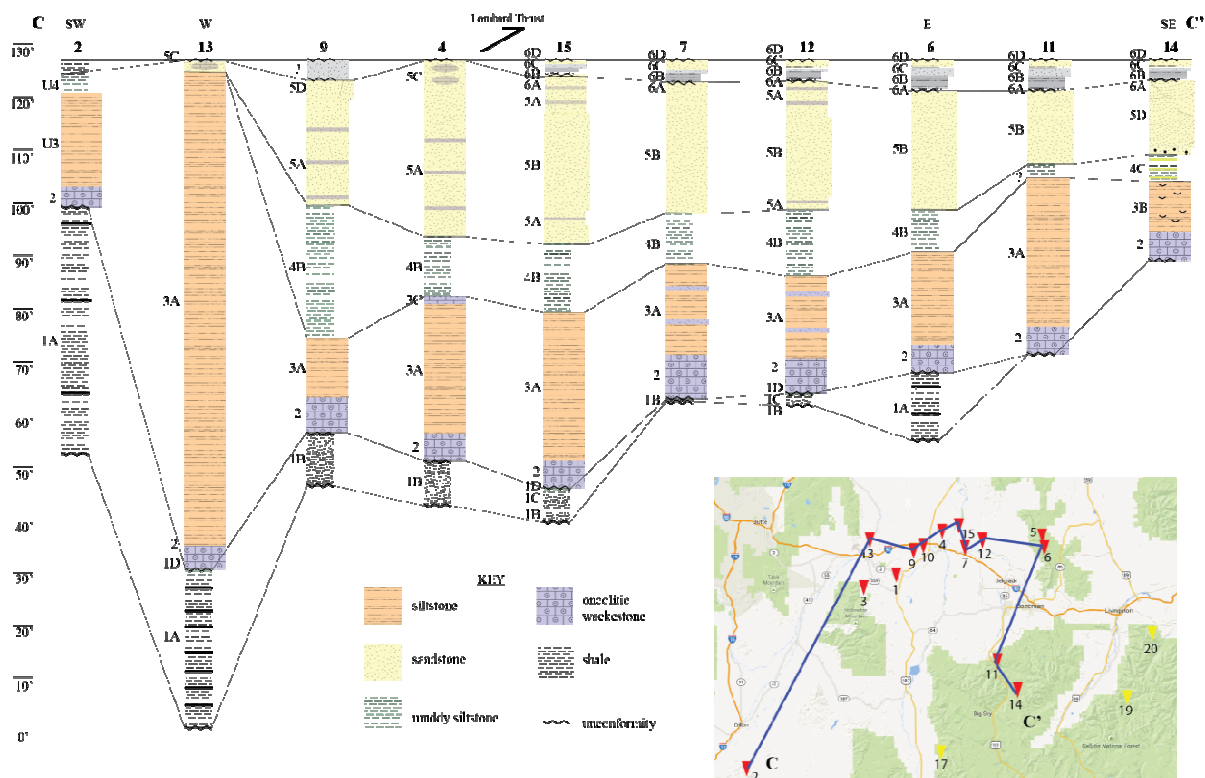


Figure 3.38 Cross section (C-C') showing Sappington lateral facies relationships in the Sappington Basin (1=Antelope Creek, 2=Ashbough Canyon, 3=Brown Back Gulch, 4=Copper City, 5=Frazier Lake, 6=Hardscrabble, 7=Logan Gulch, 8=Lone Mountain, 9=Dry Hollow, 10= Milligan Canyon, 11=Moose Creek, 12=Nixon Gulch, 13=Red Hill, 14=Moose Creek, 15=Trident). Yellow pins represent McMannis (1962) sections where Sappington is absent (16=Boulder River, 17=Cinnabar Mountain, 18=Cooke City, 19=Mill Creek, 20=Mission Creek)

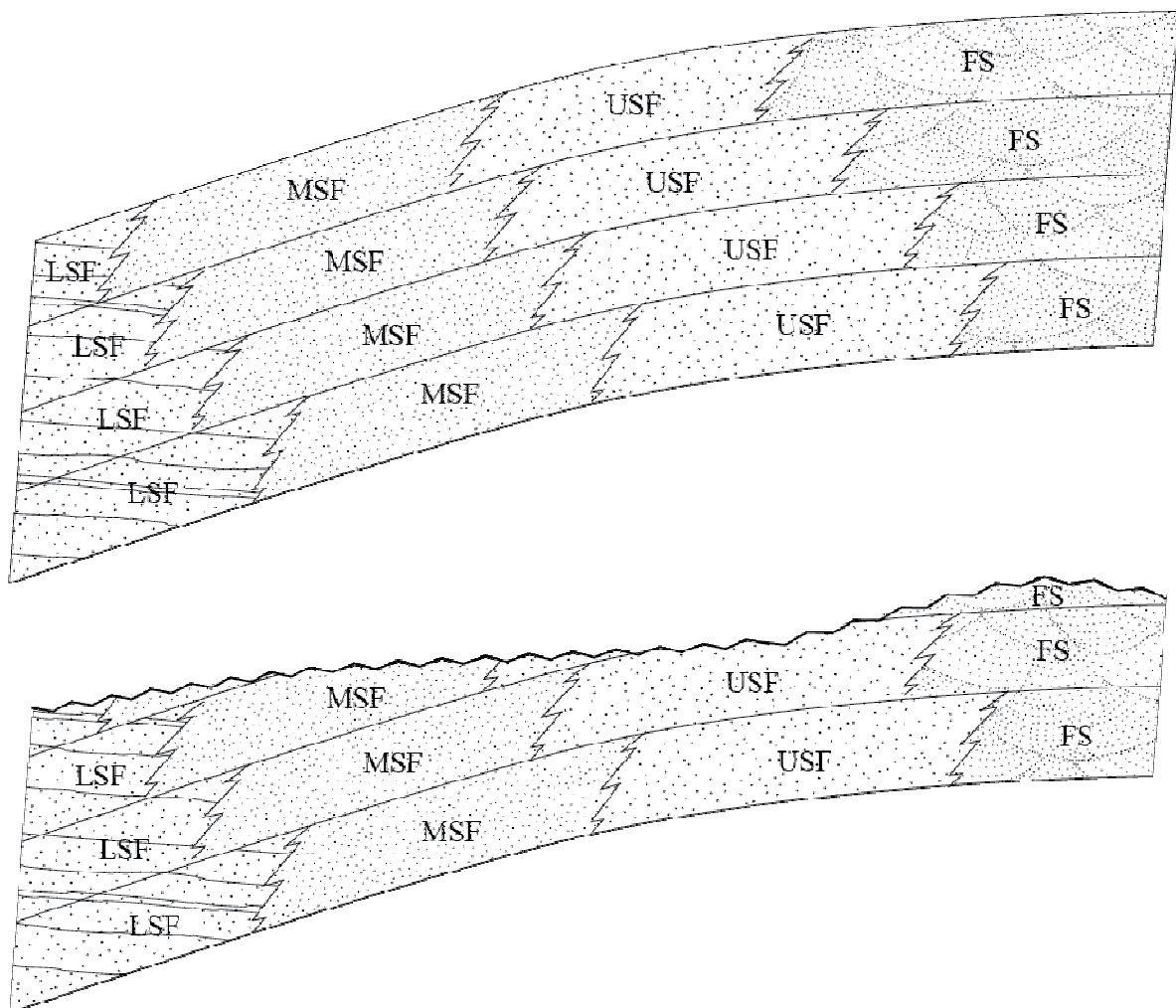


Figure 3.39 Conceptual model showing uppermost U5 differential erosion (LSF=lower shoreface, MSF=middle shoreface, USF=upper shoreface, FS=foreshore).

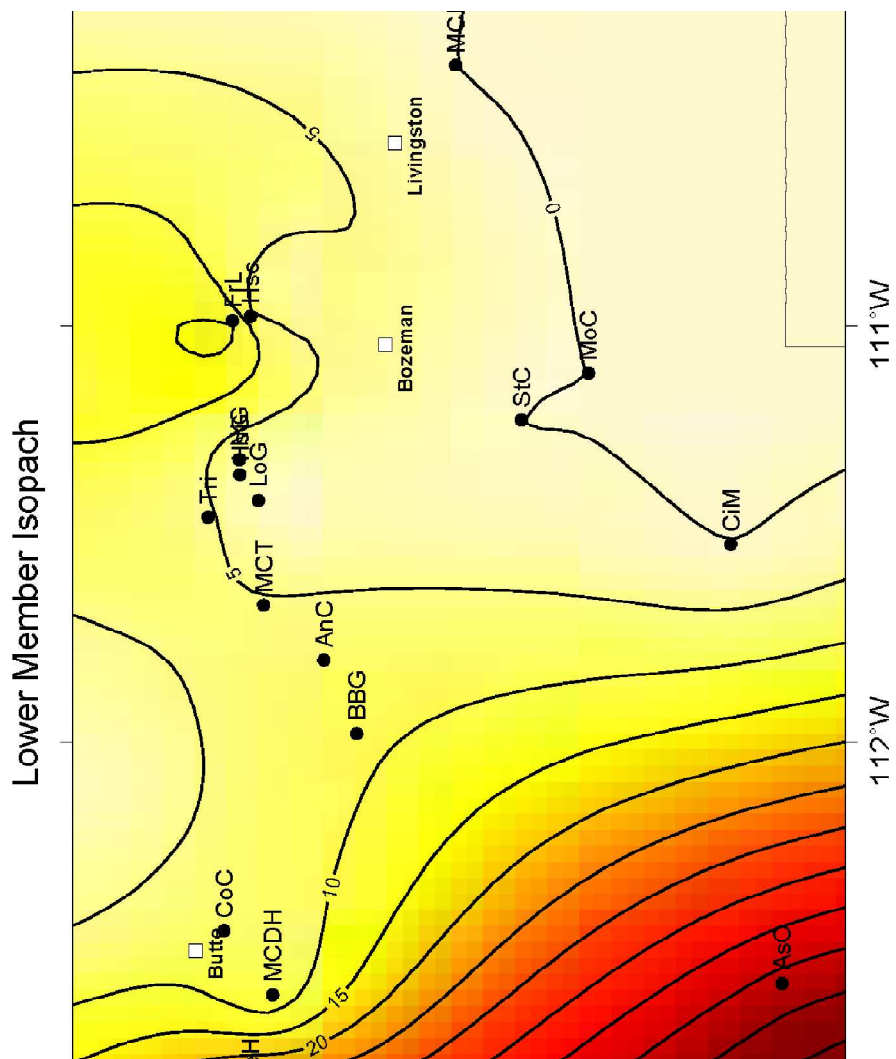


Figure 3.40 Sappington Lc
(figures were generated wi

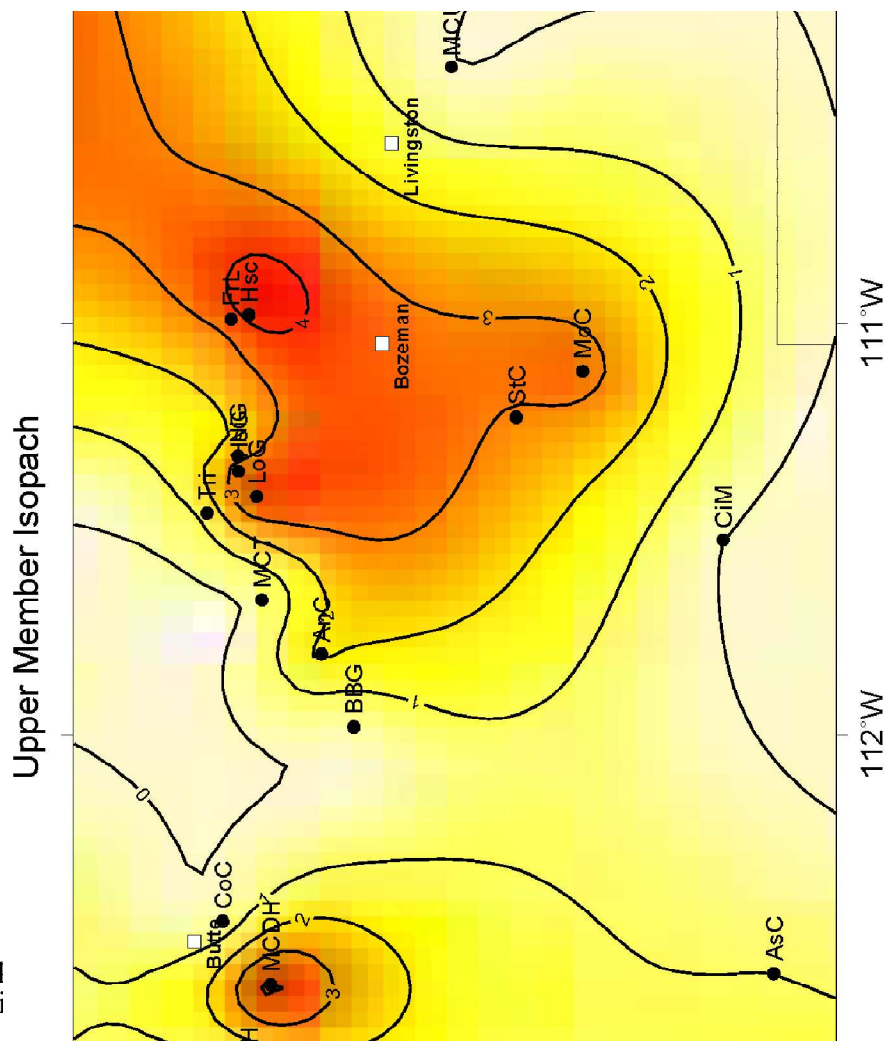


Figure 3.42 Sappington U₁
(figures were generated wi

Sequence Stratigraphic Framework

The basis of sequence stratigraphy is the sequence, which is defined as a relatively conformable succession of genetically related strata bounded at their upper surface and base by unconformities and their correlative conformities (Vail et al., 1977). Sequences are made up of systems tracts, which are defined as genetically associated stratigraphic units that were deposited during specific phases of the relative sea-level cycle (Posamentier et al., 1988). In this study, the original three part systems tract classification scheme of lowstand systems tract (LST), transgressive systems tract (TST), and highstand systems tract (HST) is used. In sequence stratigraphy the shelf break is used as the reference point for determining system tract classifications. LST is defined by deposition below the shelf break during base level fall when the rate of sedimentation exceeds the rate of accommodation space creation. LST is characterized by erosion and non-deposition above the shelf break, and by the formation of a

wedge and/or fan below the shelf break. TST is defined by deposition above the shelf break during a rise in base level when the rate of accommodation space creation exceeds the rate of sedimentation. TST is characterized by initial erosion followed by retrogradational deposition above the shelf break and minimal sedimentation below the shelf break resulting in the formation of condensed sections. HST is defined by prograding deposition during base level stand still when the rate of sedimentation exceeds the rate of accommodation space creation. HST is characterized by deposition initially above the shelf break with the potential for progradation to bring deposition below the shelf break as well. In sequence stratigraphy there are three primary surfaces of significance: sequence boundary, transgressive surface, and maximum flooding surface. The sequence boundary is an erosional surface at the base of the LST and the base of the sequence. The transgressive surface is an erosional surface at the base of the TST and represents initial flooding and deposition above the shelf break. The maximum flooding surface is a depositional surface located at the top of the TST and represents the transition from TST to HST.

Sequence stratigraphic analysis was created for use on large scales on continental margins where the seafloor transitions from a low relief shelf, crosses a shelf break, and transitions into deep water high accommodation settings such as the continental slope and abyssal plain. This complicates fitting a sequence stratigraphic framework to the Sappington because it was deposited in a low-accommodation intracratonic basin. In this type of setting a shelf break does not form or is poorly developed. The study area for this project is proposed to take place entirely above the shelf break. Consequently, lowstand deposits are not seen in the study area and are represented by a stacked sequence boundary and transgressive surfaces. The sequence stratigraphic interpretations in this study were derived solely from outcrop.

The Sappington represents approximately eight million years of deposition yet only averages 73 ft. thickness for the entire set of stratigraphic units. The thickness to time ratio of the Sappington is a function of both compaction as well as at least four unconformities representing significant lengths of time of non-deposition and erosion. Sequence boundaries are present at the following four horizons: Three Forks Formation and Sappington Lower Member (SB1), Sappington Lower and Middle Member (SB2), Sappington Middle and Upper Member (SB3), and Sappington Upper Member and Scallion Member of the

Lodgepole Formation (SB4) (Figure 3.43). The proposed sequence boundaries are seen in outcrop as a combination of a) discolored iron oxide surfaces, b) sharp surfaces separating contrasting lithologies, c) transgressive lags, and/or d) scoured erosional surfaces. Evidence for sequence boundaries is further supported by the published biostratigraphic dating of others (Sandberg et al., 1972) and unpublished biostratigraphic dating of collaborators at the University of Idaho.

The Lower, Middle, and Upper Members of the Sappington each represent sequences. The combination of the locations of sections studied within the Sappington Basin, and the low-accommodation nature of the Sappington Basin led to an incomplete systems tracts suite in each of the sequences.

Lower Member

Sequence boundary 1 (SB1) (Figure 3.43) is located between the Three Forks Formation and the Lower Member of the Sappington. A pronounced surface of discoloration (Figure 3.25), the result of oxidation from subaerial exposure, and a transgressive lag (Figure 3.22) highlight the presence of SB1. Past research in equivalent Sappington formations such as the Bakken and Exshaw Formations have called this equivalent horizon the Acadian Unconformity, which separates the Lower and Upper Kaskaskia sequences (Smith et al., 1995). However, the Paleozoic sea-level curve of Haq and Schutter (2008) identified the Acadian Unconformity as 374.5 Ma (Figure 3.44). The Wheeler Diagram presented in this paper places the SB1 unconformity at approximately 363 Ma (Figure 3.17). There lies a discrepancy of 11.5 my between the proposed age of the Acadian Unconformity and the proposed age of SB1. In addition, the geographic separation of the Acadian Orogeny with the Sappington Basin may be too great to significantly affect deposition of the Sappington. A more appropriate name for SB1 may be the Antler Unconformity due to the regional proximity of the Antler Orogeny, and the similarities in timing of SB1 with the believed onset of the Antler Orogeny. However, until more accurate ages of the Antler Orogeny are solidified and until the intraplate tectonic effects of the Antler convergent margin are better understood, classification as the Antler Unconformity should be tentative.

SB1 is the up-dip manifestation of LST1 (Figure 3.43) and represents a surface of subaerial exposure and erosion of upper Trident facies. Theoretically, LST type deposits should exist to the west out of the Sappington Basin below the shelf break in the incipient

Antler Foreland Basin. The Lower Member is interpreted as a TST (TST1) (Figure 3.43) evidenced by the basal transgressive lag, fine grain lithology of facies 1, and the minimal oxygenation environment in which the facies were deposited. During transgression, the rate of accommodation space creation exceeded the rate of sedimentation and fine grained sedimentation dominated throughout the majority of the Sappington Basin. Laterally equivalent coarser grained deposits should exist in up-dip locales, but such locales were not identified in this study. The absence of these locales does not prove or disprove their existence. In addition, proximal deposits of this nature have a lower preservation potential and may have been scalped off by LST2.

Another sequence boundary is proposed within the Lower Member and separates lithofacies 1A/1B from lithofacies 1C/1D/2 (Figure 3.25). The contact is signified by an iron oxide stained surface and a transgressive lag documented by Gutschick and Sandberg (1970). However, this surface is not widespread and requires further investigation.

Middle Member

Sequence boundary 2 (SB2) (Figure 3.43) separates the Lower Member from the Upper Member. This sequence boundary is evidenced by scouring of the Lower Member, lag channel fill of the scoured channels (Figure 3.28), and an abrupt lithologic change from U1 to U2. SB2 is the up-dip expression of LST2 (Figure 3.43), which theoretically exists to the west, distal of the shelf break. The absence of LST2 deposits means that again, similar to SB1, SB2 represents a stacked sequence boundary and transgressive surface. U2 is interpreted as representing the tail end of a TST (TST2) (Figure 3.43). Further, it signifies a different type of lithologic transgressive deposit than U1. Fine-grained siliciclastic deposition significantly slowed during U2 deposition, which allowed for carbonate deposition. The carbonates of U2 are seen in the transgressive lag (fragmented crinoid stems and brachiopod shells (Figure 3.28)). The surface between U2 and U3 is the maximum flooding surface (MFS1) (Figure 3.43) for the Middle Member sequence. U3-U5 is interpreted as a HST (HST1) (Figure 3.43) evidenced by the return of siliciclastic deposition to the Sappington Basin.

Upper Member

Sequence boundary 3 (SB3) (Figure 3.43) separates the Middle Member from the Upper Member. The sequence boundary is marked by a widespread transgressive lag (Figure

3.45) (lithofacies 6A) on top of U5. As with SB1 and SB2, the LST3 (Figure 3.43) deposits associated with the unconformity are absent, because of the location up-dip of the shelf break. Thus, SB3 represents a stacked sequence boundary and transgressive surface. The Upper Member (U6) is interpreted as a TST (TST3) (Figure 3.43) because of the limited oxygenation environment in which it was deposited. Low oxygen environments are associated with transgression because limited sedimentation and circulation creates stagnation at the sediment water interface (Wignall, 1991).

Another sequence boundary (SB4) (Figure 3.43) occurs at the contact between the Upper Member of the Sappington and the Scallion Member of the Lodgepole Formation. SB4 is characterized by scouring (Figure 3.36) of the Upper Member and the stark contrast in lithologies of the predominantly siliciclastic Upper Member of the Sappington with crinoidal packstones of the Scallion Member of the Lodgepole Formation.

Figures

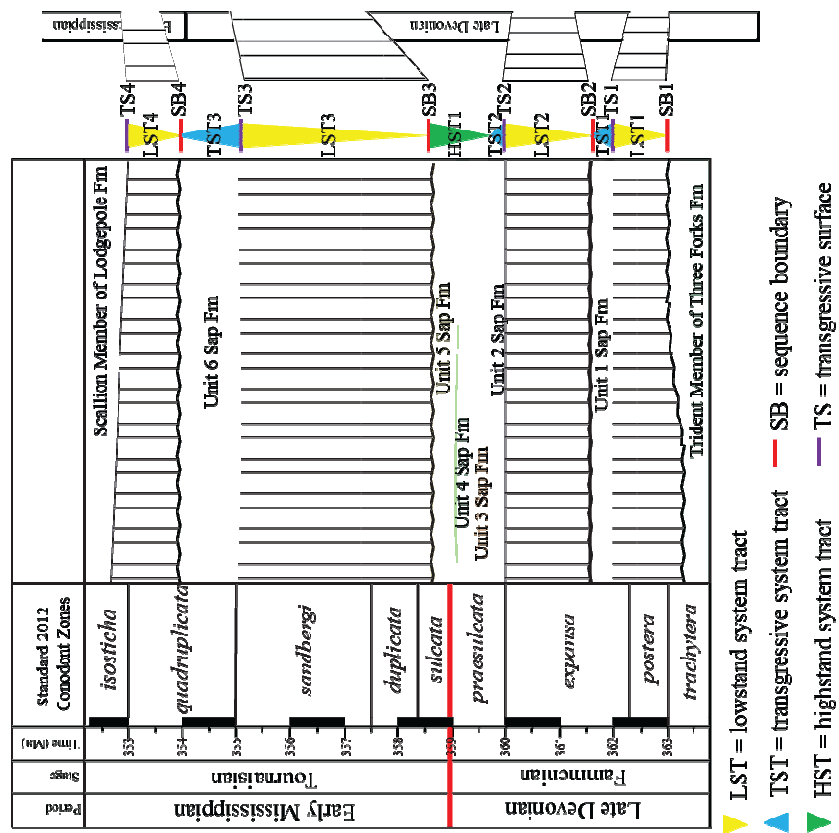


Figure 3.43 Sequence stratigraphic interpretations, (Left) relative sea-level curve, (Middle) clipped Wheeler Diagram with sequence stratigraphic interpretations to the right, (Right) Sappington stratigraphic column with sequence stratigraphic interpretations to the right. Triangles with lined shading (non-deposition) indicate the locations of LST's within a generalized Sappington stratigraphic column.

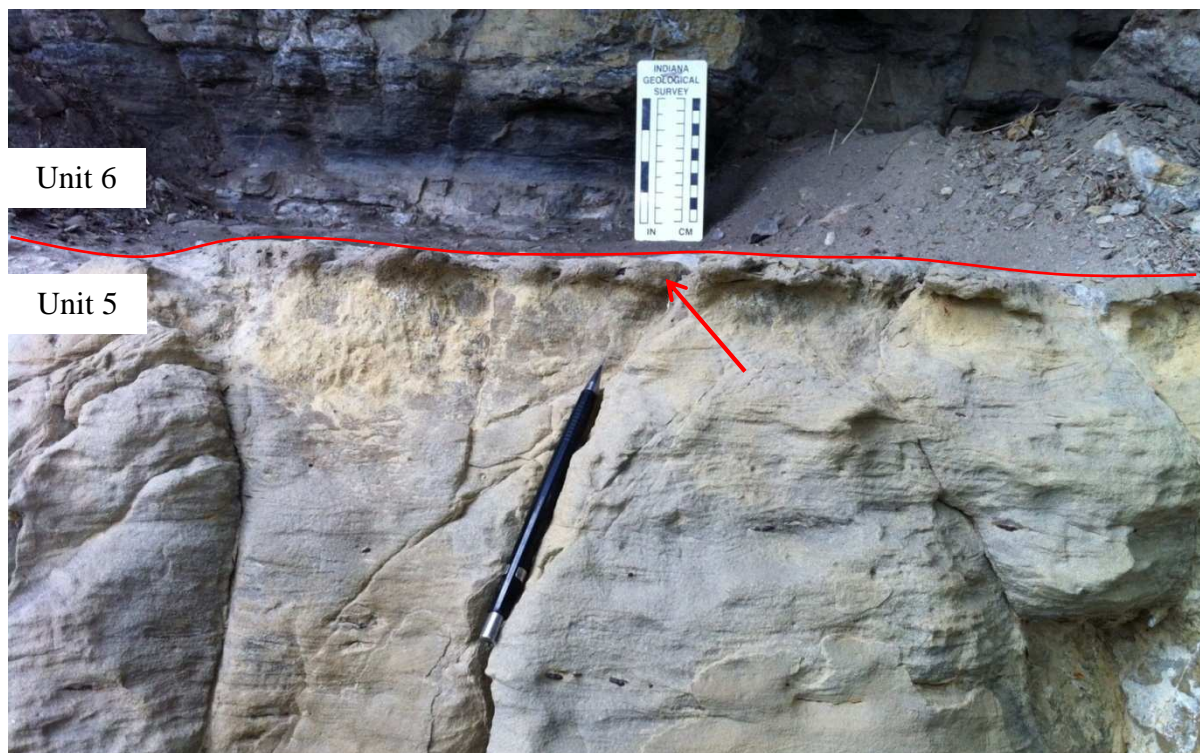


Figure 3.45 Transgressive lag (red arrow) at U5-U6 contact (photo credit: John Guthrie).

4. Discussion

Environment Interpretation Comparison

The majority of the stratigraphic units in the Sappington are broadly similar in lithologic character to what is observed in the Bakken. U4 of the Sappington is an exception to this generalized statement of comparison to Bakken units. U4 is dominated by various heterolithic bedding structures of interbedded mud and silt that could be interpreted as either a distal or proximal shift in environment from the underlying unit (U3). In previous studies, a variety of interpretations have been proposed for U4. Figure 4.1 is a comparison of the different interpretations of U4 from Gutschick et al. (1962), Nagase (2014), and this study. This study prefers the interpretation of a proximal environment shift from the underlying unit to U4 driven by abrupt sea-level fall and/or tectonic uplift. This fits within the overall trend of regression for the Sappington Middle Member and it correlates to the overall regression of the equivalent Lower Middle Member of the Bakken (Figure 4.3).

Sequence Stratigraphic Comparison to Bakken Formation

A Wheeler Diagram comparison of the Bakken (modified from Smith et al., 1995) and Sappington is presented in Figure 4.2. The Bakken Wheeler Diagram is generalized, because the development of unconformities bounding the Middle Member varies with location in the Williston Basin. The Sappington and Bakken Wheeler Diagrams vary, because of differential rates and amplitudes of subsidence and uplift in the basins associated with proximity to the Antler Convergent Margin. This difference in tectonic character resulted in the Sappington Basin being a shallower basin that was more susceptible to sea-level changes. The Lower Member of the Bakken is most similar to lithofacies 1A of the Lower Member of the Sappington, which was deposited in greater accommodation areas of the Sappington Basin to the west. The majority of Lower Member Sappington deposition in the Sappington Basin occurred in shallower, lower accommodation areas reflected by lithofacies 1B.

In the Bakken, a well-established (Angulo and Buatois, 2012) unconformity occurs at the contact between the Lower Middle Member and Upper Middle Member. Above this contact is an additional sequence of rocks that do not exist in the Sappington (Figure 4.3). The Lower Middle Member – Upper Middle Member unconformity of the Bakken is stacked with the Middle Member – Upper Member unconformity in the Sappington (Figure 4.3).

Multiple sequence stratigraphic interpretations exist for the Bakken Formation. The interpretation of Angulo and Buatois (2012) agrees with the sequence stratigraphic interpretation of the Sappington presented here (Figure 4.4).

Paleoclimate

The presence of multiple unconformities and an abundance of silt in the Sappington have implications for both polar (Gondwana) and alpine glaciation.

Unconformities, time gaps in deposition, result from periods of subaerial exposure or subaqueous sediment starvation. In the 10 my (Figure 3.17) between the end of Three Forks Formation deposition and the onset of Lodgepole Formation deposition, four prominent unconformities formed. These unconformities generally correspond to global sea-level falls (Figure 3.44), as documented by Haq and Schutter (2008), and correlate to unconformities in the Bakken and Exshaw Formations. This evidence, as well as the magnitude of base level change needed to create long term widespread non-deposition, supports global sea-level fall as the primary driving mechanism behind the Late Devonian-Early Mississippian Sappington unconformities. Historically, high-magnitude sea-level changes have been attributed to significant changes in polar glaciation, and thus the presence of high-magnitude sea-level changes in the Sappington indicates periods of increased glaciation during the Late Devonian-Early Mississippian. Late Paleozoic (Carboniferous and Permian) Gondwana glaciation events are well established (Caputo and Crowell, 1985; Crowell, 1999), but recently new evidence has been presented supporting an earlier onset of glaciation in the Late Devonian (Isaacson et al., 2008). The documentation of unconformities in the Sappington and equivalent formations (Bakken and Exshaw) further supports this theory.

The Middle Member of the Sappington is a silt-rich package of rocks with an average thickness of 62.5 ft. Soreghan et al. (2008) discussed the difficulties in manufacturing large amounts of medium- to coarse-grain size silt quartz clasts. The principal methods by which medium to coarse silt is created are: glacial grinding, frost (thermal) weathering, weathering of silt-rich protoliths, tectonic processes, salt weathering, fluvial comminution, eolian abrasion, chemical weathering, explosive volcanism, and biological origin (Soreghan et al., 2008). Of the ten processes outlined by Soreghan et al. (2008), only four: glacial grinding, weathering of silt-rich protoliths, tectonic processes, and explosive volcanism are capable of

producing the amount of silt observed in the Sappington. All of the four remaining mechanisms could be responsible for the abundance of silt in the Sappington.

Due to the required transport distances, the abundance of silt in the Sappington cannot be used as an indicator of Gondwana glaciation. However, the abundance of silt in the Sappington could have implications for alpine glaciation in the high mountains of the Acadian Orogeny, and/or the Antler Orogeny. This relationship between Sappington silt and alpine glaciation is speculative, but cannot be ruled out especially due to how little is known about the height of the mountains of the Antler Orogeny.

Figures

	Gutschick et al., 1959	Nagase, 2014	This study
U4 Descriptions			
U4 - U3 contact	Conformable	Conformable	Conformable
U4 - U5 contact	Conformable	Unconformable (forced regressive surface)	Conformable
U4 lithology	Shale	Silty dolostone with interbedded mudstone	Interbedded mudstone and siltstone
U4 sedimentary structures	Laminations, channelized lenses	Wavy laminations/lenticular, wave ripples	Lenticular bedding, wavy bedding, flaser bedding, tempestites
U4 biota	Blastoids, conchostracans, ostracodes (*from channel fill)	None	None
U4 ichnogenera	<i>Arenicolites (bifungites)</i>	<i>Planolites, Skolithos</i>	<i>Arenicolites (Bifungites), Chondrites, Macaronichnus, Planolites</i>
U4 Interpretations			
U4 - U3 contact	Silt/mud flat to mud flat	Offshore transition to offshore/offshore transition	Wave dominated shoreface to tidal dominated estuary
U4 - U5 contact	Mud flat to tidal flat/deltaic	Offshore/offshore transition to storm dominated shoreface	Tidal dominated estuary to wave dominated shoreface
U4 depositional environment	Mud flats	Open marine offshore/offshore transition	Tidal dominated estuary
Sea level	Transgression	Transgression	Regression/tectonic uplift

Figure 4.1 Comparison of U4 interpretations of Gutschick et al. (1962), Nagase et al. (2014), and this study.

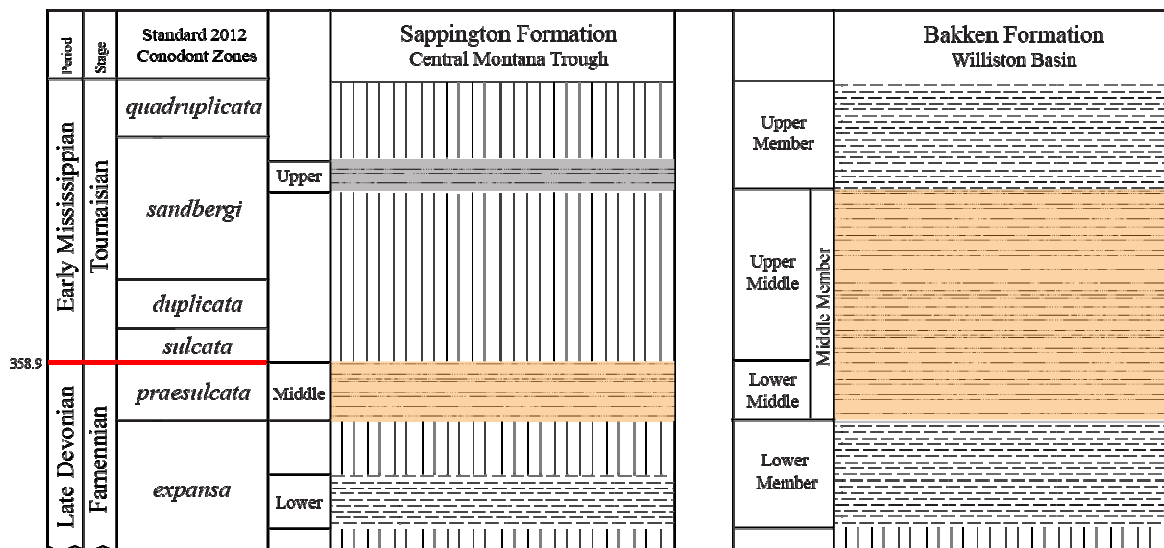


Figure 4.2 Wheeler Diagram comparison of the Bakken (modified Smith et al., 1995) and Sappington.

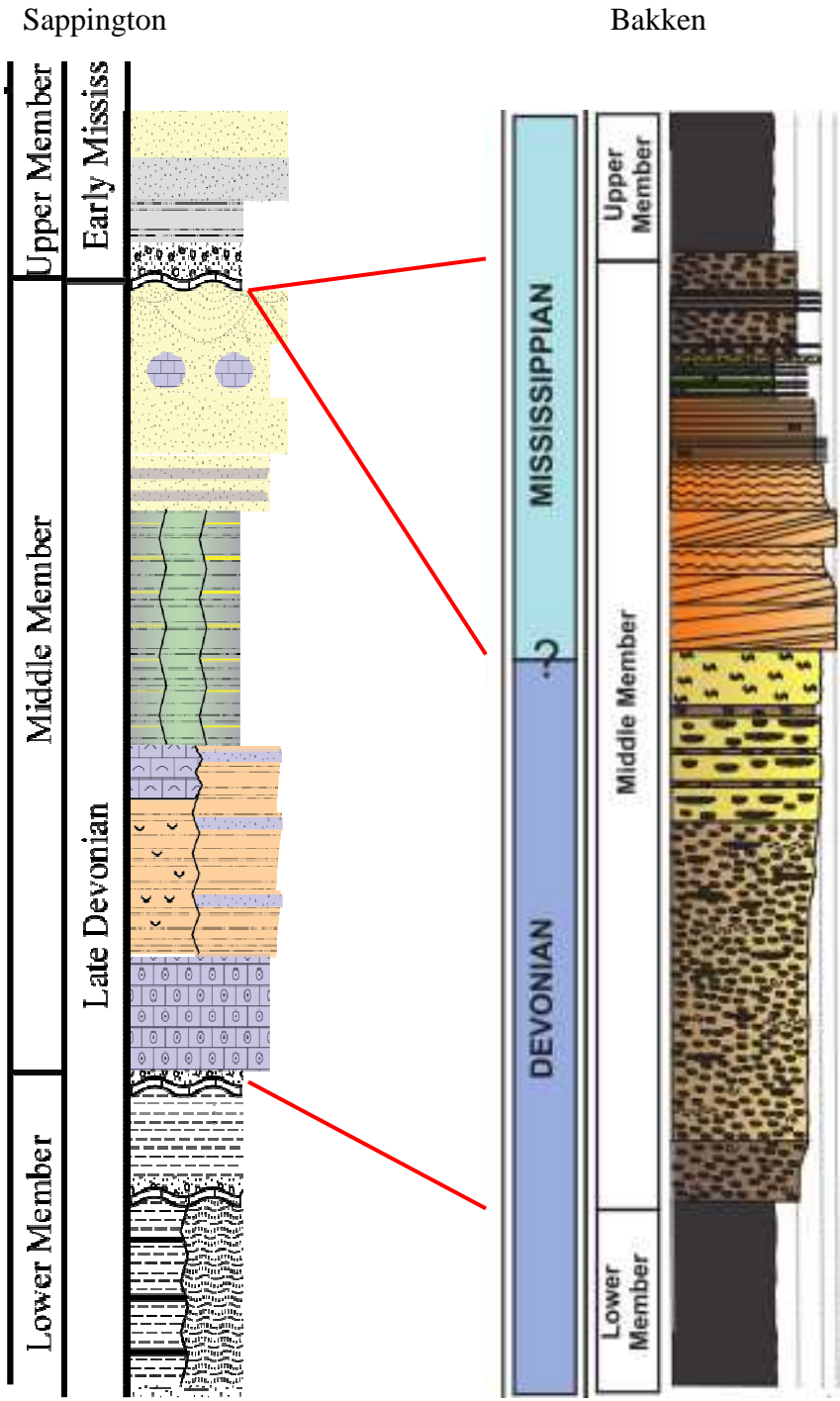


Figure 4.3 Correlation of unconformities in the Bakken (modified Angulo et al., 2008) and Sappington. The Upper Middle Member of the Bakken is proposed to not be present in the Sappington.

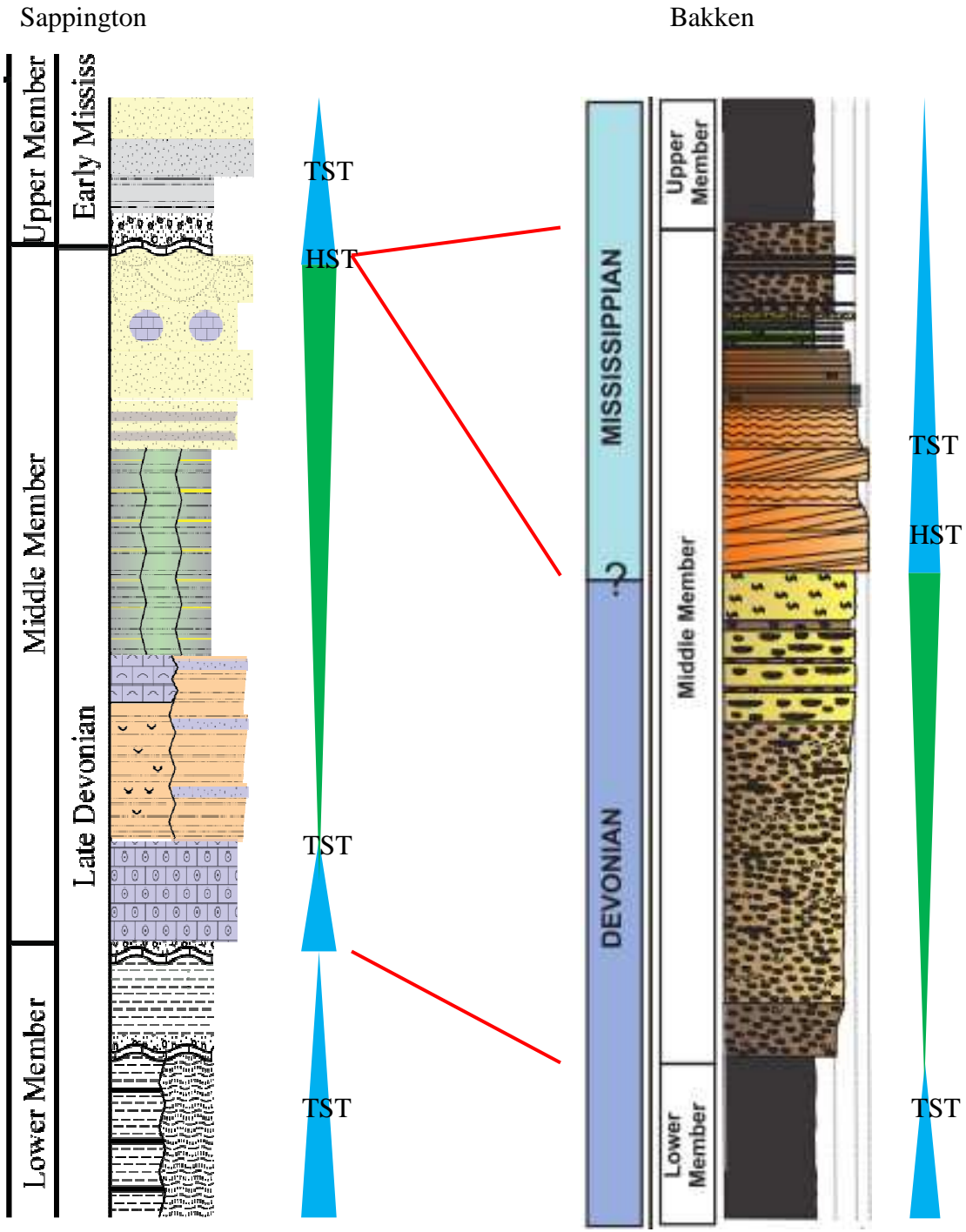


Figure 4.4 Sequence stratigraphy comparison of the Bakken (modified Angulo et al., 2008) and Sappington.

5. Conclusions

- 1) The Sappington can be subdivided into 6 stratigraphic units: Unit 1, Unit 2, Unit 3, Unit 4, Unit 5, Unit 6; and 19 lithofacies: 1A, 1B, 1C, 1D, 2, 3A, 3B, 3C, 4A, 4B, 4C, 5A, 5B, 5C, 5D, 6A, 6B, 6C, 6D.
- 2) The Sappington was deposited in a low-accommodation intracratonic basin. Depositional environment interpretations for the 6 Sappington stratigraphic units are: U1 – variable salinity, low energy, minimal oxygen flooded shelf; U2 – wave-dominated clastic starved shoreface; U3 – wave-dominated lower to middle shoreface; U4 – tidal-dominated estuary; U5 – wave-dominated lower shoreface to foreshore; U6 – minimal oxygen shoreface.
- 3) Four unconformities are present within and bounding the Sappington: Three Forks Formation – Lower Member of Sappington Formation, Lower Member – Middle Member, Middle Member – Upper Member, Upper Member of Sappington – Lodgepole Formation. These four unconformities represent four sequence boundaries (SB1, SB2, SB3, SB4). Fitting a sequence stratigraphic interpretation to the Sappington is difficult due to the low-accommodation intracratonic nature of the Sappington Basin. No lowstand systems tract deposits are present in the Sappington due to sediment bypass of the Sappington Basin. LST are represented in the Sappington by stacked sequence boundaries and transgressive surfaces. U1 of the Sappington is a TST, U2 of the Middle Member is a TST, U3-U5 is a HST, and U6 is a TST.
- 4) Stratigraphic unit isopachs and lithofacies character of the Sappington Lower and Middle Members in the study area indicate maximum accommodation to the west/southwest and thinning and pinching out on to the Beartooth Shelf to the southeast. Upper Member character indicates migration and extension of the Sappington Basin eastward to possible convergence with the Cottonwood Canyon Basin.
- 5) Bottom water eutrophication from the upwelling of deep nutrient-rich waters (Caplan and Bustin, 1999) and/or an increase in plant matter from Late Devonian land plant diversification (Algeo and Scheckler, 1998), in combination with sea-level transgression were the drivers for the creation of limited oxygen depositional environments and subsequent organic preservation in the Lower and Upper Member.

- 6) High-magnitude sea-level fluctuations created by the onset of Gondwana glaciation at the South Pole was the driver controlling periods of deposition and non-deposition (unconformities) in the Sappington Basin.
- 7) Differential low-amplitude tectonic subsidence and uplift of the western paleo-North American continental lithosphere, created by compressive stresses created at the Antler Convergent Margin (Dorobek et al., 1991), in conjunction with low-magnitude sea-level fluctuations were the driving mechanisms behind the lateral variability in lithologic character of the Sappington's six stratigraphic units and nineteen lithofacies.
- 8) Biostratigraphic dating of the Sappington (Knechtel and Hass, 1953; Sandberg and Klapper, 1967; Sandberg et al., 1972; P. Isaacson, pers. Commun., 2014; A. Warren, pers. Commun., 2014) and Bakken (Thrasher, 1985; Huber, 1986; Richards and Higgins, 1988; Richards, 1989; Karma, 1991) indicate correlation of both Lower Members, Upper Members, and the Middle Member of the Sappington with the Lower Middle Member of the Bakken. Similarities in facies character and the timing of deposition are attributed to glacially driven global sea-level cycles. Differences in facies character and timing of deposition are attributed to differences in Sappington Basin and Williston Basin architecture created from differential tectonic subsidence and uplift in the two basins.

6. References

- Achauer, Charles W. "Stratigraphy and Microfossils of the Sappington Formation in Southwestern Montana." *Billings Geological Society Tenth Annual Field Conference* (1959): 41–49.
- Adiguzel, Zeynep. "Correlation and Stratigraphic Analysis of the Bakken and Sappington Formations in Montana." Texas A&M, 2012.
- Algeo, Thomas J., and Timothy W. Lyons. "Hydrographic Conditions of the Devonian-Carboniferous North American Seaway Inferred from Sedimentary Mo-TOC Relationships." *Palaeogeography, Palaeoclimatology, Palaeoecology* 256 (2007): 204–230.
- Algeo, T. J., and S. E. Scheckler. "Terrestrial-Marine Teleconnections in the Devonian: Links between the Evolution of Land Plants, Weathering Processes, and Marine Anoxic Events." *Philosophical Transactions of the Royal Society B: Biological Sciences* 353.1365 (1998): 113–130.
- Angulo, Solange, and Luis A. Buatois. "Integrating Depositional Models, Ichnology, and Sequence Stratigraphy in Reservoir Characterization: The Middle Member of the Devonian–Carboniferous Bakken Formation of Subsurface Southeastern Saskatchewan Revisited." *AAPG Bulletin* 96.6 (2012): 1017–1043.
- Angulo, Solange, Luis Buatois, and Steve Halabura. "Paleoenvironmental and Sequence-Stratigraphic Reinterpretation of the Upper Devonian – Lower Mississippian Bakken Formation of Subsurface Saskatchewan Integrating Sedimentological and Ichnological Data." *Summary of Investigations, Saskatchewan Geological Survey* 1 (2008): 1–24.
- Anklin, J.M. and 40 others, 1993. Greenland Ice-core Project (GRIP) Members. Climate instability during the last inter- glacial period recorded in the GRIP ice core. *Nature* 364, 203–207.
- Becker, R.T.; Gradstein, F.M.; Hammer, O. "The Devonian Period." *The Geologic Time Scale 2012*. N. p., 2012. 559–582.
- Benson, Anthony L. "Devonian Stratigraphy of Western Wyoming and Adjacent Areas." *AAPG Bulletin* 50.12 (1966): 2566–2603.
- Berry, George W. "Stratigraphy and Structure at Three Forks, Montana." *GSA Bulletin* 54 (1943): 1–30.
- Blakey, R., 2013, North American Key Time-slice Paleogeographic Maps, Early Mississippian – 345 Ma (350-340), accessed October 31, 2014, http://cpgeosystems.com/images/NAM_key-345Ma_EMiss-sm.jpg.

- Blakey, R., 2005, Paleogeography and Geologic Evolution of North America, Middle Devonian (385Ma), accessed August 4, 2014, <http://www2.nau.edu/rcb7/namD385.jpg>.
- Burton, B. R., Ballard, D. W., Lageson, D. R., Perkins, M., Schmidt, C. J., and Warne, J. R., 1998, Deep drilling results and new interpretations of the Lombard thrust, southwest Montana, *in* Berg, R., ed., Proceedings of Belt Symposium III: Montana Bureau of Mines and Geology Special Paper 112, p. 229-243.
- Caplan, Mark L., R. Marc Bustin, and Kurt A. Grimm. "Demise of a Devonian-Carboniferous Carbonate Ramp by Eutrophication." *Geology* 24.8 (1996): 715–718.
- Caplan, Mark L., and R. Mark Bustin. "Devonian–Carboniferous Hangenberg Mass Extinction Event, Widespread Organic-Rich Mudrock and Anoxia: Causes and Consequences." *Palaeogeography, Palaeoclimatology, Palaeoecology* 148 (1999): 187–207.
- Crowell, J.C.V., 1999. Pre-Mesozoic ice ages: their bearing on understanding the climate system. *Geol. Soc. Amer. Mem.*, vol. 192. 106pp.
- Caputo, M.V., 1985. Late Devonian glaciation in South America. *Palaeogeogr. Palaeoclimatol. Palaeoecol.* 51, 291–317.
- Cecil, C. Blaine. *Eolian Dust and the Origin of Sedimentary Chert*. Reston, VA: N. p., 2004.
- Davydov, V.I.; Korn, D.; Schmitz, M.D. "The Carboniferous Period." *The Geologic Time Scale 2012*. N. p., 2012. 603–627.
- Dorobek, S. L. et al. "Subsidence across the Antler Foreland of Montana and Idaho: Tectonic versus Eustatic Effects." *Sedimentary Modeling: Computer Simulation and Methods for Improved Parameter Definition*. N. p., 1991. 231–251.
- Dreesen, Roland; Sandberg, Charles A.; Ziegler, Willi. "Review of Late Devonian and Early Carboniferous Conodont Biostratigraphy and Biofacies Models as Applied to the Ardenne Shelf." *Annales de la Societe geologique de Belgique, Belgian Geological Survey* 109 (1986): 27–42.
- Ettensohn, Frank R., R. Thomas Lierman, and Charles E. Mason. "Upper Devonian – Lower Mississippian Clastic Rocks in Northeastern Kentucky: Evidence for Acadian Alpine Glaciation and Models for Source-Rock and Reservoir-Rock Development in the Eastern United States." *American Institute of Professional Geologists - Kentucky Section*. N. p., 2009. 1–53.
- Fischer, A. G. and Arthur, M. A. Secular variations in the pelagic realm, in: Deep-water carbonate environments, edited by: Cook, H. E. and Enos, P., *SEPM Spec. P.*, 25, 19–50, 1977.

- Frakes, L.A., Francis, J.E., Syktus, J.I., 1992. *Climate Modes of the Phanerozoic*. Cambridge University Press, Cambridge, 274 pp.
- Grader, G. W., and Doughty, P. T. *Stratigraphy and Hydrocarbon Systems of the Sappington (Bakken/Exshaw) and Three Forks Formations in Western Montana*. 2012.
- Grader, G. W. Geological Society of America Abstract. 2005.
- Gutschick, R. C., and T. G. Perry. "Measured Sections of Sappington (Kinderhookian) Sandstone in Southwestern Montana." *AAPG Bulletin* 41.8 (1957): 1892–1905.
- . "Sappington (Kinderhookian) Sponges and Their Environment." *Journal of Paleontology* 33.6 (1959): 977–985.
- Gutschick, Raymond A., and Joaquin Rodriguez. "Biostratigraphy of the Pilot Shale (Devonian-Mississippian) and Contemporaneous Strata in Utah, Nevada, and Montana." *GSA Annual Meeting*. Vol. 26. N. p., 1978. 37–63.
- Gutschick, Raymond C., and Richard Lamborn. "Bifungites, Trace Fossils from Devonian-Mississippian Rocks of Pennsylvanian and Montana, U.S.A." *Palaeogeography, Palaeoclimatology, Palaeoecology* 18 (1975): 193–212.
- Gutschick, R. C.; Suttner, Lee J.; Switek, Michael J. "Biostratigraphy of Transitional Devonian-Mississippian Sappington Formation of Southwest Montana." *Billings Geological Society 13th Annual Field Conference* (1962): 79–89.
- Gutschick, R.C.; Rodriguez, Joaquin. "Brachiopod Zonation and Correlation of Sappington Formation of Western Montana." *AAPG Bulletin* 51.4 (1967): 601–620.
- Gutschick, R.C.; Sandberg, Charles A. "Latest Devonian Conchostracans Along Cordilleran Miogeosyncline, Alberta, Montana, Utah, and Nevada." *AAPG Bulletin Abstracts* (1970): 849–850.
- Haq, Bilal U., and Stephen R. Schutter. "A Chronology of Paleozoic Sea-Level Changes." *Science* 322 (2008): 64–68.
- Harlan, S. S. et al. "Paleomagnetism and Geochronology of Sills of the Doherty Mountain Area, Southwestern Montana: Implications for the Timing of Fold-and-Thrust Belt Deformation and Vertical-Axis Rotations along the Southern Margin of the Helena Salient." *GSA Bulletin* 120.9/10 (2008): 1091–1104.
- Huber, T. P., 1986, Conodont biostratigraphy of the Bakken Formation and lower Lodgepole Formation (Devonian and Mississippian), Williston Basin, North Dakota: Unpublished M. Sc. thesis, University of North Dakota, 274 p.

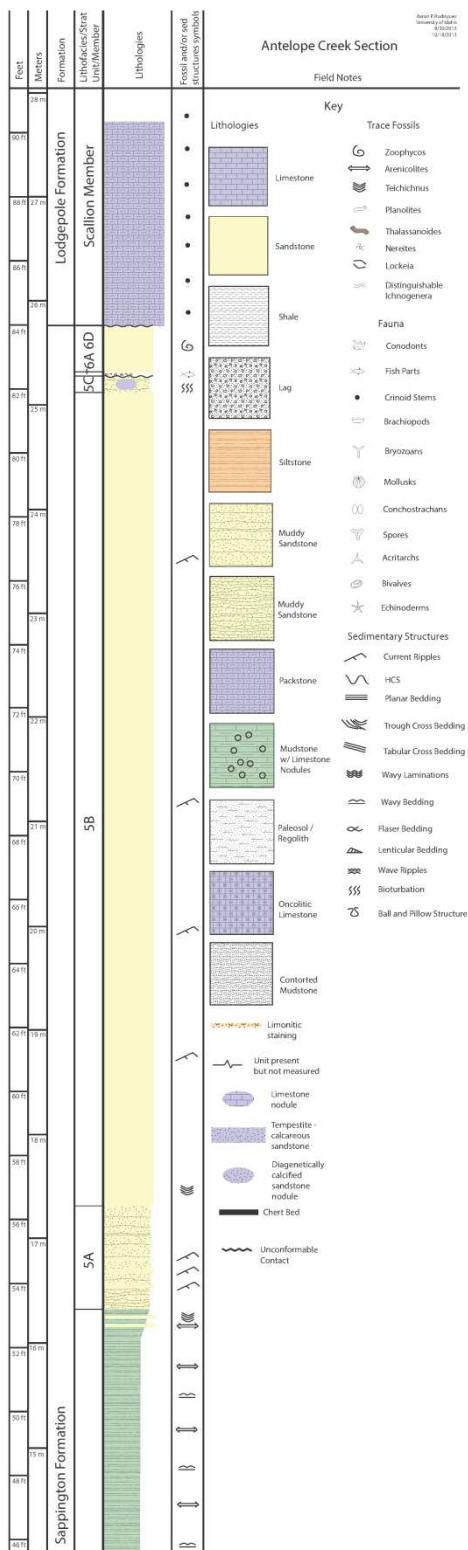
- Isaacson, P.E. et al. "Late Devonian–earliest Mississippian Glaciation in Gondwanaland and Its Biogeographic Consequences." *Palaeogeography, Palaeoclimatology, Palaeoecology* 268 (2008): 126–142.
- Karma, R., 1991, Geology and geochemistry of the Bakken Formation (Devonian-Mississippian) in Saskatchewan: Unpublished M. Sc. Thesis, University of Regina, 308 p.
- Knechtel, M. M.; Hass, W. H. "Kinderhook Conodonts From Little Rocky Mountains, Northern Montana." *Billings Geological Society 4th Annual Field Conference* (1953): 83–84.
- MacEachern, James A. "Integrated Ichnology and Sedimentology Identification of Common Ichnogenera and Primary Sedimentary Structures." 2014 : 1–92.
- Maughan, E. K., 1989, Geology and Petroleum Potential Central Montana Province U.S. Geological Survey Open-File Report OF 88-450 N.
- McMannis, W. J. "Devonian Stratigraphy Between Three Forks, Montana and Yellowstone Park." *Billings Geological Society 13th Annual Field Conference* (1962): 4–12.
- McMannis, William J. "Geology of the Bridger Range, Montana." *GSA Bulletin* 66 (1955): 1385–1430.
- Nagase, Tetsuro. "Developing a Facies Model and Sequence Stratigraphic Framework for the Devonian-Mississippian Sappington Formation in Southwestern-Central Montana." University of Montana, 2014.
- Pemberton, S. George, MacEachern, James A., Gingras, Murray K., and Bann, Kerrie L. *Trace Fossil Atlas - The Recognition of Common Trace Fossils in Cores*. SEPM, 2011.
- Perry, William J. *Oil and Gas Assessment: Montana Thrust Belt Province (027)*. N. p., 1995.
- Plint, A.G., 2010, Chapter 8, Wave- and storm-dominated shoreline and shallow marine systems. In: *Facies Models*, 4th Edition, Dalrymple, R.W. and James, N.P., eds. Geological Association of Canada, p. 167-199.
- Peterson, J. A. "General Stratigraphy and Regional Paleotectonics of the Western Montana Overthrust Belt." *Paleotectonics and Sedimentation in the Rocky Mountain Region, United States*. N. p., 1986. 57–86.
- Posamentier, H.W., Vail, P. R., 1988. Eustatic controls on clastic deposition. II. Sequence and systems tract models. In: Wilgus, C. K., Hastings, B. S., Kendall, C. G. St. C., Posamentier, H.W., Ross, C.A., Van Wagoner, J. C. (Eds.), *Sea-level Changes – An Integrated Approach*. SEPM Special Publication 42, 125–154.

- Rau, Jon L. "The Stratigraphy of the Three Forks Formation." *Billings Geological Society 13th Annual Field Conference* (1962): 51–66.
- Richards, Barry C.; Ross, Gerald M.; Utting, John. "U-Pb Geochronology, Lithostratigraphy and Biostratigraphy of Tuff in the Upper Famennian to Tournaisian Exshaw Formation: Evidence for a Mid-Paleozoic Magmatic Arc on the Northwestern Margin of North America." *Canadian Society of Petroleum Geologists* 19 (1999): 158–207.
- Richards, B. C., et al. "Carboniferous Strata of the Western Canada Sedimentary Basin." Mossop, G. D., Shetsen, I., and comp. *Geological Atlas of the Western Canada Sedimentary Basin*. 1994
- Richards, B. C., 1989, Upper Kaskaskia sequence -uppermost Devonian and lower Carboniferous, in B. D. Ricketts, ed., *Western Canadian Sedimentary Basin, a case history*: Can. Soc. Petrol. Geol., Calgary, p. 165-201.
- Richards B. C. and A. C. Higgins, 1988, Devonian-Carboniferous boundary beds of the Palliser and Exshaw formations at Jura Creek, Rocky Mountains, southwestern Alberta, in N. J. McMillan, A. F. Embry, and D. J. Glass, eds., *Devonian of the World, Vol. II, Sedimentation*: CSPG, Calgary, p. 399-412.
- Robin, Cecile; Guillocheau, Francois; Gaulier, Jean-Michel. "Discriminating between Tectonic and Eustatic Controls on the Stratigraphic Record in the Paris Basin." *Terra Nova* 10.6 (1998): 323–329.
- Sandberg, Charles A. *Nomenclature and Correlation of Lithologic Subdivisions of the Jefferson and Three Forks Formations of Southern Montana and Northern Wyoming*. N. p., 1965.
- . "Stratigraphic Section of Type Three Forks and Jefferson Formations at Logan, Montana." *Billings Geological Society 13th Annual Field Conference* (1962): 47–50.
- Sandberg, Charles A.; Klapper, Gilbert. *Stratigraphy, Age, and Paleotectonic Significance of the Cottonwood Canyon Member of the Madison Limestone in Wyoming and Montana*. N. p., 1967.
- Sandberg, Charles A.; StreeL, Maurice; Scott, Richard A. "Comparison between Conodont Zonation and Spore Assemblages at the Devonian-Carboniferous Boundary in the Western and Central United States and in Europe." *Congres International de Stratigraphie et de Géologie du Carbonifère. Krefeld 1971* (1972): 179–195.
- Savoy, L. E., and A. G. Harris, 1993, Conodont biofacies and taphonomy along a carbonate ramp to black shale basin (latest Devonian and earliest Carboniferous), southernmost Canadian cordillera and adjacent Montana: *Canadian Journal of Earth Science*, v. 30, p. 2404–2422.

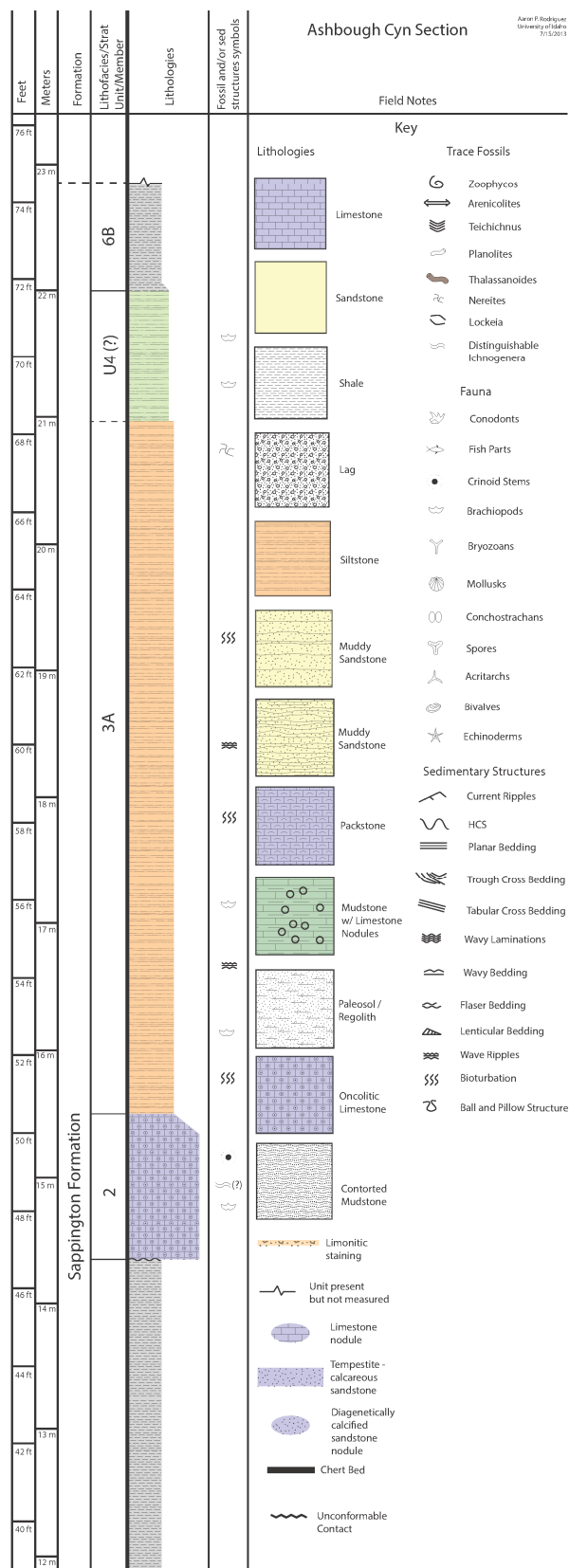
- Schietinger, Paul S. "Upper Devonian and Lower Mississippian Stratigraphy of Northwestern Montana: A Petroleum System Approach." Colorado School of Mines, 2012.
- Schmidt, Christopher J.; Neill, J. Michael. "Structural Evolution of the Southwest Montana Transverse Zone." *Rocky Mountain Association of Geologists* (1982)
- Sears, J.W., 1988, Two major thrust slabs in the west-central Montana Cordillera, in Schmidt, C.J., and Perry, W. J., editors, Interactions of the Rocky Mountain Foreland and the Cordilleran Thrust Belt: Geological Society of America, Memoir 171, p. 165–170.
- Shi, G.R., and Z.Q. Chen. "Lower Permian Oncolites from South China: Implications for Equatorial Sea-Level Responses to Late Palaeozoic Gondwanan Glaciation." *Journal of Asian Earth Sciences* 26 (2006): 424–436.
- Smith, M.G.; Bustin, R.M.; Caplan, M.L. "Sequence Stratigraphy of the Bakken and Exshaw Formations: A Continuum of Black Shale Formations in the Western Canada Sedimentary Basin." *7th International Williston Basin Symposium* (1995): 399–409.
- Sonnenberg, Stephen A., and Aris Pramudito. "Petroleum Geology of the Giant Elm Coulee Field, Williston Basin." *AAPG Bulletin* 93.9 (2009): 1127–1153.
- Soreghan, Gerilyn S., Michael J. Soreghan, and Michael A. Hamilton. "Origin and Significance of Loess in Late Paleozoic Western Pangaea: A Record of Tropical Cold?" *Palaeogeography, Palaeoclimatology, Palaeoecology* 268 (2008): 234–259.
- Thrasher, L. C., 1985, Macrofossils and biostratigraphy of the Bakken Formation (Devonian and Mississippian) in western North Dakota: Masters thesis, University of North Dakota, 292 p.
- Vail, P.R., Mitchum Jr., R.M., Todd, R.G., Widmier, J.M., Thompson III, S., Sangree, J.B., Bubb, J.N., Hatleilid, W.G., 1977. Seismic stratigraphy and global changes of sea-level. In: Payton, C.E. (Ed.), *Seismic Stratigraphy-Applications to Hydrocarbon Exploration*: American Association Petroleum Geologists Memoir, 26, pp. 49–212.
- Vuke, S.M, Lonn, J.D., Berg, R.B., Schmidt, C.J. Geologic Map of the Bozeman 30' x 60' Quadrangle Southwestern Montana. Butte, Montana: Montana Bureau of Mines and Geology, 2014.
- Wignall, Paul B. "Model for Transgressive Black Shales?" *Geology* 19 (1991): 167–170.

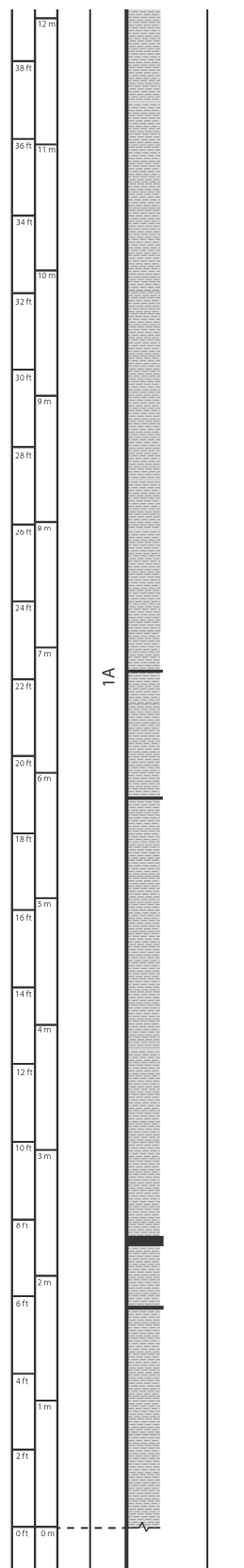
7. Appendix – Stratigraphic sections

Antelope Creek Section

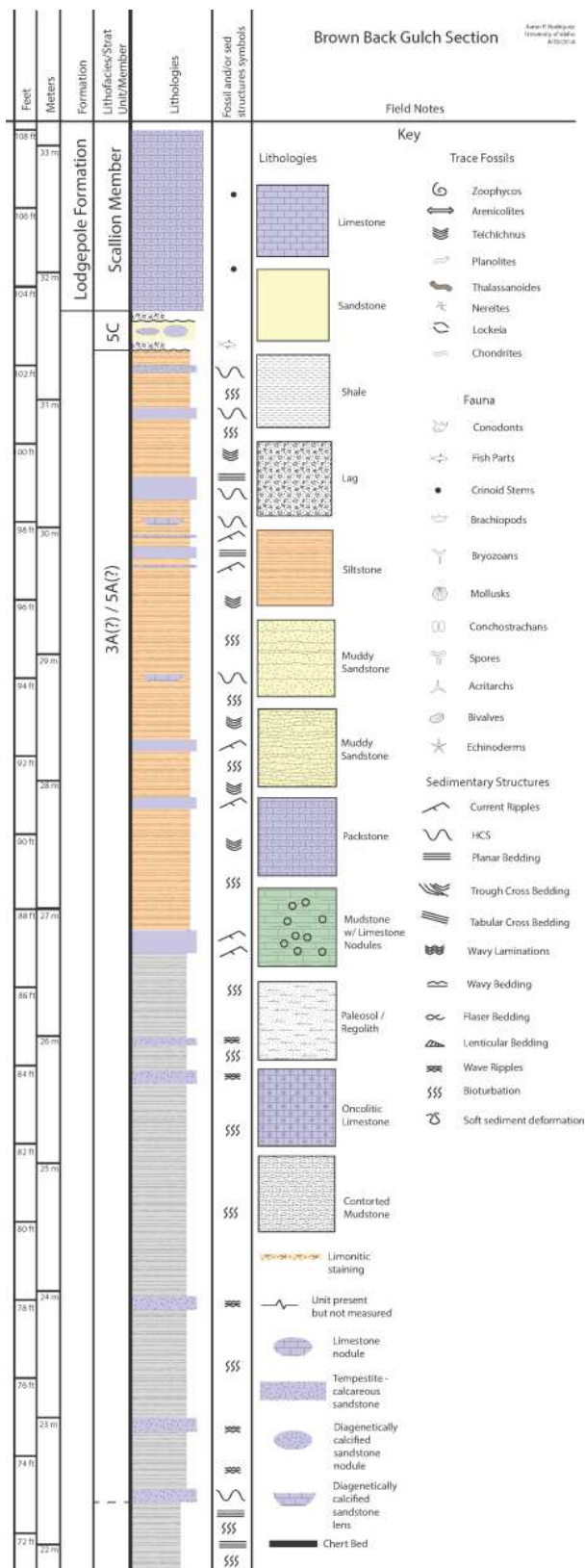


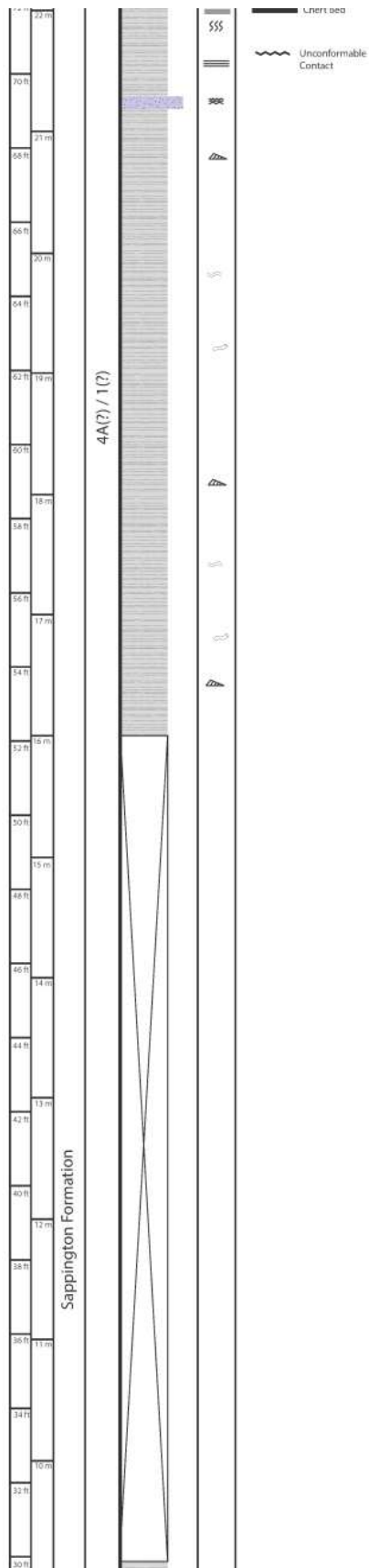
Ashbough Canyon Section



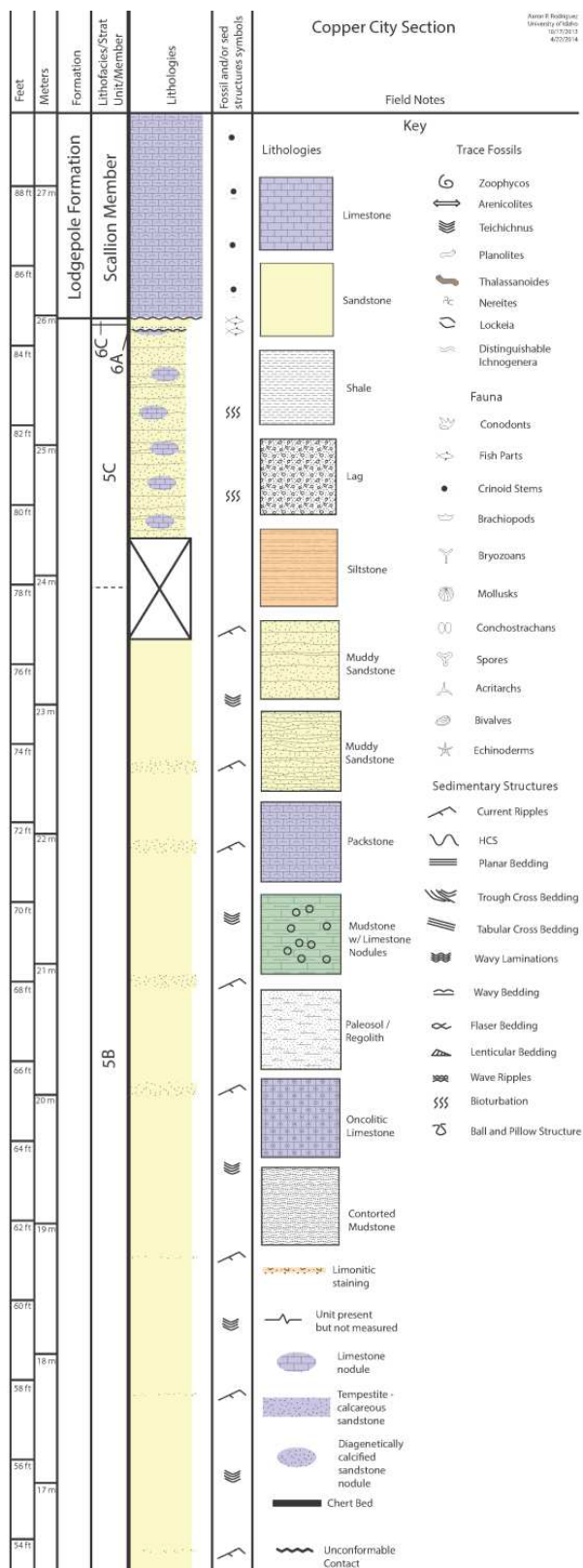


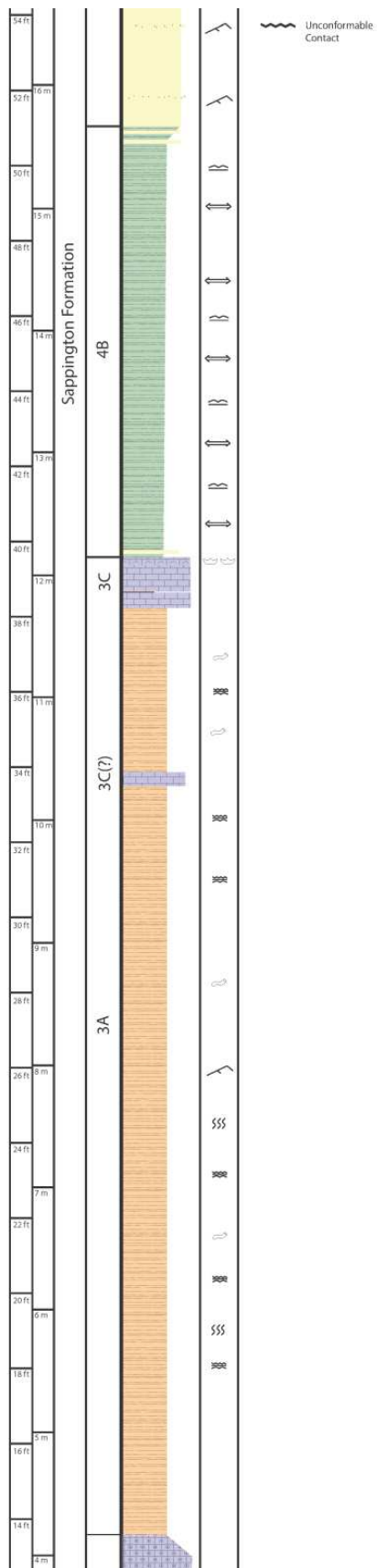
Brown Back Gulch Section

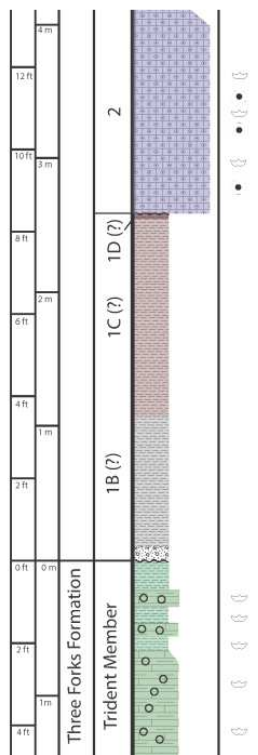




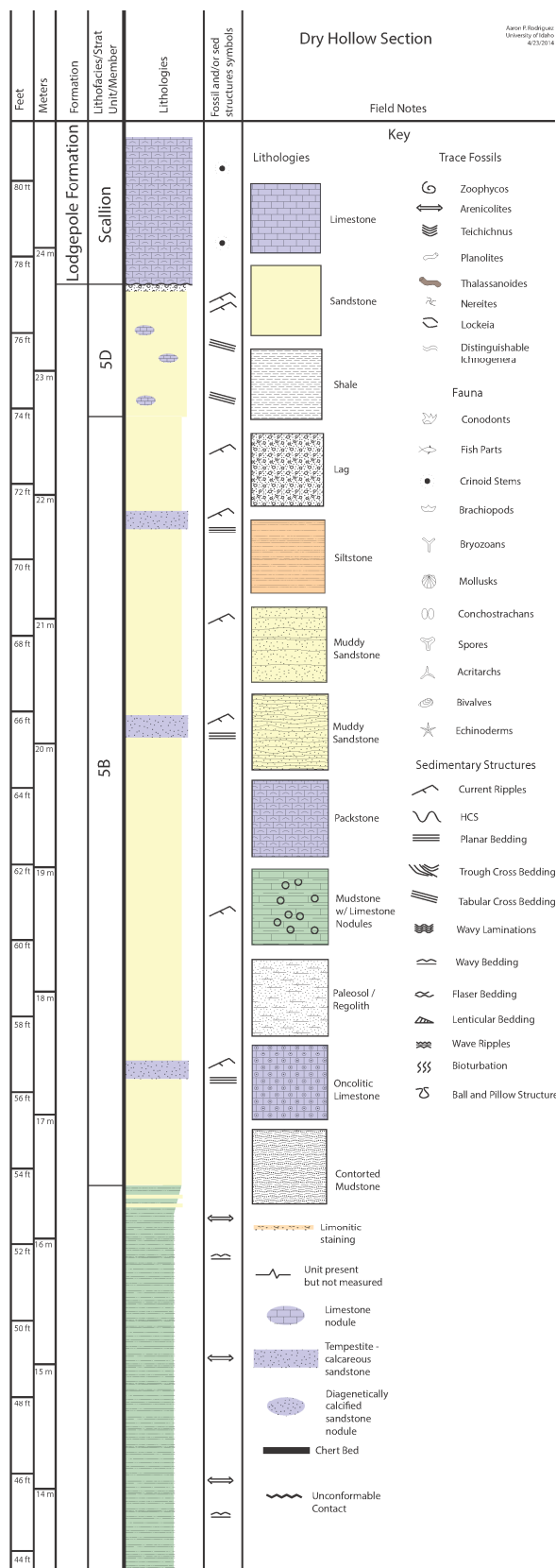
Copper City Section

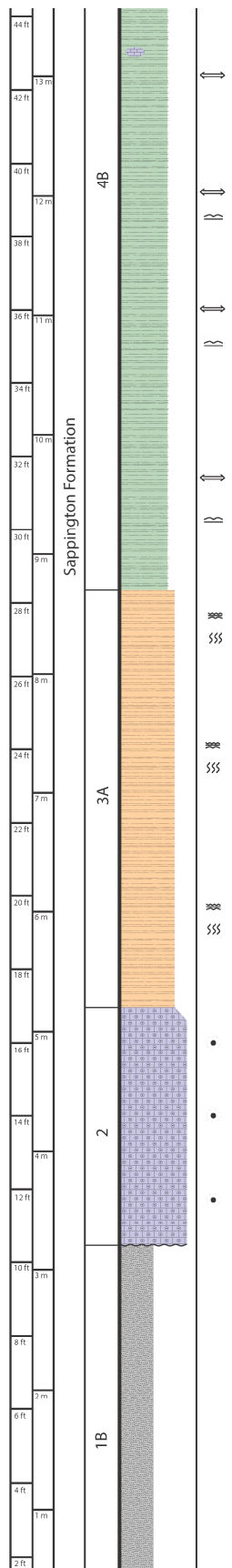


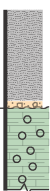




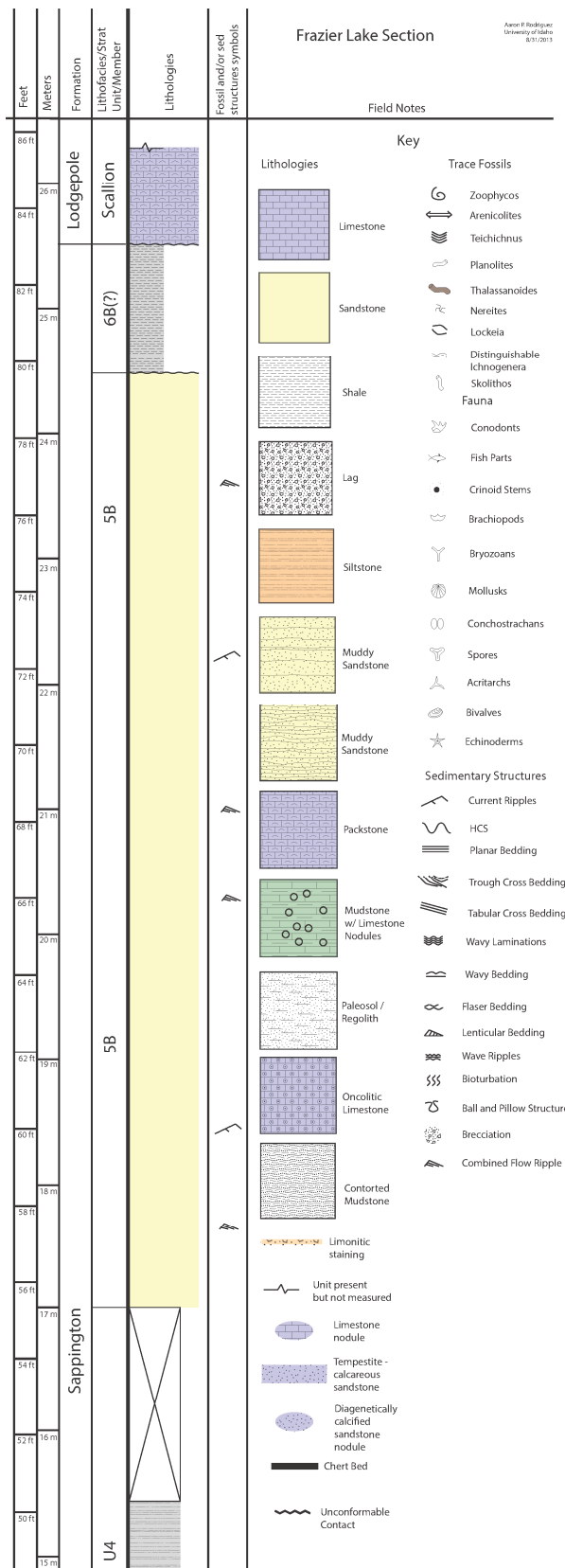
Dry Hollow Section

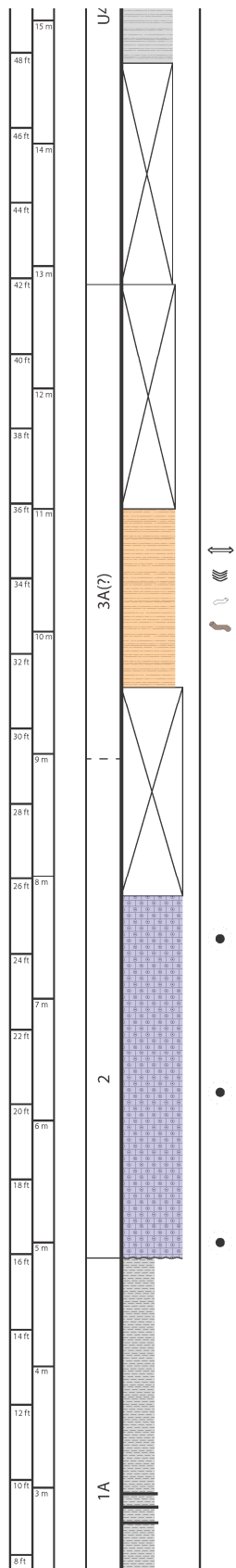


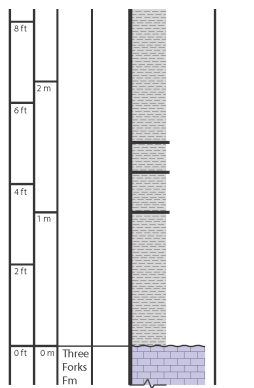


2 ft	
0 ft	0 m
3 Forks Fm	
Trident	
	

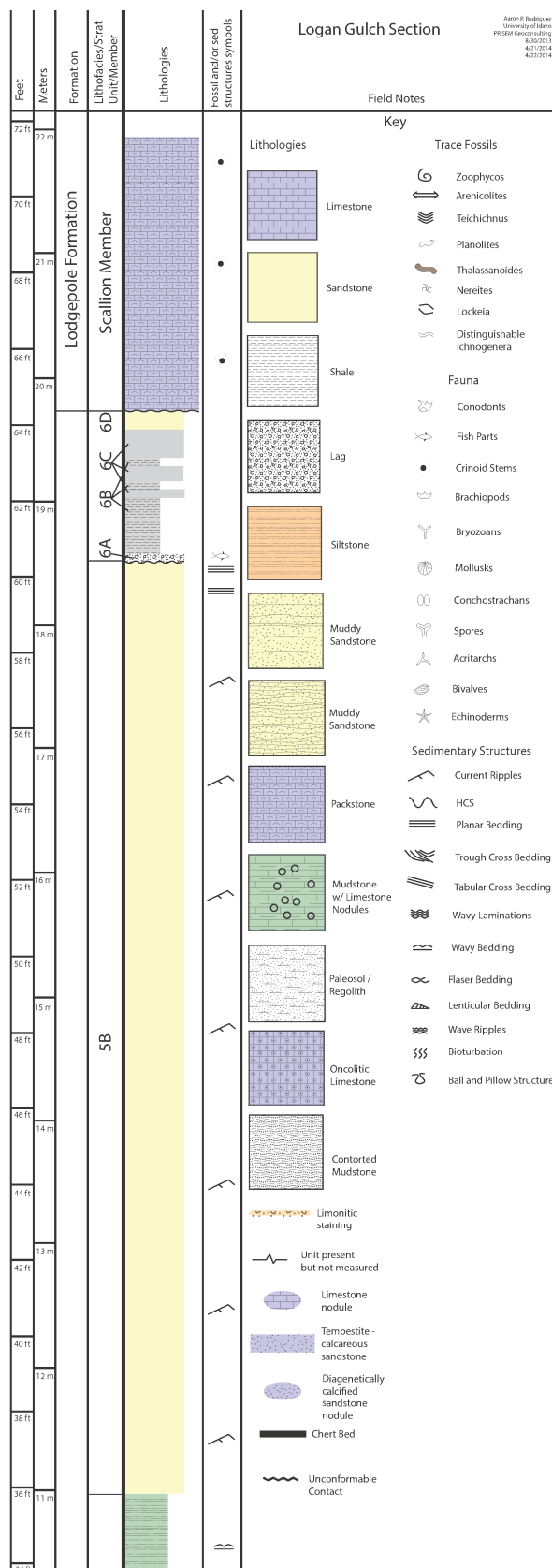
Frazier Lake Section

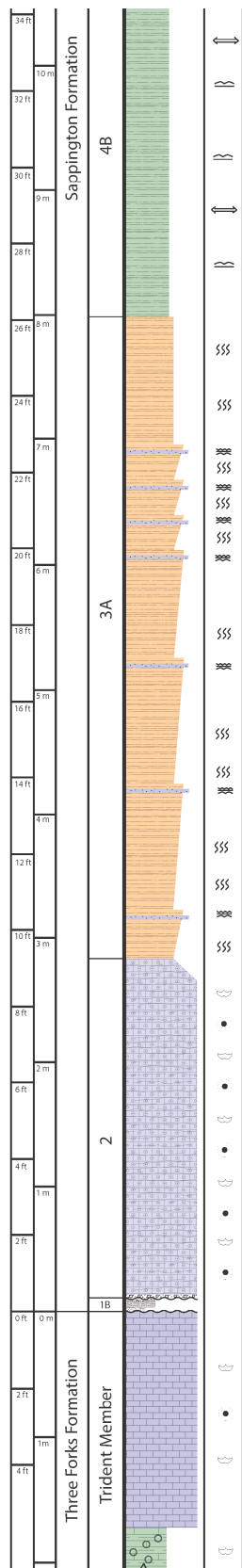




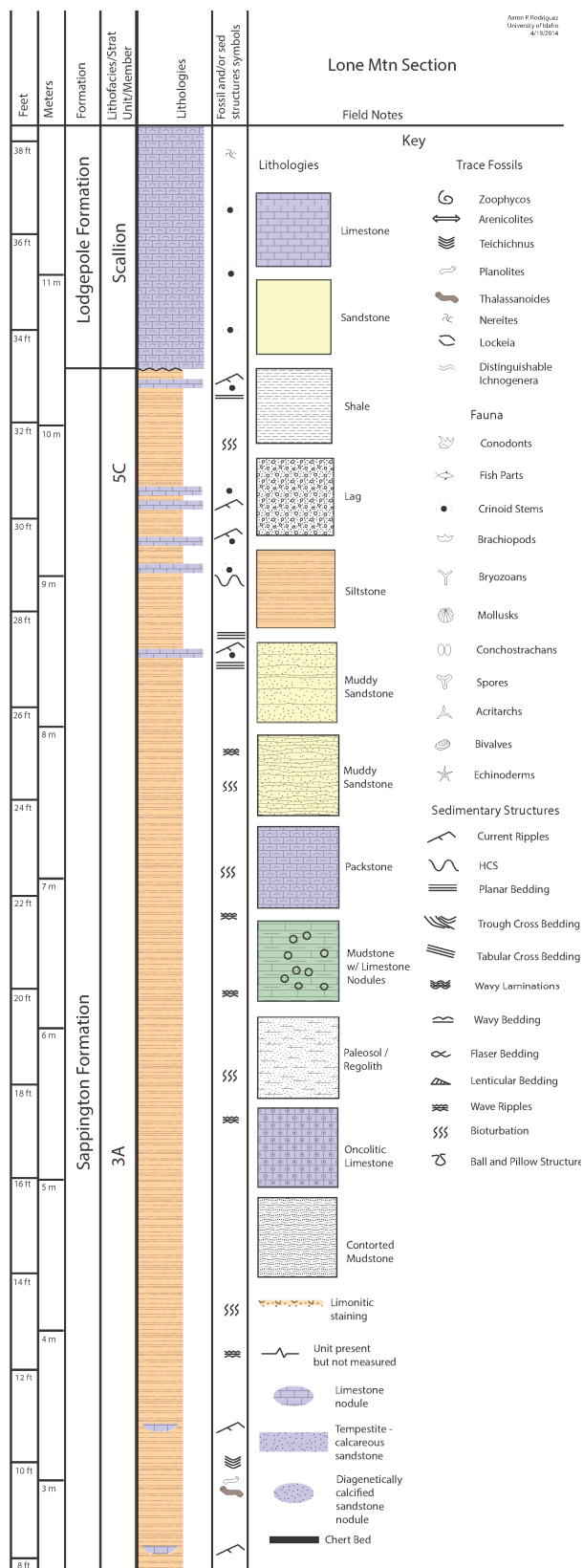


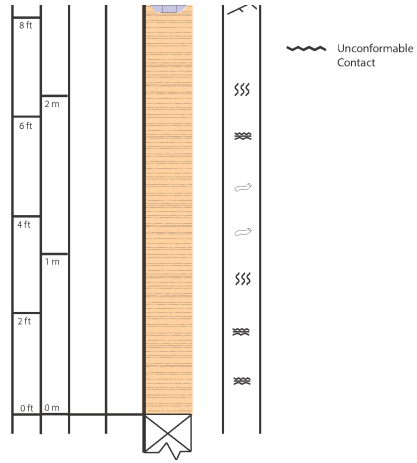
Logan Gulch Section



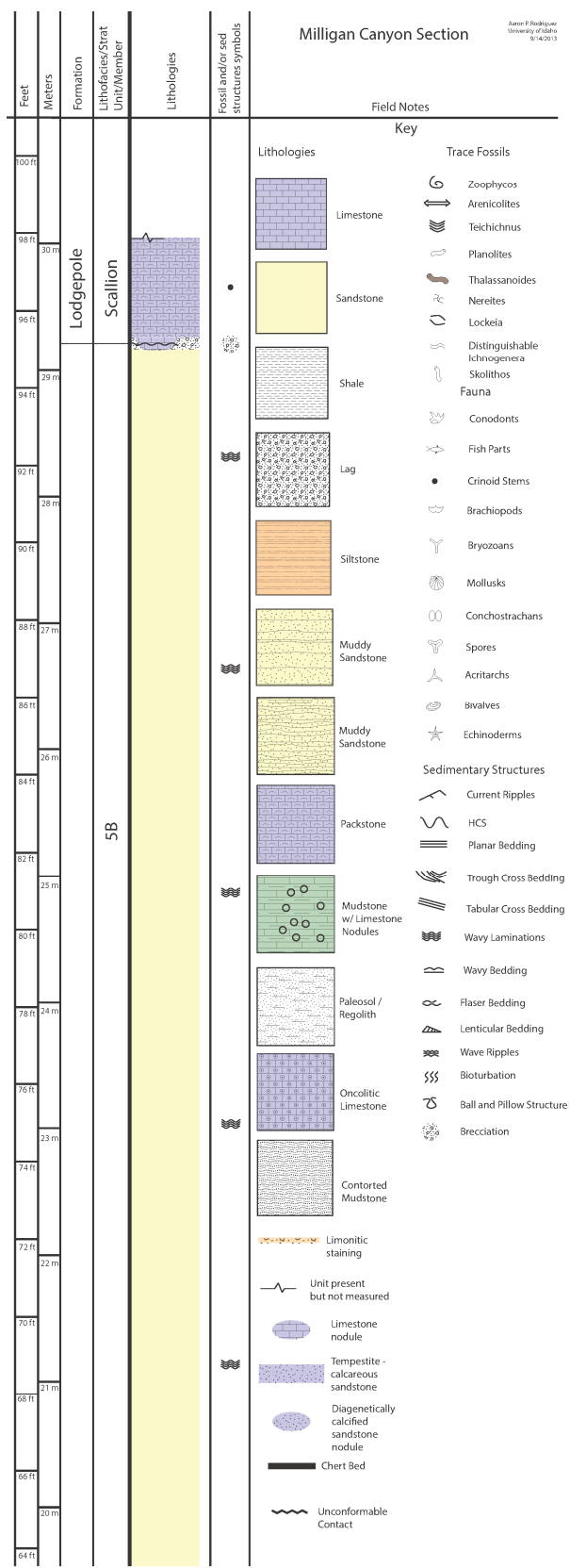


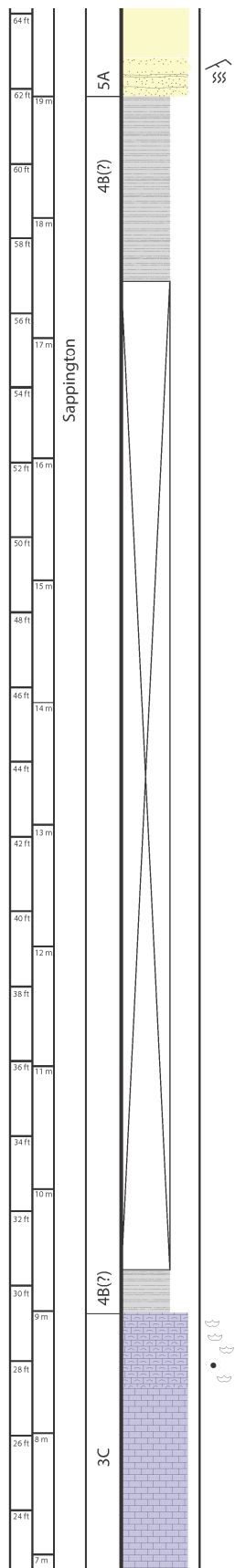
Lone Mountain Section

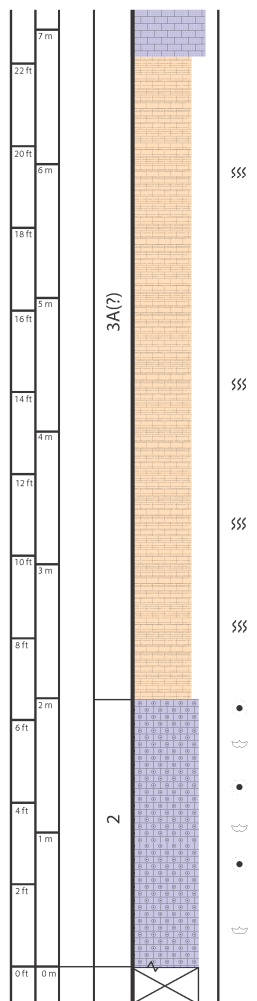




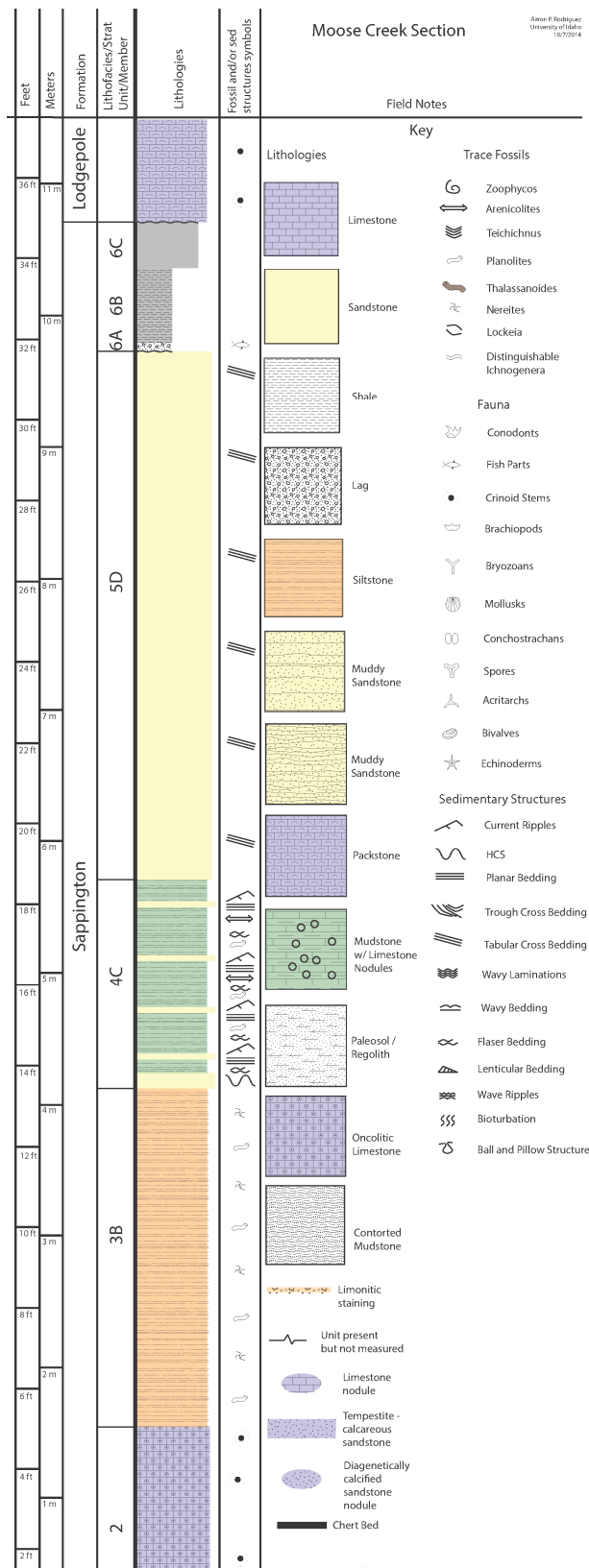
Milligan Canyon Section (Sappington type section)

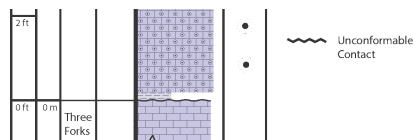




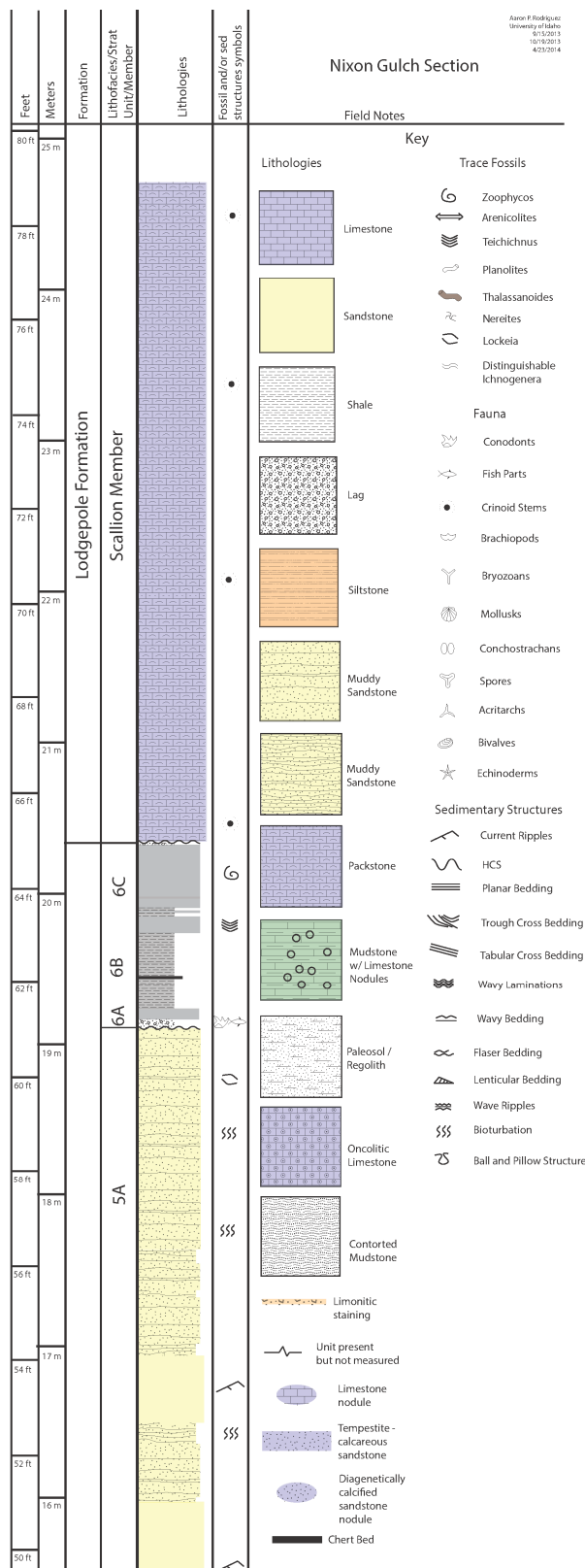


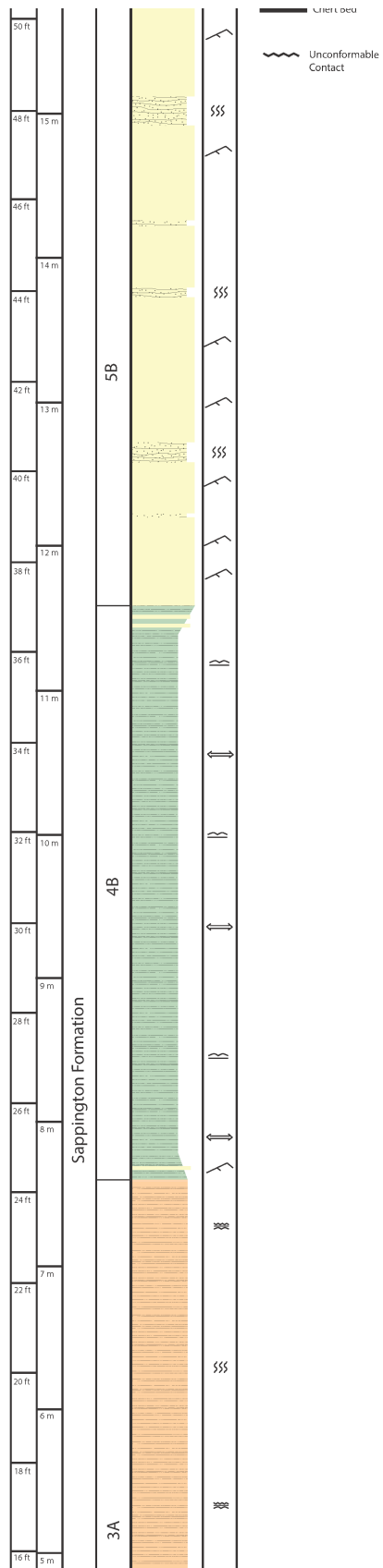
Moose Creek Section

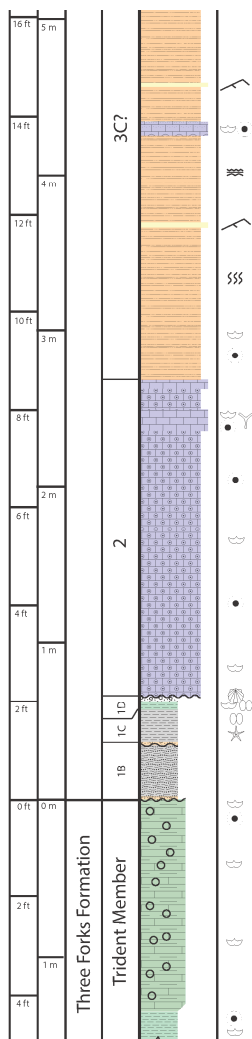




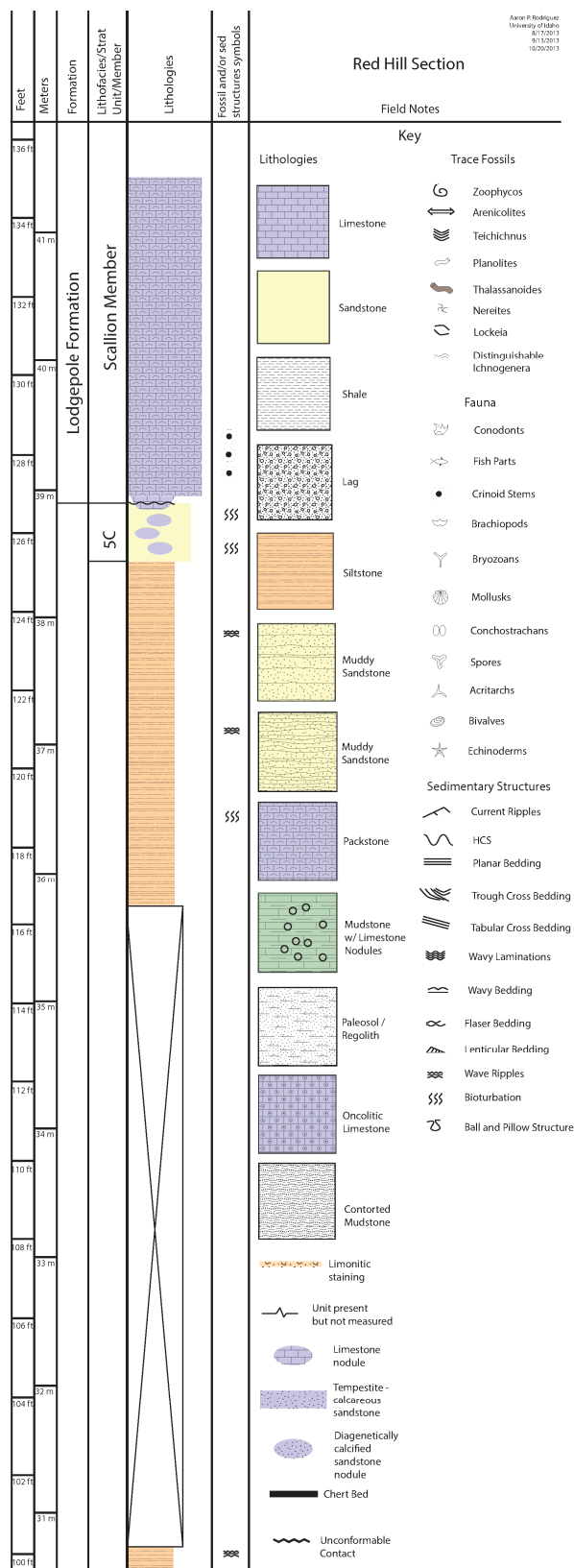
Nixon Gulch Section

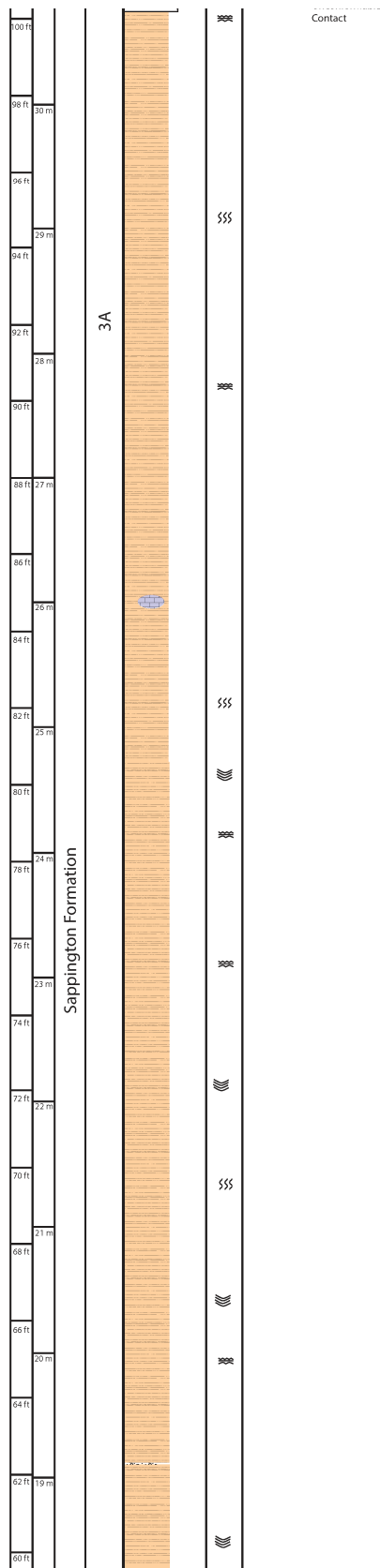


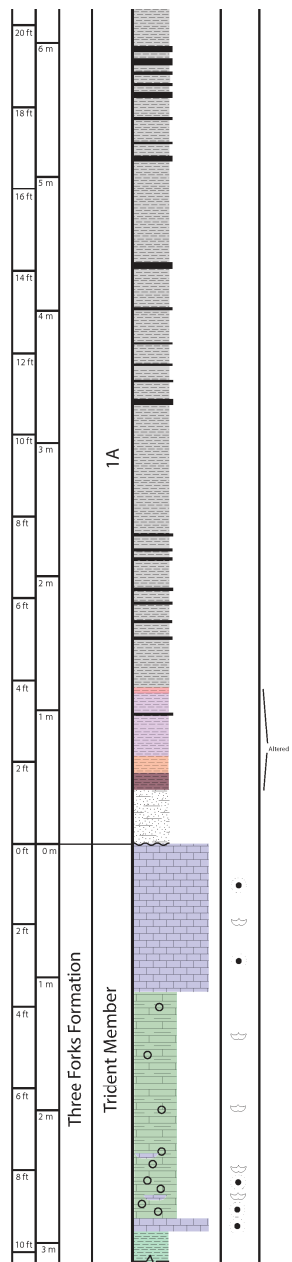




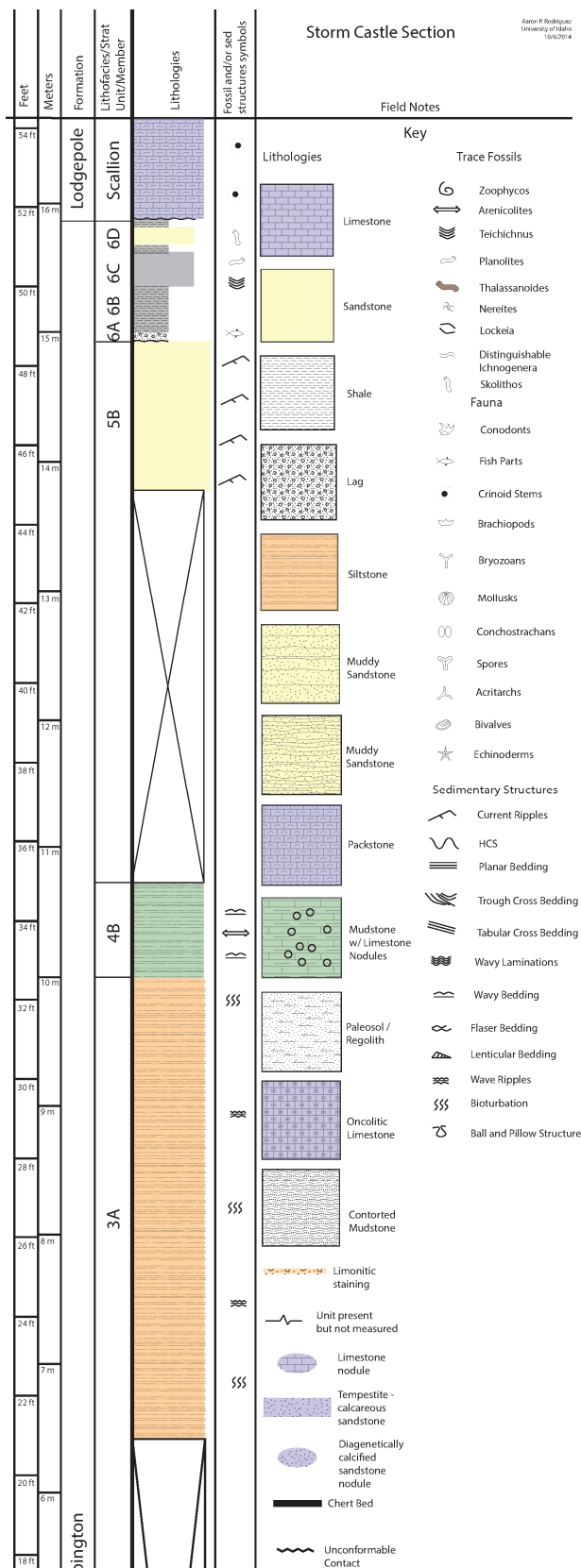
Red Hill Section

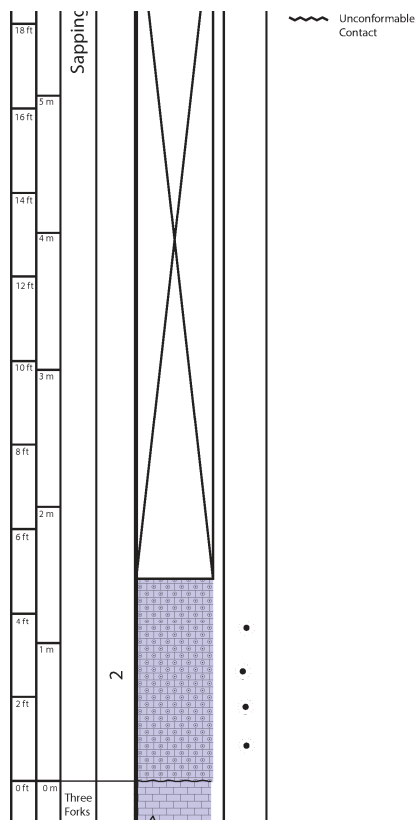




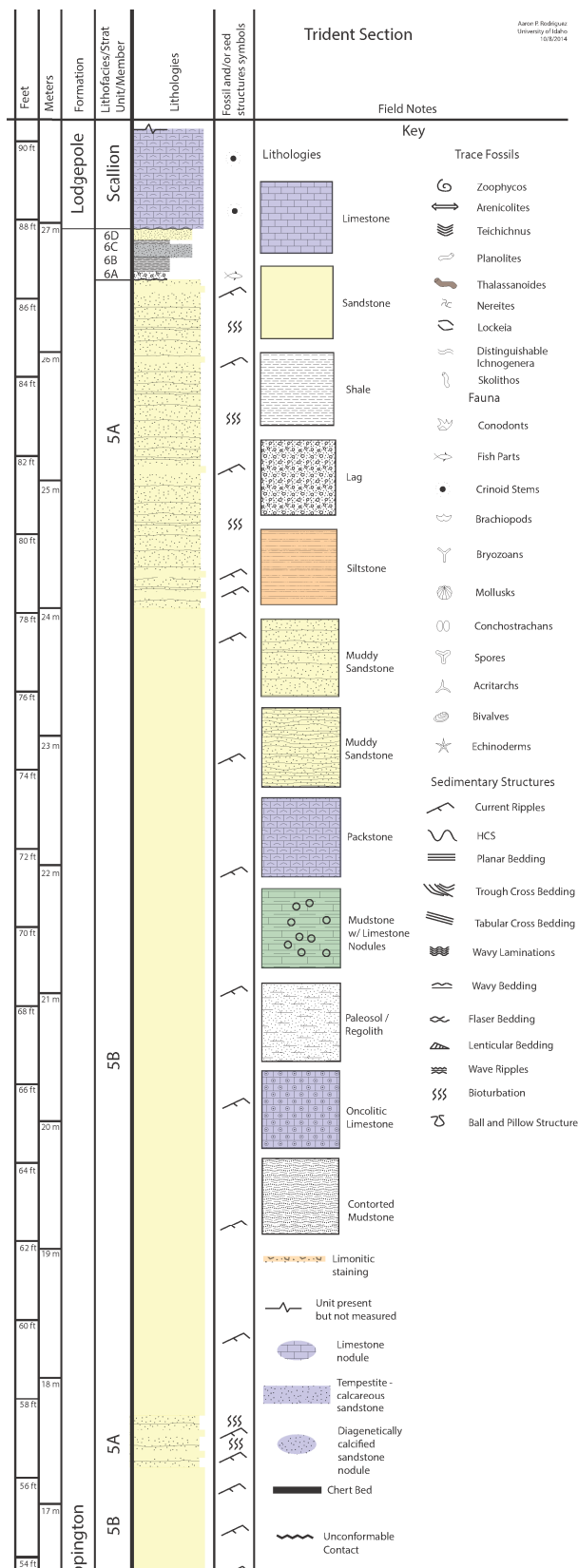


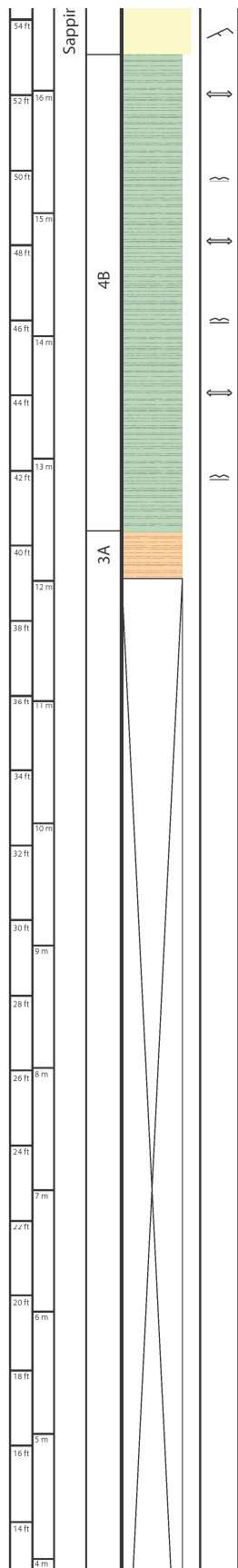
Storm Castle Section





Trident Section





Contact

